Alma Mater Studiorum – Università di Bologna
in cotutela con Università Tecnica Gebze

DOTTORATO DI RICERCA IN

CHIMICA

Ciclo 36

Settore Concorsuale: 03/A1 - CHIMICA ANALITICA

Settore Scientifico Disciplinare: CHIM/01 - CHIMICA ANALITICA

A NOVEL HYBRID THERMOCHEMICAL-BIOLOGICAL REFINERY INTEGRATED WITH POWER-to-X TECHNOLOGY FOR OBTAINING BIOPOLYMERS

Presentata da: Yusuf KÜÇÜKAĞA

Coordinatore Dottorato

Luca PRODI, Dr.

Supervisore

Cristian TORRI, Dr.

Supervisore

Serdar KARA, Dr.

Esame finale anno 2023

SUMMARY

In this study, a novel hybrid thermochemical-biological refinery integrated with power-to-x approach was developed for obtaining biopolymers (namely polyhydroxyalkanoates, PHA). Within this concept, a trilogy process schema comprising of, (i) thermochemical conversion via integrated pyrolysis-gasification technologies, (ii) anaerobic fermentation of the bioavailable products obtained through either thermochemistry or water-electrolysis for volatile fatty acids (VFA) production, (iii) and VFA-to-PHA bioconversion via an original microaerophilic-aerobic process was developed. During the first stage of proposed biorefinery where lignocellulosic (wooden) biomass was converted into, theoretically fermentable products (i.e. bioavailables) which were defined as syngas and water-soluble fraction of pyrolytic liquid (WS); biochar as a biocatalyst material; and a dense-oil as a liquid fuel. Within integrated pyrolysis - gasification process, biomass was efficiently converted into fermentable intermediates representing up to 66% of biomass chemical energy content in chemical oxygen demand (COD) basis. In the secondary stage, namely anaerobic fermentation for obtaining VFA rich streams, three different downstream process were investigated. First fermentation test was acidogenic bioconversion of WS materials obtained through pyrolysis of biomass within an original biochar-packed bioreactor, it was sustained up to 0.6 g_{COD}/L-day volumetric productivity (V_P). Second, C1 rich syngas materials as the gaseous fraction of pyrolysis-gasification stage, was fermented within a novel char-based biofilm sparger reactor (CBSR), where up to 9.8 g_{COD}/L-day V_P was detected. Third was homoacetogenic bioconversion within the innovative power-to-x pathway for obtaining commodities via renewable energy sources. More specifically, water-electrolysis derived H_2 and CO_2 as a primary greenhouse gas was successfully bio-utilized by anaerobic mixed cultures into VFA within CBSR system (V_P: 18.2 g_{COD}/L-day). In the last stage of the developed biorefinery schema, VFA is converted into biopolymers within a new continuous microaerophilic-aerobic microplant, where up to 60% of PHA containing sludges was obtained.

Keywords: Pyrolysis, Syngas Fermentation, Carbon Dioxide (CO_2) Utilization, Biochar, Volatile Fatty Acids (VFA), Polyhydroxyalkanoates (PHA).

ÖZET

Bu çalışmada, biyopolimerlerin (yani polihidroksialkanoatlar, PHA) elde edilmesi için "enerjiden-materyale" yaklaşımı ile entegre edilmiş yeni bir hibrit termokimyasal-biyolojik rafineri geliştirilmiştir. Bu konsept dahilinde, üçleme şeklinde bir proses şeması ile, (i) entegre piroliz-gazlaştırma yoluyla termokimyasal dönüşümü; (ii) uçucu yağ asitleri (UYA) üretimi için termokimyasal yöntemlerce elde edilen biyodönüşebilir ürünlerin anaerobik fermantasyonu; (iii) ve UYA-dan-PHA'ya mikroaerofilik-aerobik özel bir proses ile biyopolimer sentezi gerçekleştirilmiştir. Lignoselülozik (odunsu) biyokütlenin dönüştürülmesi önerilen biyorafinerinin ilk aşamasında; sentez gazı ve pirolitik sıvının suda çözünür fraksiyonu (WS) gibi fermente edilebilir ürünler, mikrobiyal katalizör olarak kullanılacak gözenekli biyoçar malzemesi ve sıvı yakıt statüsünde yoğun-yağ elde edilmiştir. Entegre piroliz-gazlaştırma sistemi içinde, biyokütle verimli bir şekilde biyokütlenin kimyasal enerji içeriğinin %66'sına kadarını temsil eden fermente edilebilir ara ürünlere dönüştürülmüştür. İkincil aşamada, yani VFA-zengin sıvıların elde edilmesi için uygulanan anaerobik fermantasyonda, üç farklı alt proses incelenmiştir. İlk fermantasyon testi, biyokütlenin biyokömür yataklı orijinal bir biyoreaktör içinde pirolizi yoluyla elde edilen WS malzemelerinin asidojenik biyodönüşümüdür ve 0,6 gCOD/L-gün verimlilik (V_P) değerlerine ulaşılmıştır. Sonra, entegre piroliz-gazlaştırma aşamasının gaz fraksiyonu olarak C1 bakımından zengin sentez gazı malzemeleri, yenilikçi biyoçar bazlı biyofilm difüzör reaktörü (CBSR) içinde fermente edilmiş ve 9.8 gCOD/L-gün V_P'ye ulaşılmıştır. Üçüncü olarak, yenilenebilir enerji kaynakları yoluyla malzeme elde etmenin yenilikçi yolu, "power-to-x" konseptine dayanan homoasetojenik biyodönüşümdür. Yani, su elektrolizinden üretilen H_2 ve birincil sera gazı olarak CO_2, anaerobik kültürler tarafından CBSR sistemi içinde UYA'ya başarıyla dönüştürülmüştür (V_P 18.2 gCOD/L-gün). Geliştirilen biyorafineri şemasının son aşamasında, VFA %60'a kadar PHA içeren çamurların elde edildiği sürekli mikroaerofilik-aerobik mikro-tesis içinde biyopolimerlere dönüştürülmüştür.

Anahtar Kelimeler: Piroliz, Sentez Gazı Fermantasyonu, Karbon Dioksit Kullanımı, Biyoçar, Uçucu Yağ Asitleri, Polihidroksialkanoat (PHA).

ACKNOWLEDGEMENTS

Firstly, I would like to express my gratitude to my supervisors, Dr. Cristian Torri and Dr. Serdar Kara for their all kind of supports during my doctoral study.

During my PhD journey, that started in Gebze Technical University (GTU), I was lucky enough to spend more than two years of period in University of Bologna (UniBo) under a specific "co-tutelle" (co-tutorship) agreement between UniBo and GTU for awarding a double doctoral degree. These have been a great experience and I want to thank all parties of UniBo for their hospitality and willingness to accommodate me. I would like to thank also to the people who encouraged and supported me from my home university (GTU) for conducting an internationally collaborated PhD.

I am also grateful to all my dear colleagues, friends and professors from both Turkish and Italian side who made this tough journey a pleasant for me.

Lastly, I acknowledge the Council of Higher Education of Turkey (YOK) for the financial support received during the first year of research activities at UniBo, within the YUDAB international scholarship. Likewise, I would like to thank Scientific and Technological Research Council of Turkey (TUBITAK) for the scholarship provided within 2214A research fellowship programme during the second year at UniBo. Besides, I acknowledge the research fund received from GTU within the BAP projects programme, which was used to conduct preliminary experiments at GTU.

Lastly, I dedicate this work to my dear wife Şeyma and to my lovely family…

TABLE of CONTENTS

LIST OF ABBREVIATIONS AND ACRONYMS

Abbreviations and Acronyms		Explanations
V_P	:	Volumetric Productivity
gr	:	Gram
GJ	:	Gigajoule
kg	:	Kilogram
kmol	:	Kilomole
mL	:	Milliliter
min	:	Minute
s	:	Second
M	:	Mass
MW	:	Molecular Weight
V	:	Volume
p	:	Density
µL	:	Microliter
eV	:	Electron Ionization
m/z	:	Mass to Charge Ratio
Da	:	Dalton
C	:	Concentration
t	:	Time
ε	:	Yield
l	:	Microbial Growth
ω	:	Unreacted Portion
ADF	:	Aerobic Dynamic Feeding Process
APL	:	Aqueous Pyrolysis Liquid
AS	:	Anhydrosugars
BES	:	Bromoethane Sulfonate
C1	:	One-carbon molecules
CBSR	:	Char-Based Biofilm Sparger Reactor
COD	:	Chemical Oxygen Demand
DAD	:	Diode-Array Detection
DIET	:	Direct Interspecies Electron Transfer

DMC	:	Dimethyl Carbonate
EBPR	:	Enhanced Biological Phosphorus Removal Process
FTP	:	Fischer-Tropsch Process
GHG	:	Greenhouse Gas
GC	:	Gas Chromatography
GC-MS	:	GC Mass Spectrometry System
GC-TCD	:	GC With Thermal Capture Detector
HfMBR	:	Hollow Fiber Membrane Reactor
HHV	:	Higher Heating Value
HPLC-SEC	:	High-Performance Liquid Size Exclusion Chromatography
HMW	:	High Molecular Weight
HRT	:	Hydraulic Residence Time
HTB	:	Hybrid Thermochemical-Biological
IDE	:	Integrated Developing Environment
LMW	:	Low Molecular Weight
MWD	:	Molecular Weight Distribution
MMC	:	Mixed Microbial Cultures
MW	:	Molecular Weight
OLR	:	Organic Loading Rate
ORP	:	Oxidation Reduction Potential
PHA	:	Polyhydroxyalkanoates
PHB	:	Polyhydroxy Butyrate
PL	:	Pyrolytic Lignin
PS	:	Polystyrene
PyP	:	Pyrolysis Products
SEM	:	Scanning Electron Microscope
SRT	:	Sludge Residence Time
SSC	:	Single Strain Culture
toe	:	Tons of Oil Equivalent
VFA	:	Volatile Fatty Acids
VSS	:	Volatile Suspended Solids
WS	:	Water-Soluble Pyrolysis Liquid
WI	:	Water-Insoluble Pyrolysis Products

LIST OF FIGURES

LIST OF TABLES

1. INTRODUCTION

1.1. Aim and Scope

The scope of thesis was mainly composed of, (i) thermochemical processing (e.g. pyrolysis, gasification) of lignocellulosic biomass to obtain bioconvertible (i.e. bioavailable) and stable intermediate compounds such as one-carbon (C1) rich syngas and saccharated bio-oil; (ii) biological upgrade of those intermediates into organic fatty acids (VFA) by anaerobic fermentation, (iii) and intracellular synthesis of biopolymeric materials (namely, polyhydroxyalkanoates, PHA) as final products via VFA-consuming mixed microbial cultures (MMC). This type of biorefineries which integrates thermochemical conversion and biological processes are called as hybrid thermochemical-biological (HTB) systems [1]. Even though HTB biorefinery is a quite recent and relatively immature approach yet is still quite interesting due to it can depolymerize refractory biomasses including the ones which are not suitable for hydrolysis.

In this research study, pyrolysis was initially chosen as the platform process for thermochemical conversion of biomass. Then, biochar gasification was included to maximize the bioavailable compounds originated from lignocellulosic biomass. Both pyrolysis and gasification processes are known as easy-to-setup and effective thermochemical process that can be conducted in flexible scales varying from bench-scale systems (gr/day) to large-scale thermochemical factories (tones/day).

Power-to-material (i.e. power-to-x) approach was also combined with the research study, as an alternative pathway to obtain totally sustainable biopolymers, where renewable power originated H_2 gas via water-electrolysis and CO_2 as a main greenhouse gas was aimed to be bioconverted into VFA by means of anerobic fermentation (more specifically homoacetogenic metabolism). As in line with the final target, VFA obtained through this secondary simpler pathway, were also proposed to be used in PHA accumulation biological process. A simplified graphical abstract of the proposed integrated biorefinery system combined with power-to-x approach is visualized in Figure 1.1. Finally, it was aimed to reveal overall product yield from one unit biomass to one-unit biopolymeric PHA material.

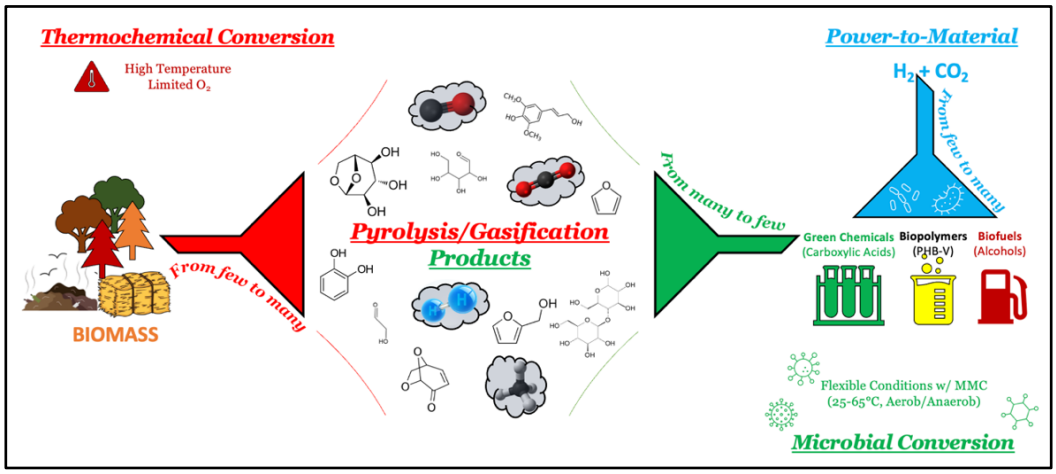

Figure 1.1: Graphical abstract of the proposed integrated biorefinery.

Each main process of the proposed biorefinery schema which combines the hybrid thermochemical-biological and power-to-x pathways are going to be discussed in detail under different sections. The preliminary investigations and the processes which were found as non-ideal in terms of process optimization, are not included into the main chapters, yet they will be shared in detail as Appendixes. Here in below, all the following chapters together with a short description of their content are shared:

- Thermochemical Conversion: Pyrolysis-gasification integrated thermochemical process for maximizing bioavailable compounds originated from lignocellulosic biomass.
- Water Soluble PyP Fermentation: Acidogenic fermentation of bioavailable pyrolysis products (PyP), more specifically and mainly water-soluble fraction of pyrolytic liquid (WS) into organic fatty acids via biochar attached MMC.
- Syngas Fermentation: Bioconversion of gaseous products (syngas) of thermochemical conversion into organic fatty acids within a novel char-based biofilm sparger reactor (CBSR) by acetogenic MMC.
- H_2/CO_2 Fermentation: Chemoautotrophic bioconversion of water-electrolysis derived green H_2 and CO_2 as an abundant greenhouse gas with homoacetogenic attached-grown mixed cultures within CBSR system.
- VFA to PHA Bioconversion: Development and testing of a fully continuous microaerophilic-aerobic biological micro-plant, which utilizes VFA-rich streams via a peculiar microbial consortium that accumulates intracellular PHA as a final product.

- Overall Conclusion: An overall image to the developed integrated biorefinery and performance evaluation will be shared.

1.2. COD as Single Unit Approach

The assessment of yields obtainable by HTB methods, and their comparison with second-generation technologies, require the definition of a common unit of "chemical energy", which can be easily applicable in both aqueous biological systems and thermochemical processes. To date, tons of oil equivalent (toe), corresponding to 41.85 GJ, is the most widely used chemical energy unit to compare oil, biomass fuels and power sources in energy systems. Such a measure is intrinsically related to oil and requires analyses (namely higher heating value HHV, or elemental analysis) that are difficult or inaccurate if performed in aqueous solutions. As such, relying on 'toe' is quite difficult in HTB processes, whereas the use of COD or theoretical oxygen demand, usually adopted in many biotechnological approaches [2], could be of great importance in comparing different HTB systems.

COD is a widely used parameter to track organic matter content of waste-waters and is defined as the number of equivalent amounts of oxygen required to fully oxidize all available organic compounds in a given volume or weight of sample. Even though it is appearing as a very specific parameter by this basic definition, COD can also be considered as an indicative measurement of available chemical energy stored in samples. One mass unit of COD (kg) corresponds a certain amount of organic matter which requires one kg of oxygen to be completely oxidized to carbon dioxide (CO_2) and water. By definition, 0.125 kmol of electrons found in energy-rich bonds of organic molecules correspond to 1 kg of COD due to the stoichiometry of redox reactions [3].

1 kg of COD (otherwise named as kgCOD, 1 kgO, or kgO_2) is defined as the amount of organic matter in a given volume that needs 1 kg of oxygen to be completely oxidized. The highest COD is that of hydrogen (8 $kgCOD/kgH_2$), whereas the COD of organic materials ranges between 0.2 (oxalic acid) and 4 (methane) kgCOD/kg. Natural occurring substrates typically shows a narrow COD range between that of glucose (1.07 kgCOD/kg) and lignin (2.3 $kgCOD/kg_{feedstock}$). Due to the stoichiometry of redox reactions, 1 kg of COD corresponds, by definition, to 0.125 kmol of electrons packed into the energy-rich bonds of organic compounds by photosynthesis or

electrosynthesis [4][5]. For instance, 0.125 g of H_2 (1 g of COD) through water electrolysis requires an electric current equal to 12 kC/gCOD against an electric potential of more than 1.23 V. If the reaction is reversed, the maximum stored chemical energy that can be recovered as electric power is:

$$\frac{MJ}{gCOD} = \frac{12440\ C \cdot 1.23\ V}{gCOD} = 15.3\ \frac{kJ}{gCOD} \cong \mathbf{15}\ \frac{MJ}{kgCOD} \quad (1.1)$$

15 MJ/gCOD can be obtained by several independent approaches as the typical "energy content" of 1 kg of COD. In fact, due to stoichiometry, both COD and HHV are correlated to elemental compositions [6]. This is because both COD (exactly) and HHV (empirically) are proportional to the number of bonds that are broken during combustion to form the stable bonds of H_2O and CO_2. Even considering that the different chemical bonds are characterized by slightly different bond energy, this amount of energy released by oxidation of 1 kg of COD range in a quite narrow range between 12 MJ/kgCOD (graphite) and 18 MJ/kgCOD (carbon monoxide). This slight variability in HHV/COD ratio of organic compounds is actually the driver which can support the anaerobic processes (e.g. anaerobic digestion of glucose to CH_4, anaerobic fermentation of glucose to ethanol) feasible with net energy gain. In fact, according to thermodynamic principles, biocatalysts allow to exploit paths that are within limits of two fundamental rules extensively elucidated elsewhere [7]:

i) The COD of reagents should be equal to the COD of products. Given that oxidants have negative COD (e.g. oxygen -1 gCOD/g, by definition) this assumption is valid in both anaerobic and aerobic systems.
ii) Organism can exploit just favorable "COD pathways", which are those that foresee a decrease in HHV/COD ratio or oxidize a part of COD [8].

The advantage of considering COD as a single platform unit to track the flow of chemical energy, COD can also be used to calculate overall balance (hereinafter as COD balance) instead of mass balance, since it can be applied to all kind of materials can be found in biorefineries. Because the COD of reagents should be equal to the COD of products. Given that oxidants have negative COD (e.g. oxygen -1 gCOD/g, by definition) this assumption is valid in both anaerobic and aerobic systems. From this information, it is possible to establish that 1 kg of COD as PyP can theoretically

be transformed in 1 kg of COD of fermentation products, such ethanol, butanol or VFAs.

Within this kind of complex biorefinery approach, where thermochemical conversion, anaerobic fermentation and PHA bio-accumulation processes are combined, it is a challenge to track whole system through a single unit. However, COD as a useful direct measurement of chemical energy in both liquid (e.g. pyrolytic liquids, fermentation broth, PHA-rich suspension), solid (e.g. biochar, PHA-granules) and gas (e.g. CO, CH_4, H_2) in/out materials of the biorefinery, will be used as the single unit for performance evaluation and product yields, as we proposed and discussed in detail elsewhere [3].

2. THERMOCHEMICAL CONVERSION

2.1. Introduction to HTB

To date, most of the efforts to obtain drop-in biofuels or chemicals from second and third generation feedstock were spent only on biological or thermochemical approaches [9]. At the interface of these compartmented approaches, hybrid thermochemical-biological (HTB) processes are an interesting, although immature, field of research. Although HTB represents a relatively new research domain, the potential of biology to alleviate, or even solve, specific technical issues related to thermochemical process and, more specifically, pyrolysis and gasification, was demonstrated by several groups [9]–[13].

In pyrolysis, biomass is heated with minimal or exempt from oxygen at 350-600°C. Heat easily breaks polymers resulting in the production of a vapor stream enriched in pyrolysis products (PyP) and a carbonaceous residue (char or biochar). The stream of PyP is subsequently cooled down, yielding a gas and a liquid product (pyrolysis liquid, formed by water and organic substances). Being a relatively simple process, pyrolysis allows the treatment of a large array of different feedstock, representing one of the most reliable pathways for depolymerizing the slowly biodegradable fractions of biomass [14]. Although pyrolysis is a high-rate method to depolymerize biomass, the high temperature used in the process implies a lower selectivity of the reaction, especially when complex feedstock is considered [15]. HTB approaches aim to exploit microorganisms as a sort of "biological funnel" [16], to decrease the complexity of PyP and unlock advanced utilization of thereof [1]. Different HTB schemes based on pyrolysis and gasification have been proposed and investigated during the last two decades [7], [9]–[12], [17] Although some challenges (mainly related to low volumetric productivity) remains relevant [18], Syngas fermentation by single microbial strains (or single strain culture, SSC) is the most mature HTB approach, with two commercial exploitation attempts (Coskata and INEOS Bio, finally bankrupted) and one commercially available process (Lanzatech) in 2021 [19]–[22]. HTB processes based on pyrolysis can address some of the limitations of syngas fermentation but poses two additional challenges: toxicity and bioavailability [23]. Toxicity depends on pyrolysis process (feedstock and pyrolysis conditions), PyP detoxification strategies and by adopted microorganisms (or

consortia in MMC) with their own tolerance levels towards PyP. On the contrary, bioavailability depends solely on feedstock and pyrolysis conditions.

Another suitable thermochemical technology for HTB approach is gasification, a commercial technology for the thermal conversion of biomass into C1 (CO, CH_4, CO_2) and H_2 rich syngas materials (i.e. synthesis gas) in the absence of oxygen. The suitability of this technology for the latter biological process in HTB concept is originating from the "Wood–Ljungdahl" (i.e. Acetyl-CoA) pathway of strictly-anaerobic acetogens who were discovered as early as 1932. *Acetogenesis* are capable of converting some inorganic C1 gasses (namely, CO and CO_2) and hydrogen (H_2), into organic fatty acids (i.e. VFA), that can be used as a direct product in chemical refineries (e.g. for vinyl acetate, cellulose acetate, resins production) and/or as a platform chemical to be upgraded for advanced biomaterials such as PHA [24].

This chapter proposes to establish a robust integrated thermochemical conversion pathway for maximizing the chemical energy yield of bioavailable products from lignocellulosic (i.e. wooden) biomass. For this purpose, an integrated pyrolysis-gasification system was proposed.

More specifically, a representative wooden biomass (namely fir sawdust) was first pyrolyzed under different temperature conditions (450 – 650 °C) to investigate the chemical energy yields (COD basis) of bioavailable PyP, namely, WS of condensables (i.e. aqueous tars, aqueous pyrolysis liquid), and gas products (i.e. syngas). Later, the most dominant product of pyrolysis, namely biochar, whose composition is mostly carbon, thereof not considered as a bioavailable product, were gasified under CO_2 environment, into CO and H_2 rich syngas mixture. The choice of CO_2 as oxidizing agent instead of widely-used O_2 and air, was mainly for expanding environmental-friendly approach, by means of proposing the use of CO_2 rich off-gasses originated from the aerobic fermentation section of the PHA process {Chapter 6}. Hence, utilizing CO_2 for gasification purpose, induces both reducing greenhouse gas (GHG) pollution, and generation of syngas to be used as biochemical energy source for the production of green chemicals (e.g. VFA) and biomaterials (e.g. PHA). The COD yields of different biochars obtained at different pyrolysis temperatures were identified. Finally, the tested thermochemical conditions, were scenarioized for the determination of most advantageous flow diagram to the latter biological conversions.

2.2. Methodology

2.2.1. Experimental Set-Up for Thermal Conversion

Pyrolysis and gasification experiments were performed in a fix bed reactor system. The apparatus was consisted of a quartz cylindrical reactor (710 mm length and 40 mm Ø), where biomass was inserted by a quartz cylindrical sample holder (300 mm length and 27 mm diameter). The quartz reactor was positioned inside a tubular furnace and followed by a water-containing gas impinger and a small cyclone unit both submerged into ice during the experiments. A cotton trap was placed just after the cyclone unit to capture the fine aerosols before to 10L sized laminated foil gasbag (Supel™ Inert Foil, 10L) for storing the produced gas materials. Besides, a peristaltic pump was positioned before the reactor and a loop line was created for gas flow in the set-up, by using modified polyamide tubing (⌀ 6mm OD) laminated with double layer silicone and aluminum foil, for avoiding leaks of highly permeable gasses (e.g. H_2) as described elsewhere {Chapter 3.2.2.1} [25]. In addition, an extra gasbag was positioned before the peristaltic pump, to be used as oxidant gas (CO_2) storage, only for gasification tests (Figure 2.1).

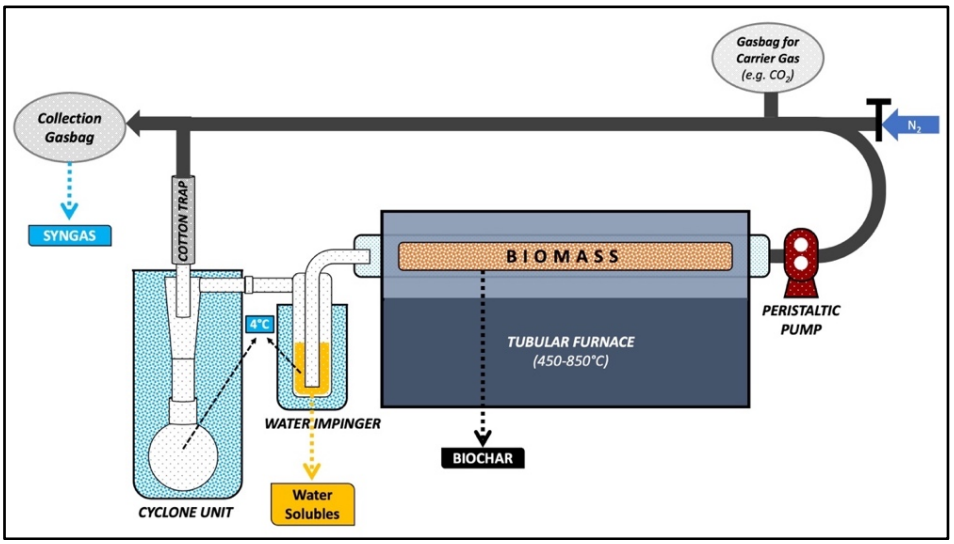

Figure 2.1: Flow-diagram and units of the fixed bed pyrolysis-gasification set-up.

2.2.2. Pyrolysis Conditions

Three different temperature conditions were tested during the pyrolysis of lignocellulosic biomass experiments, namely, 450 °C, 550 °C, and 650 °C. For this

purpose, sawdust biomass originating from fir tree, which belongs to pine family (*Pinaceae*), were used as feedstock. Before each batch pyrolysis test, the fixed bed furnace system was flushed with excess amount of N_2, for several minutes to strip away atmospheric O_2. Then, 30 g of pre-dried biomass feedstock were compacted inside the biomass holder and inserted into the pre-heated zone (Figure 2.2). Immediately after, gas recirculation was started at 225 mL/min flowrate to sustain the fluids inflow towards to the traps and the gas collection bag. Each temperature condition was tested in triplicates under same operational conditions, and residence time (20 min ± 5). At the end of each test, heating and peristaltic pump instantly stopped, quartz reactor was cooled down rapidly (≈5 min) under N_2 flow. WS liquid trapped inside the impinger, and produced biochar was collected manually and stored in proper conditions until the analysis. Water-insoluble portion (WI) of condensable pyrolysis products (i.e. pyrolytic liquid, bio-oil), or in other names of condensable tars, dense-oil, or pyrolytic lignin (PL), were scraped away by acetone washing of each glassware unit (namely, quartz reactor, sample holder, gas impinger, cyclone, and cotton-trap) of the apparatus. Produced gasses (i.e. syngas, synthesis gas, pyrogas) were stored inside a sealed air-tight gasbag.

Figure 2.2: Fixed-bed furnace apparatus during a pyrolysis test.

2.2.3. Gasification Conditions

Gasification tests of the biochar samples, obtained from the pyrolysis of biomass under different temperature conditions, were conducted in the same experimental apparatus used for pyrolysis (Figure 2.2) with an addition of oxidant gasbag prior to the peristaltic pump (Figure 2.1). CO_2 was provided as oxidant gas in a CO_2/C ratio of 1.5 (± 0.07) according to the work of Sadhwani et al. [26]. Preheated quartz reactor at

850 °C was flushed with excess amount of CO_2 gas for several minutes prior to the insert of sample holder with compacted biochar. The rest of operation was same as pyrolysis experiments {Chapter 2.2.2}.

CO_2/C ratio was calculated according to the below formula, where the symbols of $M_{biochar}$, $\#_C$, $MW_{biochar}$, V_{CO2}, and ρ_{CO2} were representing amount of gasified biochar (g), number of carbon elements in the biochar molecular formula, molecular weight (MW) of biochar sample ($g/mole$), total volume of initial CO_2 gas (L), and density of CO_2 respectively (2.1).

$$\left[\frac{M_{biochar}(g)\ x\ 12\left(\frac{g_C}{mole}\right) x\ \#_C}{MW_{biochar}\left(\frac{g}{mole}\right)}\right] \div \left[V_{CO_2}(L) x\ \rho_{CO_2}\left(\frac{g}{L}\right)\right] \quad (2.1)$$

2.2.4. Analytical Methods

Biomass feedstock, pyrolysis products (biochar, WS, WI, and pyrogas), and gasification products (syngas, and char) were analyzed according to the following procedures, for determining the COD content and characterization of each material.

Quantification of VFA were carried out by following the previously published method elsewhere [27]. For this purpose, a given amount of bioliquid sample (0.1 mL) was directly poured in a GC vial (volume 2 mL) and added sequentially with 0.1 mL of $KHSO_4$ saturated solution, 0.1 mL of NaCl saturated solution, and 0.1 mL of internal standard solution (2-ethyl butyric acid 1 mg/mL in deionized water). Then, 1 mL of dimethyl carbonate (DMC) was added, and the closed vial was vigorously shaken to favor the liquid-liquid extraction from the water solution into DMC. After the two phases settled the sample was injected by an autosampler into the split/spitless injector (spitless conditions, 250°C) of an Agilent 7820A gas chromatography mass spectrometry system (GC-MS). The syringe of the autosampler was programmed to take 1 µL of the solution to be injected at a fixed height from the top of the vial (10 mm), corresponding to the layer of DMC. Analytes were separated with a DB-FFAP polar column (Agilent, 30 m length, 0.25 mm ID, 0.25 mm film thickness) with a helium flow of 1 mL/min. The initial oven temperature was set to 50°C (5 min) and increased to 250°C (10°C min^{-1}). Detection was made with a quadrupole mass spectrometer Agilent 5977E operating under electron ionization at 70 eV with full scan mode acquisition at 1 scan s^{-1} in the 29-450 m/z range. Identification was based on the

retention time, mass spectra of the pure compounds and by library mass spectra matching (NIST). Quantification was made from the peak area integrated by extracting characteristic ions from the total ion current.

COD concentration of the liquid samples were conducted by using a Quick-COD analyzer (LAR Process Analyzer AG) following the ASTM D6238-98 method based on thermal oxidation at 1200 °C.

Silylation allows the extension of GC-MS analysis to a large amount of highly polar compounds. In a GC vial (2mL), 50 µL of liquid sample was dried under nitrogen at ambient conditions. Then, 100 µL of N,O-Bis(trimethylsilyl)trifluoro-acetamide with trimethyl-chlorosilane (BSTFA), 100 µL acetonitrile, 50 µL of 3-chlorobenzoic acid as the internal standard at 1 mg/mL in acetonitrile, and 10 µL of pyridine were poured on the dried sample. The sample was heated at 75 °C for 90 minutes. Then, 0.5 mL of ethyl acetate was added into the vial prior to the GC-MS analysis. 1 µL of the silylated sample was injected with an autosampler at 280°C in spitless mode in a GC-6850 Agilent equipped with HP-5MS column (Agilent). The initial oven temperature was set at 50 °C for 5 minutes, then a temperature ramp was applied at 10 °C-min^{-1} heating rate up to the 325 °C where the oven held for 10 minutes at the end. Mass spectra were recorded under electron ionization (70 eV) at a frequency of 1 scan-s^{-1} within the m/z 50–450 range.

Molecular weight distributions (MWD) of liquid samples were analyzed by a high-performance liquid size exclusion chromatography (HPLC-SEC). Samples were filtrated with a nylon filter (0.45µm) and 20µL of liquid sample were injected to the HPLC-SEC system using ultra-pure water as solvent. Hardware of the Agilent 1200 series HPLC instrument was consisting of; Agilent 1260 series ALS, Agilent 1260 series TCC, PL aquagel-OH-20 column, an Agilent Diode-Array Detection (DAD) G1315D detector, and an Agilent 1260 Infinity II G7162A Refractive Index Detector (RID) detector. Different standards of polyethylene-glycol were prepared in water and analyzed for a linear calibration curve between 200 to 10000 Da. Signals were collected by both RID and DAD detectors. Molecular ranges were determined through polyethylene-glycol standards in a range from 1450 to 10000 Da.

A gas chromatography system with thermal capture detector (GC-TCD 7820A, Agilent Technologies) was used to determine gas components. The GC-TCD had three packed columns (HAYASEP 80-100 mesh, HAYASEP 0 80-100 mesh, and

MOLSIEVE 5A 60-100 mesh) placed in series, to determine the concentration of N_2, H_2, CH_4, CO_2 and CO with following program: 9 min at 50°C, then 8°C min^{-1} to 80°C.

2.3. Results and Discussion

2.3.1. Pyrolysis of Biomass

Fir sawdust as a representative lignocellulosic biomass, was pyrolyzed under three different temperature conditions, namely 450 °C, 550 °C, and 650 °C, to investigate the chemical energy distribution of PyP at COD basis. As expected, higher temperature yielded less biochar (37%$_{COD:COD}$) as compared to the lower temperature conditions. On the other hand, water-insoluble PL portion was corresponding 10% of overall COD for low (450 °C) and medium (550 °C) temperature conditions, while at high temperature (650 °C) it reached up to 15%. More critically, bioconvertible pyrolysis products (i.e. bioavailable PyP) which were previously defined as C1-rich gaseous products (i.e. syngas, pyro-gas) and water-soluble condensables (WS, or aqueous pyrolysis liquid (APL)), showed an increasing trend by raised temperatures. COD yields to the WS portion was detected as 31%, 33%, and 34% for low, medium, and high temperature conditions respectively. Meantime, pyro-gas portion was reached up to the 15% of overall COD at high temperature, while it was only 6% at low temperature (Figure 2.3). In conclusion, biochar was still the main product in terms of chemical energy at each condition. For this reason, a secondary thermochemical conversion was proposed, namely biochar gasification, to maximize the overall yield of biomass originated bioavailable products.

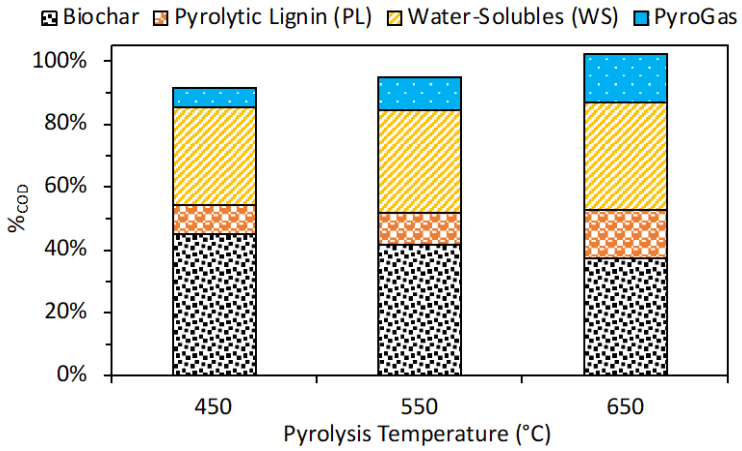

Figure 2.3: COD yields of pyrolysis products at different temperatures.

Analyses of WS fraction of pyrolysis products obtained from all temperatures tested, were carried out to reveal an approximate chemical characterization (Figure 2.5), since being the WS an extremely complex mixture of chemicals their full characterization was beyond the scope of this work. An overall molecular weight distribution (MWD) of each WS sample were conducted by HPLC-SEC technology. In addition, some selected constituents of WS, such as acetic acid, butyric acid, levoglucosan, furfural, furfural-5-methyl, 2-furanmethanol were quantified by GC-MS methods and presented as COD percent. In particular, organic acids and levoglucosan levels are quite significant in terms of bioavailability of WS, since organic acids are well known substrates for many microbial communities, and levoglucosan as an anhydrous sugar was previously reported to be easily biodegradable compound by several studies [28]–[31]. At this point, low temperature pyrolysis at 450 °C was provided the highest yields with 6.9%, 0.4%, and 6.4% for acetic acid, butyric acid, and levoglucosan in terms of product COD against to the biomass COD.

2.3.2. Biochar Gasification

In this section, gasification performance of biochars obtained by biomass pyrolysis at different temperature conditions, were investigated for revealing the yield of fermentable syngas molecules. For this purpose, biochars were gasified under CO_2 environment at 850 °C constant temperature. As a result, biochars obtained through the low pyrolysis temperature, was ended up with a significant yield of syngas (Figure 2.4). More specifically, syngas yields were estimated as 29%, 23%, and 12% for the biochars obtained from low, medium, and high pyrolysis temperatures, respectively.

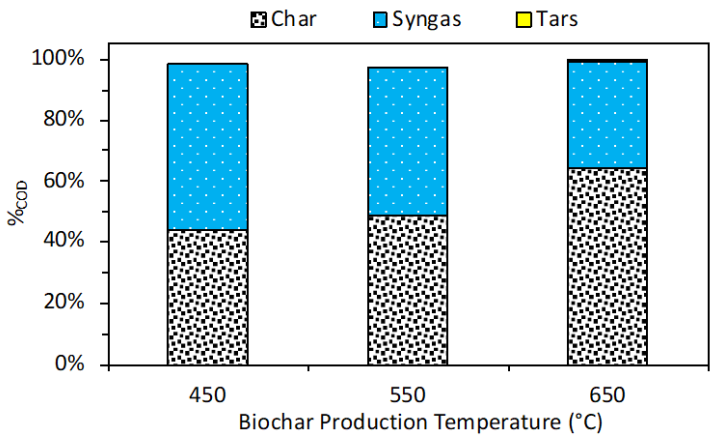

Figure 2.4: COD yields of biochar gasification tests.

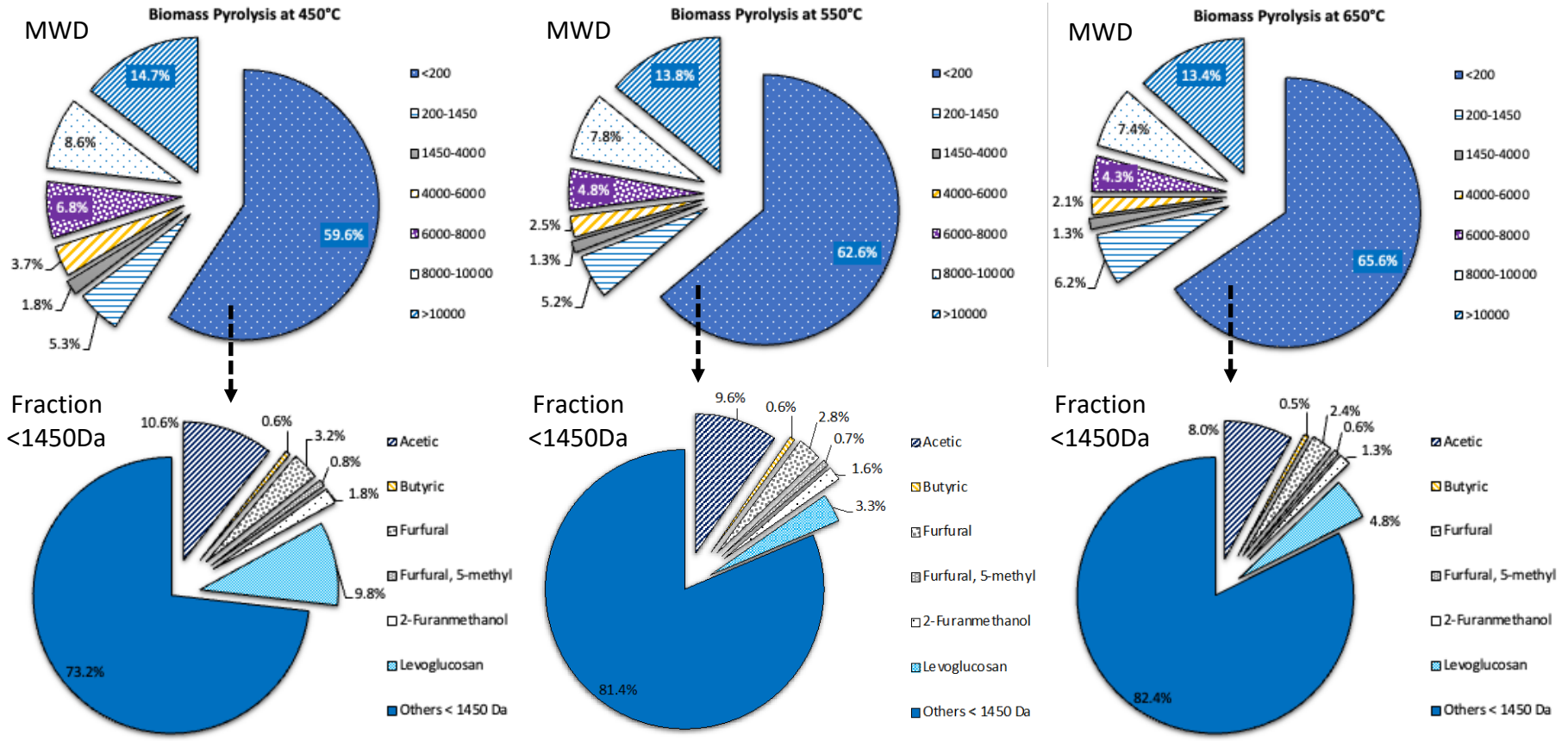

Figure 2.5: Chemical characterization of water-soluble pyrolytic liquid (WS); molecular weight distributions (MWD) are in the upper, GC-MS detectable fractions (MW < 1.45kDA) are presented in the below.

2.4. Conclusion

The purpose of this section was to find out the most advantageous integrated pyrolysis-gasification scenario for obtaining higher yields of bioavailable compounds from lignocellulosic biomass, to be used in the further biological processes within the proposed hybrid biorefinery. According to the thermochemical experiments, biomass pyrolysis at high temperature (650 °C) followed by biochar gasification, was found out as less advantageous as compared to the others, with an overall 61% COD yield into the bioavailables. Meanwhile, the other two scenarios with pyrolysis at lower temperatures was shown a quite similar overall yield in terms of bioavailable compounds (namely 66%$_{COD}$). However, pyrolysis at low temperature (450 °C) followed by biochar gasification at 850 °C was provided a slightly higher (>0.5% $_{COD}$) bioavailable compounds (Figure 2.6). Given the fact of this scenario was revealed also higher yields of VFA and anhydrosugars, it was identified as the optimal thermochemical pathway.

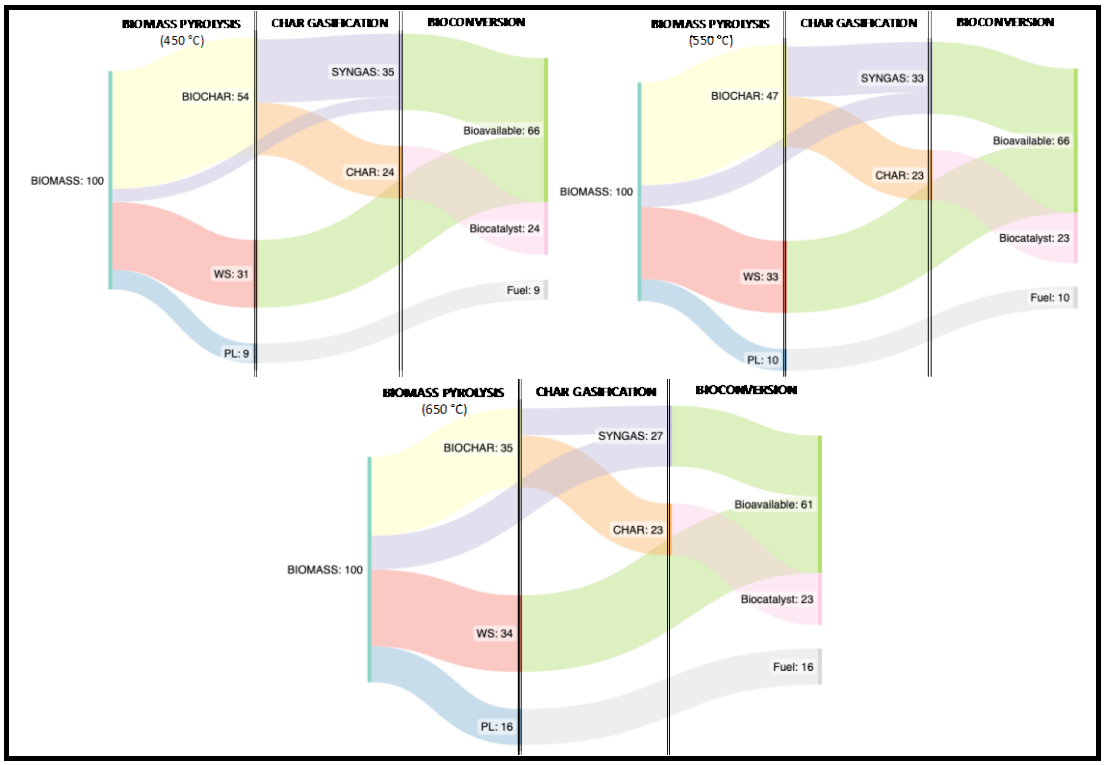

Figure 2.6: COD basis flow diagrams of thermochemical conversion scenarios.

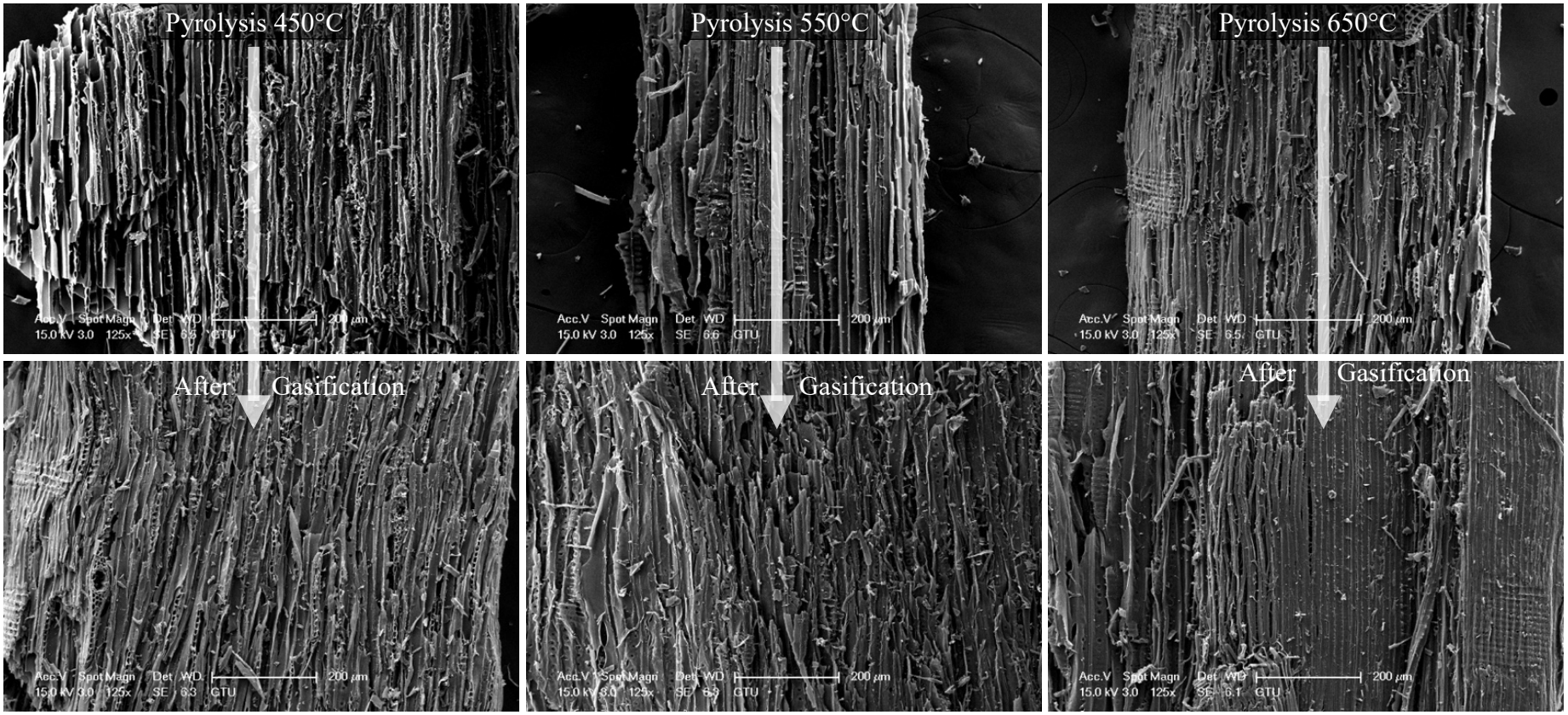

Figure 2.7: Magnified imaging of biochar and char samples obtained by SEM.

3. WATER-SOLUBLE PyP FERMENTATION

The coupling of pyrolysis and acidogenic fermentation was here proposed as a new hybrid thermochemical-biological method to circumvent the hydrolysis bottleneck within lignocellulose valorization schemes. Pyrolysis products of fir sawdust, i.e., WS together with some recessive amounts of CO-rich syngas, were tested as feedstock for VFA production (Figure 3.1). WS/syngas conversion to VFA was particularly challenging due to the combined effect of substrate (WS) and product (VFA) inhibition. To solve such an issue, a new type of bioreactor based on packed biochar, and a new acclimatization/bioaugmentation procedure consisting of co-feeding WS/syngas and glucose, were proposed and tested. The gradual switch from glucose to WS was monitored through various analytical techniques, observing the transition toward a "*pyrotrophic*" MMC able to convert WS/syngas into VFA. Even without selective inhibition of methanogens, the main fermentation products were VFA (mainly acetic, butyric and caproic acid), whose profile was a function of the WS/glucose ratio. Although the achieved volumetric productivity was lower (<0.6 gCOD L^{-1} d^{-1}) than that observed in sugar fermentation, bioaugmented *pyrotrophs* could convert headspace CO, most of GC-MS detectable compounds (e.g. anhydrosugars) and a significant portion of non-GC-MS detectable compounds of WS (e.g. oligomers with MW<1.45 kDa).

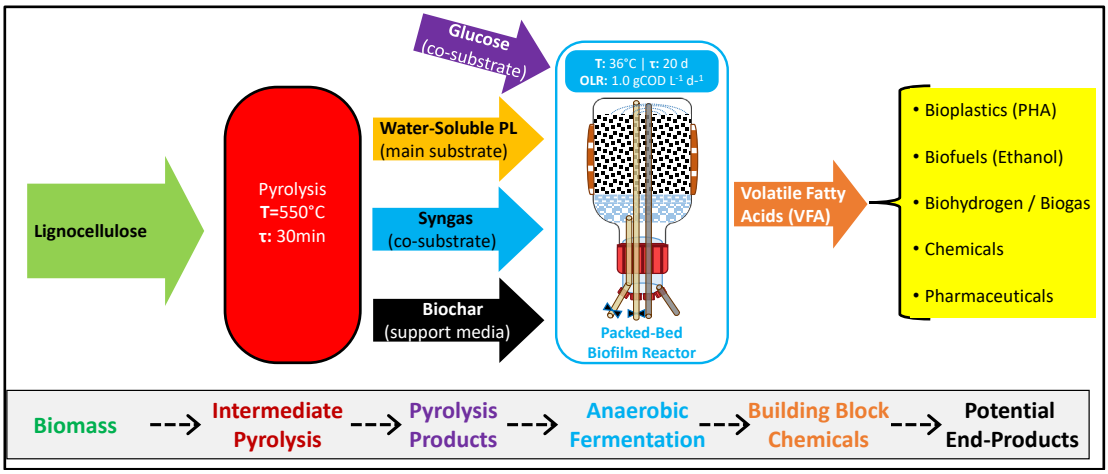

Figure 3.1: Abstract figure for the bioconversion of water-soluble pyrolytic liquid (WS) as a main substrate for acidogenic fermentation.

3.1. Introduction to WS Fermentation

Lignocellulosic biomass is a renewable and potentially sustainable raw material for obtaining value-added chemicals and bio-materials. However, due to its heterogeneous and refractory physicochemical structure, lignocellulose is not easily bioavailable for biological conversion processes. The depolymerization of the slowly biodegradable fractions of lignocelluloses can be achieved by pyrolysis, namely heating at 350-650°C in the absence of or with minimal oxygen, which can convert a large array of different feedstock into; a vapor stream enriched in pyrolysis products (PyP: water, gas and condensable organics) and a carbonaceous residue (char or biochar) [32]. The main product of intermediate and fast pyrolysis is the liquid phase (i.e., bio-oil, pyrolytic liquid, pyrolysis tar etc.), which can be easily fractionated into water-soluble (aqueous phase) and water-insoluble (organic phase) fractions.

Although pyrolysis is a high-rate and reliable technology, the high temperature used in the process implies a low selectivity of the depolymerization reaction, with the production of a mixture that cannot be used as it is in drop-in applications [15]. One of the most interesting approaches for upgrading PyP is HTB biorefinery, a "biological funnel" [33] that can decrease the complexity of pyrolysis products and unlock advanced utilization of thereof [1].

Summing up all bioavailable constituents of PyP, namely gas (syngas or synthesis gas) and WS portions, pyrolysis can deliver more than half of the chemical energy of a biomass, providing a performance that is better than what can be obtained by means of hydrolysis-based scheme [3]. Syngas is biodegradable and can be anaerobically converted to various target chemicals like hydrogen alcohols and VFAs [1]. The main issue related to syngas conversion is the low water solubility of CO and H_2 as well as the eventual presence of highly toxic contaminants (e.g. hydrogen cyanide or NO_x) [34], which are typically more relevant for gasification derived syngas [35]. HTB processing of WS, which is the most relevant bioavailable fraction of PyP, is severely less studied. Such mixture, whose composition is still under study, is made by VFA, anhydrosugars (AS), hydroxy acetaldehyde, polar phenols (e.g. di or tri-hydroxybenzenes), anhydro-oligosaccharides formed by cellulose ejection, humin, and hybrid oligomers formed by lignin and cellulose [36]–[38]. WS is bioavailable and partially biodegradable [39], [40], and selected fractions of WS (e.g. AS and VFA) were successfully converted with HTB schemes by several authors [13], [41]–[44] .

Whole WS can be converted to methane by anaerobic digestion in 55-76% yield [45], [46], and healthy microbial consortia can degrade most of the GC-MS detectable portion of WS [28], [47], [48].

The addition of biochar and the use of suitable microbial mixed consortia (hereafter called "*pyrotrophs*" [7]) allows to exploit syngas and a large portion of WS organics for the production of biochemical intermediates [51] [44]. In particular, whereas methanogenic activity could be selectively inhibited, *pyrotrophs* could be used to convert syngas/WS into VFA, which in turns can be used as chemical or biochemical building blocks for the production of several products [49].

To date, there is only one work for conversion of pyrolysis condensable compounds into VFA [50]. *Lemos et al.* fermented a solution of 11 gCOD L^{-1} (about 1% by weight) of pyrolysis liquid from fast pyrolysis of chicken beds; with 2 d of hydraulic residence time (HRT) at 30°C, 6.2 gCOD L^{-1}as VFA were obtained, corresponding to 54% yield and volumetric productivity equal to 3.1 gCOD L^{-1} d^{-1}. Such concentration and productivities of VFA were suitable for direct PHA production using MMC [51]. Therefore, the author tested a combined anaerobic-aerobic system, demonstrating a final yield of PHA of 19% and an overall volumetric productivity of 0.7 gCOD L^{-1} d^{-1}.

Besides the work of *Lemos et al.* [50], several works focused on WS biomethanation often reported a significant VFA accumulation in the system, even when biogas production was completely absent. *Torri and Fabbri* [44] and *Hübner et al.* [28] tested low-temperature WS from wood pyrolyzed at 400°C (at 35 gCOD L^{-1}) and digestate pyrolyzed at 330°C (at 30 gCOD L^{-1}) in a batch test for a long time, showing that such high concentrations inhibit the methane production, giving a significant acidogenic activity. In both cases, total VFA concentration increased during the process, suggesting a biological conversion of PyP into VFA. Although these studies were not optimized for VFA production, the overall VFA yields (29% and 41%, respectively) were significant, and the final concentration (about 10 gCOD L^{-1}) of VFA reached the level of self-inhibition of acidogenesis due to the toxicity of undissociated VFA. *Hübner et al*. [52] also tested a similar concentration of WS obtained at 420 and 530°C observing the inhibition of both methanogenic and acidogenic activity.

As a whole, the limited available literature suggests that it could be possible to convert WS into VFA, even if, at the best of the author's knowledge, continuous

conversion of WS into VFA was never demonstrated. This chapter aimed to fill this research gap by investigating the coupling of pyrolysis and fermentation to produce VFA. To demonstrate the reliability of such coupling, all the bioavailable PyP, namely syngas and WS, were provided to a packed bed biofilm reactor. Nonetheless, given the possible applications of clean syngas, the reactor was designed as a bio-filter and targeted to the conversion of WS, the less valuable part of pyrolysis products, into a broth rich in VFA.

As confirmed by several preliminary fermentation tests [53], the most challenging aspect of PyP fermentation is the strong inhibition arising from WS's phenols and furans. For this reason, a special attention was given to the WS, to investigate its acidogenic bioconversion capability in presence and absence of biochar material, as a detoxifying agent. To establish the system's performance and confirm the pyrotrophic activity, the biodegradation of pyrolysis products and the yield of fermentation intermediates (VFA, methane and other GC-MS detectable compounds) were quantified with two different acidogenic fermentation tests lasting 83 and 114 days. The effect of biochar addition, acclimatization and glucose-aided bioaugmentation was evaluated, highlighting the potential and pitfalls of converting WS into VFA.

3.2. Methodology

3.2.1. Pyrolysis Conditions

WS and syngas used for the experiments were obtained through intermediate pyrolysis of fir sawdust with a fixed bed pyrolizer (Figure 2.1), as detailed in the previous sections {Chapter 2.2}, yet without cyclone unit.

A series of sequential pyrolyzes were done prior to the fermentation experiments for obtaining substrate test materials. About 5 grams of dry biomass were pyrolyzed at intermediate pyrolysis conditions for 30 minutes residence time at each batch run of the pyrolysis reactor. Constant temperature (550 °C) was maintained in the horizontal lab-scale tubular furnace. About 10 L of Nitrogen gas (N_2) was initially provided, at 1 L/min rate for 10 min, to purge the air from the pyrolysis system. Subsequently all available gas was continuously recirculated by a peristaltic pump (at 100 mL/min flow-rate) to avoid dilution of the produced syngas components during the pyrolysis of

biomass. One impinger containing 50 mL of distilled water was connected and placed inside an ice-bucket to the outlet of the quartz reactor. In this way, nearly all water-soluble condensable part of pyrolysis products (i.e. APL) was collected inside the impinger (i.e. water trap) and distinguished from acetone-soluble pyrolytic lignin portion which was named as WI. A cotton trap was placed just after the water-trap to capture the fine aerosols. Gaseous pyrolysis products (syngas) were collected inside a laminated foil gasbag. The solid carbonaceous fraction (biochar) was collected at the end of each pyrolysis.

Biomass feedstock and all the PyP were analyzed to determine the COD content of each PyP and the overall balance. COD yields of PyP were varying from 14% to 35% for syngas, WS, water-insoluble (mostly pyrolytic lignin, PL), and biochar (Table 3.1). Syngas with a calculated COD of 440 (±55) mgCOD L^{-1}_{syngas} , obtained from the sequential batch pyrolysis (performed on weekly basis) were stored in laminated foil gas bags (Supel™ Inert Foil 1L) and the most abundant gas product was carbon monoxide (CO) with 31% average concentration (Table 3.1). A pre-portioned concentrated WS stock solution (194.8±4.8 gCOD L^{-1}) stored refrigerated (-20°C) and used throughout the long-term fermentation experiment. Being the WS an extremely complex mixture of chemicals [54], their full characterization was beyond the scope of this work, yet a detailed analytical characterization of the WS was carried out according to *Torri et al* [55] and shown in detail (Figure 3.2). WS molecular constituents, which were considered relevant for fermentation and/or were monitored during the experiment were: acetic acid (5.5%, as gCOD/$gCOD_{WS}$), hydroxy acetaldehyde (4.5%), levoglucosan (2.9%), mannosan (1.4%), ethanediol (0.8%), catechol (0.3%), 4-methyl-catechol (0.3%). The rest of non-quantified low molecular weight compounds (LMW<1.45 kDa) was presented as others in Figure 3.2.

Table 3.1: COD yields of PyP, composition of syngas, and WS concentration.

PyP Yields:	$\%_{COD}$	Syngas: 13.5% (±1) , WS: 34.5% (±5) , PL: 14.4% (±3) , Biochar: 35.4% (±2)
Syngas Constituents:	*v/v*	CO: 31% (±5) , H_2: 0.4% (±1) , CH_4 9% (±1) , CO_2: 16% (±6) , N_2: 43% (±5)
WS Concentration:	$gCOD\ L^{-1}$	194.8 (±4.8)

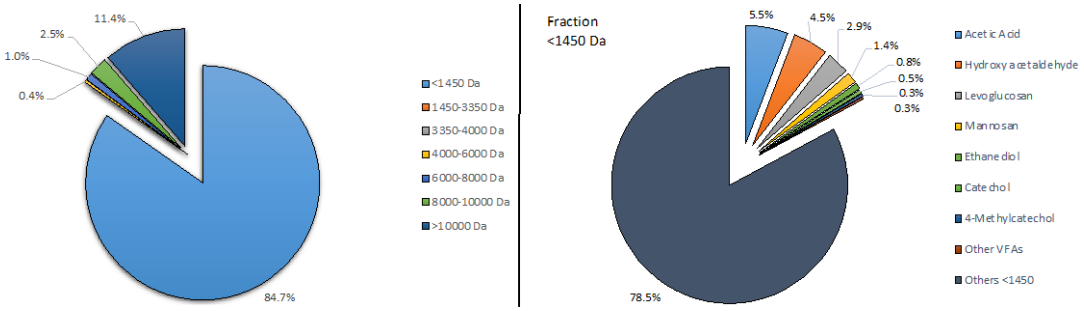

Figure 3.2: WS characterization: MW distribution by HPLC-SEC (left) and main GC-MS detectable compounds (right).

3.2.2. Tailor-made Char-bed Bioreactor System

Bioreactors are commonly used apparatuses generally equipped with several built-in specifications for the investigation of biological treatment studies. Each bioreactor test may require different types of specialty such as heating, agitation, re-circulation and some further technologies like online sensoring. Even though there are many ready-to-use fabricated bioreactors available in the market with a cost usually over than 1000 €, it is often not possible to access those advanced (but inflexible) systems for many students, young-researchers or small-scale private R&D companies. In this part of study, a new low cost (≈100€) packed-bed anaerobic bioreactor was developed, and all methodological details are shared. Some preliminary tests were conducted to verify the developed bioreactor system's credibility in terms of leak-tightness, accurate gas monitoring, temperature controlling, and mass balance (COD-eq) coverage, which all have shown a very promising performance.

Biofilm bioreactor technologies mainly provides a higher conversion yield because of a better interaction occurring between substrate material and the microbes [56]. This also provides a less-suspended, much clearer effluent as compared to slurry systems [57]. Sands, stones, ceramics and recently some polymeric materials have been commonly used as filtering media [56], [58]. However, there is a little attempt to use non-inert materials such as pyrolysis derived biochar, which have a great potential for stimulating biological activities with its unique porous structure [59]–[63].

The use of biochar in biological systems has recently started to be seen as a very promising and efficient strategy for enhancing the anaerobic microbial activity [64], [65]. Some of the main advantages of the application of charcoal-like pyrolysis derived biochar material, for enhanced anaerobic digestion by means of its unique physiochemical porous structure, are reported as; contribution to pH buffering [66],

mitigation of several inhibition phenomenon such as ammonia and VFA inhibitions [44], [67], [68], providing a faster start-up period by shortening the lag-phase duration [59], stimulating the substrate removal rate resulting in a better product (i.e. biogas) yield [69]. Although there are several promising reports about the use of biochar for anaerobic digestion (i.e. biomethanation) purposes are available in the literature, no attempt was found for the use of biochar material as a packing material for the more specific anaerobic biotechnology purposes such as acidogenic fermentation (VFA production), solventogenic bioreactions (e.g. bio-ethanol synthesis), anaerobic conversion of gaseous materials, or bio-utilization of unconventional substrates (e.g. aqueous pyrolytic liquid).

Single-board microcontrollers are known as easy-to-use and affordable digital controller systems. *Arduino* is one of the most widely known microcontrollers which is based on open-source Integrated Developing Environment (IDE). With its cost-competitive hardware tools and free-to-access software, *Arduino* can also serve as a very useful platform for digital controlling of special-made reactors for biochemical research purposes. The cost-benefits make this microprocessor widely affordable, even for quite complicated tasks such as the control of a lab-scale bioreactor. The main use of *Arduino* in chemistry is the field of automated bioreactor monitoring and datalogging (also known as "ChemDuino"), whereas is less frequently applied for bioreactors controlling [70], [71].

In order to investigate the anaerobic conversion of unconventional substrates (e.g., pyrolytic liquids, syngas) flexible, robust and easily customizable bioreactors are needed. That kind of bioreactors often require controlling of some operational parameters such as liquid/gas flow, temperature, and agitation etc. Besides, a real-time monitoring of the bio-chemical reactions (e.g., biogas production rate, pH monitoring etc.) are also substantial in most of the cases. Two main aspects were targeted by the tailor-made bioreactor development (hereinafter called also 'tetrapod'), which are relevant for that purpose; packed-bed bioreactor assembly that allow to obtain satisfactory mass and COD balance (1), and a simple real time controlling system by means of Arduino technology (2).

3.2.2.1. Design and Construction

Schematic diagram of the tetrapod bioreactor system is presented in Figure 3.3. Shortly, the bioreactor system consists of two parts:

i) Glass bottle part that is equipped with the heating system: A standard half-liter laboratory type of glass-bottle (i.e., duran bottle, pyrex glass-bottle) was used upside-down.

ii) Four-ported special-cap together with liquid recirculation pump: There are four ports available at the bottom for the purposes of gas injection, gas sampling, liquid sampling/injection, and liquid recirculation. This peculiar cap was the inspiration of the 'tetrapod' naming due to its appearance. The glass-mouth, the four screw-openings and the surrounding screw-caps were manufactured as water-tight materials by using silicone O-ring septa for each screw cap. Nonetheless, since bio-liquid fills the cap from inside, this avoids the risk of any gas leakage from the bottom. In this way gas molecules would stay in the top head-space which is the bottom of the glass-bottle where there is no leaking risk.

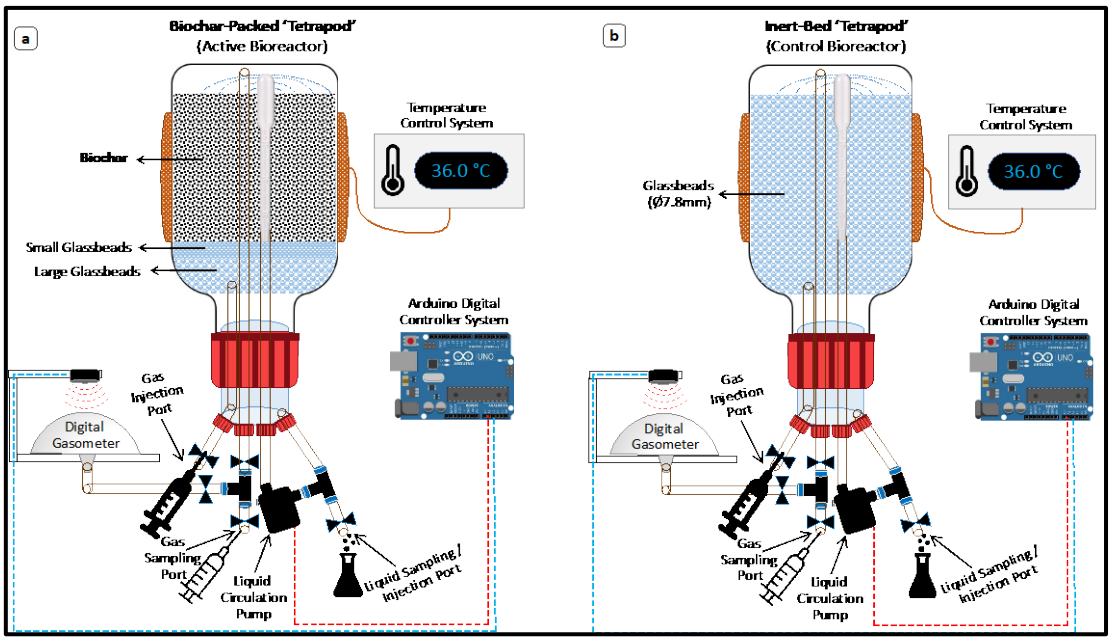

Figure 3.3: Schematic diagram of the tailor-made packed-bed bioreactor system: a) Biochar-packed bioreactor, b) Inert-bed bioreactor.

Two identical tetrapod bioreactors were assembled, but with different packing materials. First one with the coarse biochar packing material which will be called 'biochar-packed tetrapod' or active bioreactor. The latter is 'inert-bed tetrapod' (also control bioreactor) where glass beads were the only packing material. The control bioreactor with inert-bed was designed to evaluate the effect of biochar addition in terms of anaerobic bioconversion efficiency. Biochar used as packing material is a commercial charcoal provided by "Romagna Carbone s.n.c." (Italy) which was

obtained from orchard pruning biomass (apple, grapevine, pear, peach) with a slow pyrolysis process at 500°C and a residence time of 3h, in a kiln of 2.2m in diameter and holding around 2 ton of feedstock [72].

In anaerobic cultivation reactors, especially when involving the strict-anaerobes, it is very important to guarantee a perfect sealing all through the system to avoid any cross-contamination of gases. There are two main reasons for this; one is that anaerobic microbes are quite sensitive to oxygen exposure, and the second is to obtain a good mass and COD balance of the system. Preliminary tests showed that the main experimentally relevant issue of small-scale reactor is the air leakage, namely the input of air into the reactor without significant change into gas volume [53]. Without special devices and using standard approaches for anaerobic digestion tests, a COD loss mainly (but probably not only) due to O_2 permeation into silicon hoses, was found and estimated in almost 38 mL-d^{-1} of oxygen. Such phenomena, even if acceptable for short term anaerobic digestion of biodegradable substrates, is not acceptable for long term fermentation of PyP, in which long lag phases could increase the length of the study and, consequentially, the total COD loss. To fix the O_2 permeation issue, several mock tetrapod bioreactors structures were assembled, filled with hydrogen or helium (most penetrable gases), and tested for gas leaks through GC-TCD analysis of the headspace through time. Such tests provided some key hints to minimize leakages [53].

'Tetrapod' bioreactor was designed to have all joints and sealing submerged in water. This allows to easily detect any leaky joints and, thanks to low gas solubility in the liquid, to minimize permeation of gases through correctly sealed joints. Besides joints, the external hoses, connectors, and sampling valves revealed to be a large source of minor leaks due to gas permeation and relatively high surface area (given small reactor volume), and therefore were improved to obtain a perfectly gas-tight conditions. For this purpose:

- All the external equipment was connected by quick-connect pneumatic connectors which are well-used gas-tight systems for industrial purposes. All the connection adapters and the sampling valves were quick-connect pneumatic fittings (⌀ 6 mm) which showed a good barrier performance.
- Tubing was performed with laminated hoses, which were manufactured by wrapping an aluminum foil onto polyamide hose (⌀ 6mm OD) using silicone as layer binder and final coating (Figure 3.4).

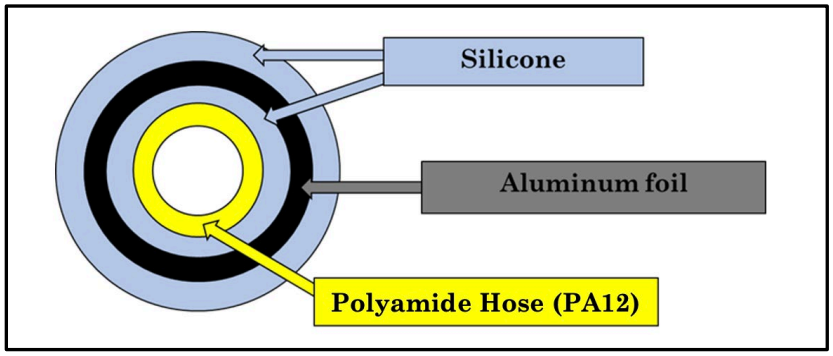

Figure 3.4: Cross-section view of upgraded hose for minimizing leaks.

Liquid recirculation and sampling: It is important to ensure the homogeneity of packed-column bioreactor for keeping the bio-filter media wet, which is vital for the attached-growth microbes. Moreover, in order to allow the contact between biofilm and gases, the packed-column pores should not be permanently filled with liquid. It follows that, given the variable hydraulic conductivity of packed column, overflowing of bioliquid above the filter media is also another critical point to be avoided. For this reason, a regulatable pulsed mode of water recirculation system was applied for the 'tetrapod' bioreactor. An Arduino based script allows the submersible-type mini pump to work for adjustable time, with a flow capacity of 240 L/hr. Therefore, circumventing somewhat difficult procurement of a pump with specific discharge rate, which in turn depends on the hydraulic conductivity of filling media.

The mini pump was connected to a hose through the same multilayer approach. First the hose was fitted to the pump, thereafter a silicone layer was applied to seal the two parts. To prevent any acetic acid contamination, usually presented in silicone paste, the system was left working with water overnight. Then, all the acetate-contaminated washing-water was discharged.

The sprinkling system at the top of filter bed was built using a modified plastic Pasteur pipette. Pipette filler was used as a terminal part of the recirculation system. The opposite part (tip) was firstly cut to remove the narrowing needle part, then connected to a hose and fixed with a cable tie. On the pipette filler, holes with ≈ 2.0mm diameter were made with a hot soldering needle in a symmetric distribution that allows a homogenous liquid distribution to all directions. The size of the holes was tuned in order to force the liquid to spread onto entire packed bed and to avoid clogging with entrained particles.

Bio-liquid samplings were made by using disposable plastic syringes via 'liquid sampling port' equipped with a quick-connect pneumatic valve. The liquid port was placed just before the water-pump for sustaining a well-mixed liquid sampling.

Gas feeding, off-gasses volume measurement, and gas sampling: Available off gasses were removed at each operational day by graduated gas-tight disposable syringes and total amount in terms of milliliters (mL) were recorded.

Gas samplings throughout the experiments were made using a quick-connect valve of the 'gas sampling port' by using graduated disposable syringes which allow withdrawal of a known amount of gas sample. Prior to each gas sampling, all available headspace gas and gasbag gas was mixed by using sampling syringe. Such operation allowed a better homogenization between the gasbag and the headspace of the reactor, providing a much representative gas sample of the whole system.

Only for the PyP co-fermentation experiment where pyrolysis originated syngas were also used as a co-substrate, syngas feedings were made by the graduated syringes at each operational day.

Temperature control system: Heating and temperature control system were developed to operate the bioreactor at desired mesophilic temperature range (34-38 °C). The heating system consists of two elastic resistance pads placed on the walls of the bioreactor bottle, a thermocouple fixed to the liquid recirculation hose, and a digital thermostat that provides power to the resistances depending on the measured temperature value. The digital thermostat had a 0.1 °C level of sensitivity for adjusting the set temperature level. Moreover, a folding thermal jacket (made by aluminum foil) was placed to cover the entire walls of the glass bottle for sustaining a constant and homogeneous distribution of temperature in the packed-bed reactor.

3.2.2.2. Experimental set-up

Two identical tetrapod bioreactors were filled with different packing materials, as mentioned before (Figure 3.3). Table 3.2 provides all set-up details of the assembled tetrapod bioreactors. The inert-bed control reactor was filled with 480g (dry-weight) of large glassbeads with 8mm outer diameter (OD) (Figure 3.5), which corresponds to ≈305 (± 15) mL net filter-bed volume in total. The active bioreactor was packed with biochar, which was supported onto two layers of different size of glassbeads. To prevent biochar entraining into recirculation flow, 325 g of small glassbeads with 4mm OD were layered below biochar and, 200g of large glassbeads (OD 8mm), below them.

The multilayer glassbead media as a retainer for the upper biochar-media part, was corresponding around 205mL net occupied volume and the rest filter-bed volume was occupied by coarse biochar materials.

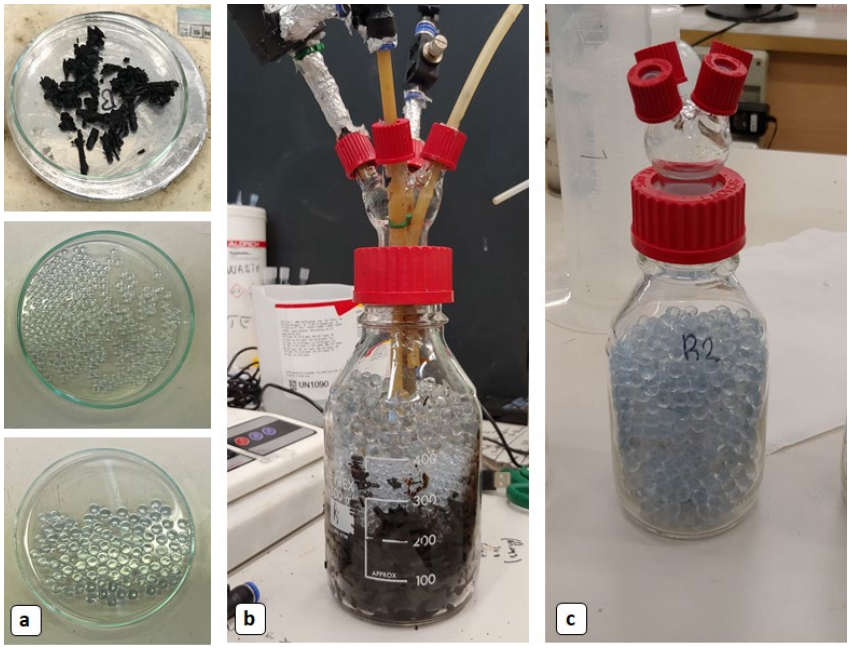

Figure 3.5: a) Packing materials, b) Biochar amended tetrapod, c) Inert-bed tetrapod.

Table 3.2: Set-up parameters of the bioreactor system for PyP fermentation.

Parameters / Details	**Biochar-Packed (Active) Bioreactor**	**Inert-Bed (Control) Bioreactor**
Reactor Type	Anaerobic Packed-Bed Bioreactor	Anaerobic Packed-Bed Bioreactor
Filter Type	Carbonous Porous Media	Non-porous Inert Media
Packing Material(s)	Coarse Biochar + Small Glassbeads + Large Glassbeads*	Large Glassbeads
Packing Ratios (V:V)	36% + 40% + 24%	100%
Operating Temperature	36 °C ± 2	36 °C ± 2
Liquid Recirculation Rate	220 L/hr	220 L/hr
Reactor Total Volume	620 mL	620 mL
Filter-Bed Volume	≈ 305 ± 15 mL	≈ 305 ± 15 mL
Liquid Volume	200 mL	200 mL
Headspace Volume	≈ 115 ± 15 mL	≈ 115 ± 15 mL
Biochar Amount	100 g (in wet basis**)	n/a

** Grain diameters of the glassbead filter medias were; Ø7.8mm for large ones, and Ø4.0mm for small ones. ** Biochar water content was 69% (M:M).*

Assembling of tetrapods was made following a restricted procedure that allows to set-up the bioreactor in the best configuration possible for gas and liquid recirculation. Firstly, keeping the bottle vertical, the gasbag tube connector and liquid recirculation tube with the modified Pasteur pipette, were inserted in the central part of the half-liter sized bottle. Thereafter, biochar, small glassbeads, and big glassbeads were added for the biochar packed tetrapod. For the control reactor, all big glassbeads were added in one time. The addition of all layers allowed to fix the long tubes previously inserted. Tubes had to be longer than the bottle itself, so that after the connection of the special cap, there should be a residual outside part for connecting all the necessary external equipment (pump and external gasbag). After this step, the specially-designed screw cap was sealed to the bottle. The special cap was designed with four small ports on the external side and with a restricted neck at inside part. This restriction allowed to avoid falling down of filter media grains (glassbeads) into the internal side of the four-small ports. The four small-caps were removed to facilitate the passing of the pipes through the holes, and later re-connected. The last two pipes of the tetrapods, for pump input and gas injection port were connected at the end. The gas input pipe should enter some millimeters inside the big glassbeads layer if possible. The pump input pipe, instead, must enter as short as possible inside the cap, in order to avoid dead volumes. Finally, caps were completely sealed, and the pump was connected to the recirculation system. Before to connect the external gasbag, assembled tetrapod must firmly be turned upside down, allowing the inside layer to maintain the exact order needed. After the bioreactor was fixed into a stable support in upside down position, gasbag and heating system were attached.

Pictures were taken from the start-up of the first anaerobic experiment conducted in the assembled tetrapod system. Figure 3.6.a shows the clean biochar-packed bioreactor on the left and clean inert-bed bioreactor on the right, prior to the operation. In Figure 3.6.b, one of the tetrapods was recently inoculated and started an anaerobic test. After the start-up, the tetrapod was covered by the thermal-jacket to keep the bioreactor in a more standardized temperature condition (Figure 3.6.c).

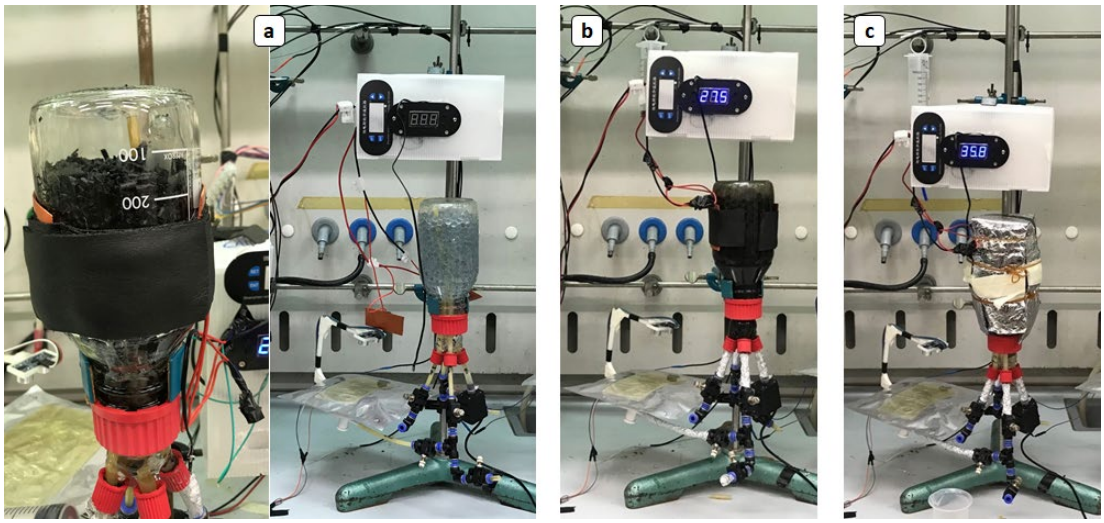

Figure 3.6: Operational start-up steps: a) Before operation; biochar packed at left, inert-bed on right, b) Freshly inoculated, c) On-going with a thermal jacket.

3.3. Operational Start-up

Packed-bed bioreactors were previously inoculated during the preliminary tests [53] with a digestate from an industrial anaerobic digester treating mainly grape pomace, distillery stillage and wastewater treatment sludges (supplied by Caviro Extra S.p.A., Faenza, Italy). The inoculum was a suspension with the following characteristics: pH 7.8, total COD 78.7 ± 0.7 gCOD L^{-1}, and suspended COD 74.0 ± 0.7 gCOD L^{-1}. A modified cultivation medium was prepared based on *Temudo et al.* [73] (Table 3.3). Nutrient supplementation was provided by assuming an average 5% microbial growth yield ($gCOD_{growth}/gCOD_{WS}$) and a C:N:P ratio of microbial biomass of 100:5:1. The equation used for estimating the required medium amount is provided in the subsequent section together with all the other formulations that have been used in this part of thesis study.

Table 3.3: Anaerobic basal medium.

Chemical Compounds	**Molecular Formula**	**Concentration** (g/L)
Ammonium chloride	NH_4Cl	13.425
Potassium dihydrogen phosphate	KH_2PO_4	7.815
Sodium chloride	NaCl	2.919
Sodium sulfate decahydrate	Na_2SO_4-$10H_2O$	0.573
Magnesium chloride hexahydrate	$MgCl_2$-$6H_2O$	1.201
Ferrous sulfate heptahydrate	$FeSO_4$-$7H_2O$	0.031
Calcium chloride	$CaCl_2$	0.006
Tri-tert-butyl borate	$H3BO_4$	0.001
Sodium molybdate dihydrate	Na_2MoO_4-$2H_2O$	0.001
Zinc sulfate heptahydrate	$ZnSO_4$-$7H_2O$	0.032
Cobalt (II) chloride monohydrate	$CoCl_2$-H_2O	0.009
Copper (II) chloride dihydrate	$CuCl_2$-$2H_2O$	0.022
Manganese (II) chloride tetrahydrate	$MnCl_2$-$4H_2O$	0.025
Nickel (II) chloride hexahydrate	$NiCl_2$-$6H_2O$	0.005
EDTA	$C_{10}H_{16}N_2O_8$	0.500

3.3.1. Formulas and Calculations

In this part all the calculation methods used in this part of study (namely, PyP Fermentation) will be explained in detail with corresponding formulas. Each equation will be followed by its unit-based formulation with italic letters to provide a clear presentation. First formula is related to medium concentration level calculation:

$$20.0\,\frac{\text{gCOD}}{\text{Liters}}\ \text{x}\ \frac{15\ \text{gCOD Microbial Mass}}{100\ \text{gCOD}}\ \text{x}\ \frac{5\ \text{g Nitrogen}}{100\ \text{g Microbial Mass}} = \frac{0.15\ \text{g Nitrogen}}{L}$$

$$\frac{0.15\ \text{g Nitrogen}}{L}\ \text{x}\ 53.5\ \frac{\text{g NH}_4\text{Cl}}{\text{mole NH}_4\text{Cl}}\ \text{x}\ \left(14.0\ \frac{\text{g Nitrogen}}{\text{mole NH}_4\text{Cl}}\right)^{-1} = \frac{0.57\ \text{g NH}_4\text{Cl}}{L} \qquad (3.1)$$

$$\frac{0.57\ \text{g NH}_4\text{Cl}}{L}\ \text{x}\left(13.425\ \frac{\text{g NH}_4\text{Cl}}{\text{Liters medium}}\right)^{-1} \cong \frac{42.5\ \text{mL Medium}}{L}$$

HRT of the continuous reactor operation was calculated as follow, where [V_{Liq}] corresponding the total wet-volume (i.e. active volume) of the bioreactor set-up, and [Q_{Liquid}] as the daily liquid feeding/discharging rate:

$$\mathrm{HRT} = \frac{V_{Liq}}{Q_{Liquid}} \quad \left| days = \frac{mL}{\frac{mL}{day}} \right| \tag{3.2}$$

Organic loading rate (OLR) were calculated as follow, where [COD_X] as the measured COD concentration of each substrate material and [%X] as the substrate ratio depending on the feeding regime.

$$\mathrm{OLR} = \left[(\mathrm{COD_{WS}} \times \%_{\mathrm{WS}}) + (\mathrm{COD_{GLU}} \times \%_{\mathrm{GLU}}) + (\mathrm{COD_{CH_4}} \times \%_{\mathrm{CH_4}})\right] \times (HRT)^{-1}$$

$$\frac{gCOD}{L \cdot day} = \left[\left(\frac{gCOD}{L} \times \%\right) + \left(\frac{gCOD}{L} \times \%\right) + \left(\frac{gCOD}{L} \times \%\right)\right] \times (days)^{-1} \tag{3.3}$$

COD concentration of the gas input (syngas) and gas output (biogas) were calculated as follows, where [COD_{GAS}] as the overall COD concentration of the gaseous mixture, [C_X] as the percent concentrations of each gas component measured by GC-TCD, and [COD_X] as the COD constant of each gas component in g-COD/L unit (e.g. H_2: 0.71, CO: 0.71, CH_4: 2.85).

$$\mathrm{COD_{GAS}} = \left(\mathrm{C_{H_2}} \times \mathrm{COD_{H_2}}\right) + \left(\mathrm{C_{CO}} \times \mathrm{COD_{CO}}\right) + \left(\mathrm{C_{CH_4}} \times \mathrm{COD_{CH_4}}\right)$$

$$\frac{gCOD}{L} = \left(\% \times \frac{gCOD}{L}\right) + \left(\% \times \frac{gCOD}{L}\right) + \left(\% \times \frac{gCOD}{L}\right) \tag{3.4}$$

Total COD concentration of VFAs in the WS and fermentation effluents were calculated by below equation, where [COD_{VFA}] as the overall COD concentration of the liquid sample, [C_X] as the concentration of each VFA component measured by GC-MS, and [COD_X] as the COD constant of each VFA component in g-COD/g unit (e.g. Acetic: 1.1 , Propionic: 1.5 , Caproic: 2.2).

$$\mathrm{COD}_{VFA} = \left(\mathrm{C_{Acetic}} \times \mathrm{COD_{Acetic}}\right) + \left(\mathrm{C_{Propionic}} \times \mathrm{COD_{Propionic}}\right) + \cdots$$

$$\frac{gCOD}{L} = \left(\frac{g}{L} \times \frac{gCOD}{g}\right) + \left(\frac{g}{L} \times \frac{gCOD}{g}\right) + \cdots + \left(\frac{g}{L} \times \frac{gCOD}{g}\right) \tag{3.5}$$

Total input [M_{In}] values were calculated by following equation, where [$t_{Experiment}$] represents the total duration (time) of the experiment, and [Σt_{Batch}] corresponds the duration of the batch mode operation when no feeding was provided to the bioreactor:

$$\mathrm{M}_{IN} = \left[\mathrm{OLR} \times \left(t_{Experiment} - \sum t_{Batch}\right)\right]$$
$$gCOD = \left[\left(\frac{gCOD}{L-day}\right) \times \left(days - \sum days\right)\right] \quad (3.6)$$

Total output [M_{Out}] value which is corresponding the sum of the removal of both gas and liquid materials in line with the principle of continuous operation were calculated by the following equation**.** [$C_{Liq\text{-}Out}$] is the measured COD concentration of the effluent liquid and [$V_{Liq\text{-}Out}$] is the amount of discharged liquid at its corresponding day, while [$C_{Biogas\text{-}Out}$] as the measured concentration of the bioreactor system's off-gas and [$V_{Biogas\text{-}Out}$] is the total volume of the discharged gas on that day.

$$\mathrm{M}_{OUT} = \sum\left[\left(C_{Liq-Out} \times V_{Liq-Out}\right) + \left(C_{Biogas-Out} \times V_{Biogas-Out}\right)\right]$$
$$gCOD = \sum\left[\left(\frac{gCOD}{L} \times L\right) + \left(\frac{gCOD}{L} \times L\right)\right] \quad (3.7)$$

COD recovery as an indicator parameter is included to the calculations for showing the COD balance efficiency of the experiment which takes into account of 'Total Input' and 'Total Output' parameters. Given the fact that the COD trapped inside the packed-bed was not monitored, this definition does not fully correspond the total COD balance, yet it still provides beneficial information about the recovered overall materials in terms of COD.

$$\text{COD Recovery} = \frac{\mathrm{M}_{OUT}}{\mathrm{M}_{IN}} \mathrm{x}\ 100$$
$$\% = \frac{gCOD}{gCOD} \times 100 \quad (3.8)$$

Daily net VFA [L_{VFA}] production has found a critical monitoring parameter by the authors, since it provides a direct tool to observe the target products' productivity and estimated by the following equation. In the formula, [$Cvfa_T$] represents the current

(last) measured COD-eq VFA concentration, [$Cvfa_{T-1}$] is the one previous VFA measurement and [$V_{Effluent}$] is the discharged amount of liquid from the bioreactor which is basically based on the HRT.

$$L_{VFA_{DAY-T}} = \left[\left(V_{Liq} \times \left(C_{VFA_T} - C_{VFA_{T-1}}\right)\right) + \left(C_{VFA_{T-1}} \times V_{Effluent}\right)\right]$$
$$\frac{gCOD}{day} = \left[\left(L\left(\frac{gCOD}{L} - \frac{gCOD}{L}\right)\right) + \left(\frac{gCOD}{L} \times L\right)\right] \quad (3.9)$$

Total produced net VFA [M_{VFA}] amount is also estimated for each set or phase of experiment to calculate further critical parameters such as VFA productivity and VFA yield. This defined parameter is calculated by following the next equation.

$$\mathrm{M}_{VFA} = \sum\left[\left(L_{VFA_{DAY_1}}\right) + \left(L_{VFA_{DAY_2}}\right) + \cdots + \left(L_{VFA_{DAYn}}\right)\right]$$
$$gCOD = \sum\left[\left(\frac{gCOD}{day}\right) + \left(\frac{gCOD}{day}\right) + \cdots + \left(\frac{gCOD}{day}\right)\right] \quad (3.10)$$

Volumetric productivity [V_P] is defined directly based on the net VFA production and estimated by the following equation.

$$\mathrm{Q}_P = \frac{\mathrm{M}_{VFA}}{t_{Experiment} \times V_{Liq}}$$
$$\frac{gCOD}{L - day} = \frac{gCOD}{day \times L} \quad (3.11)$$

One another critical parameter for the performance evaluation of the target products is the net VFA yield [ε_{VFA}] which is calculated by this following equation.

$$\varepsilon_{VFA} = \frac{\mathrm{M}_{VFA}}{\mathrm{M}_{OUT}} \times 100$$
$$\% = \frac{gCOD}{gCOD} \times 100 \quad (3.12)$$

Formulas related to overall COD mass balance estimations will be presented in the following equations. Total adsorbed organic material [A] in terms of COD was

based on a measurement. It is simply calculated by the total COD mass detected by subsequential dual washing of packing-bed with excess amount of distilled water (3.13). While microbial growth [l] is a hypothetical estimation value, defined by the difference between the total input and the sum of total output and adsorbed material (3.14). Lastly, another hypothetic parameter was defined to estimate unreacted portion (ω) of substrates (3.15).

$$A = (\mathrm{C_{Wash1}} \times \mathrm{V_{Wash1}}) + (\mathrm{C_{Wash2}} \times \mathrm{V_{Wash2}})$$
$$gCOD = \left[\left(\frac{gCOD}{L} \times L\right) + \left(\frac{gCOD}{L} \times L\right)\right] \quad (3.13)$$

$$l\ (\mathrm{gCOD}) = M_{IN} - (M_{OUT} + A)$$
$$gCOD = [gCOD - (gCOD + gCOD)] \quad (3.14)$$

$$\omega\ (\mathrm{gCOD}) = \sum (C_{Liq-Out} \times V_{Liq-Out}) - M_{VFA}$$
$$gCOD = \sum \left[\left(\frac{gCOD}{L} \times L\right) + \left(\frac{gCOD}{L} \times L\right)\right] - gCOD \quad (3.15)$$

3.4. Analytical Methods

3.4.1. Chemical Analysis

The pH of liquid materials was conducted with a bench type multiparameter device (SI Analytics, Lab 845). Liquid samples were centrifuged at 5000 rpm for 10 minutes prior to the chemical analysis, namely COD, VFA, silylation and HPLC-SEC, by following the procedures described in the previous section {Chapter 0}. Likewise, gas components were analyzed by the same GC-TCD procedure.

3.4.2. DNA Extraction, Microbial Analysis (16S rRNA) and SEM

At the end of each set of experiments, packed-bed bioreactors were rinsed with an excess amount of distilled water two times and all the washing liquid was collected. Subsequently, the washing liquids were centrifuged for 15 min at 5000 RPM, the

supernatant was discharged, and the precipitated sludge was collected. Additionally, the packing materials (biochar and glass bead) of the bioreactors were recovered at the end of the co-fermentation experiment. All microbial samples (sludge and packing material) were freeze-dried at -65 °C and 1.0 mbar vacuum conditions before the biological assays and scanning electron microscope (SEM) analysis. Biochar samples were gold-coated before to SEM and photographed by Philips XL30S-FEG.

Total DNA was extracted from 500 mg of freeze-dried samples using the DNeasy PowerSoil Kit (QIAGEN, Hilden, Germany) following the manufacturer's instructions with a slight modification, homogenization step was performed in a FastPrep instrument (MP Biomedicals, Irvine, CA, United States) by three 1-min steps at 5.5 movements per sec. Total DNA was quantified by using NanoDrop ND-1000 (NanoDrop Technologies, Wilmington, DE) and 25 ng was used for the amplification step of the V3-V4 hypervariable region of the 16S rRNA gene using the 341F and 785R primers carrying Illumina adapter overhang sequences [74]. Briefly, the thermal cycle consisted of initial denaturation at 95°C for 3 min, 25 cycles of denaturation at 95°C for 30 s, annealing at 55°C for 30 s and an elongation step at 72°C for 30 s, and a final elongation step at 72°C for 5 min. PCR products were purified by using Agencout AMPure XP magnetic beads (Beckman Coulter, Brea, CA) and Nextera Technology was used to prepare indexed libraries by limited cycle PCR reaction. After a further clean-up step as described above, libraries were normalized to 4 nM and pooled. The samples pool was denatured with 0.2 N NaOH and diluted to a final concentration of 6 pM with a 20% PhiX control. Sequencing was performed on Illumina MiSeq platform using a 2 x 250 bp paired end protocol, according to the manufacturer's instructions (Illumina, San Diego, CA).

Raw microbial sequences were processed using a pipeline combining PANDASEQ[75] and QIIME2 [76]. High-quality reads, obtained by a filtering step for length (min/max = 350/550 bp) and quality with default parameters in QIIME2, specifically, reads with an expected error per base E = 0.03 (i.e., 3 expected errors every 100 bases) were discarded, based on the phred Q score probabilities. The resulted reads were clustered into Amplicon Sequence Variants (ASVs) using DADA2[77]. Taxonomy was assigned using the VSEARCH algorithm[78] against SILVA database [79]. All the sequences assigned to eukaryotes (i.e., chloroplasts and mitochondria) or unassigned were discarded. Microbial compositional analysis was performed using the R Software.

3.5. Results and Discussion

3.5.1. WS Mono-Substrate Fermentation

As mentioned in the introduction and confirmed by several preliminary fermentation tests, the most challenging part aspect of PyP fermentation is the strong inhibition arising from WS's phenols and furans [44], [53]. For this reason, in this set of experiments, WS was used as a solo substrate material to investigate its acidogenic bioconversion capability in presence of biochar (Active Reactor) and without biochar (Control Reactor), under a semi-controlled pH conditions (Figure 3.8).

To investigate the effect of lower OLR on the inhibition effect (Table 3.4), the influent concentration level [$C_{SUBSTRATE}$] was kept constant at 5 g-COD/L during the whole test, while decreasing OLR from 0.50 to 0.25 g-COD/L-day in the 2nd half of the test (Phase II). Each phase of the tests has ended up with a batch period which is shown on the profile graphs. Consequential to the complete inhibition of MMC, detected as accumulation of GC-MS detectable WS constituents, the fermenters were switched to batch mode phases until complete levoglucosan biodegradation was back detected.

Table 3.4: Operational conditions adopted in the WS fermentation experiment.

Parameters	**Units**	**Control Reactor**		**Active Reactor**	
		Phase I	Phase II	Phase I	Phase II
$C_{SUBSTRATE}$	*g-COD/L*	5,0		5,0	
OLR	*g-COD/L-day*	0,50	0,25	0,50	0,25
HRT	*days*	10,0	20,0	10,0	20,0
Operational Time	*days*	52	31	38	45

First weeks of operation at the active reactor, total VFA were found quite stable over 4 gCOD-L^{-1}. However, a possible inhibition related to WS constituents was occurred and VFA values approximately halved. Whenever the continuous feeding has stopped and the first batch mode started after the 3rd week of continuous operation, VFA values were started to increase back and reached to the 3 gCOD-L^{-1} (Figure 3.7).

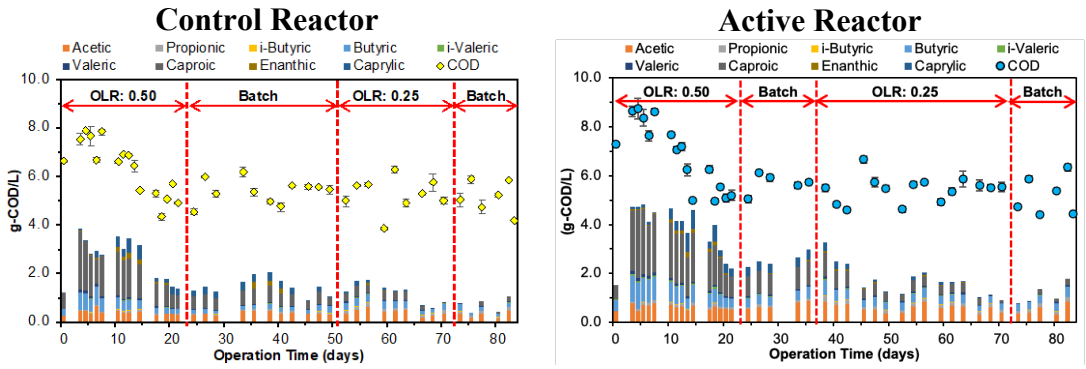

Figure 3.7: VFA and COD profile of WS fermentation effluents.

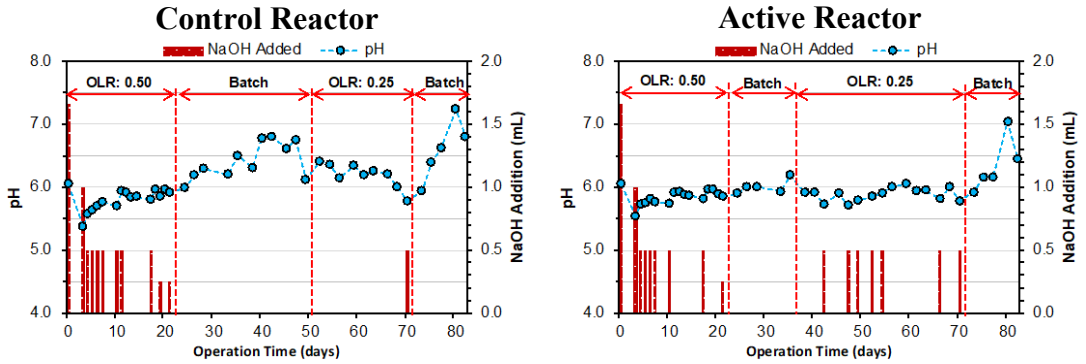

Figure 3.8: Alkaline additions and pH profile of WS fermentation effluents.

In the meantime, all the available levoglucosan content was completely degraded in a very short time (Figure 3.10). This was showing that inhibition of MMC due to the WS's components was not irreversible. Later on, HRT was doubled from 10 days to 20 days with the same feeding concentration, meaning that OLR was halved. Interestingly, VFA values have started to decrease again immediately after, even though the levoglucosan and mannosan levels were still quite low which was indicating a continuous uptake of the WS molecules. This phenomenon might be explained by another reason rather than inhibition by WS components, which could be the insufficient nutrition amount due to the extremely low OLR. A clear outcome is, lowering the OLR can be a solution of inhibitory effects of WS, yet is not productive.

Daily positive net CO_2 amounts throughout the experiment were implying that microbial respiration was active always (Figure 3.9), although some days were minimal.

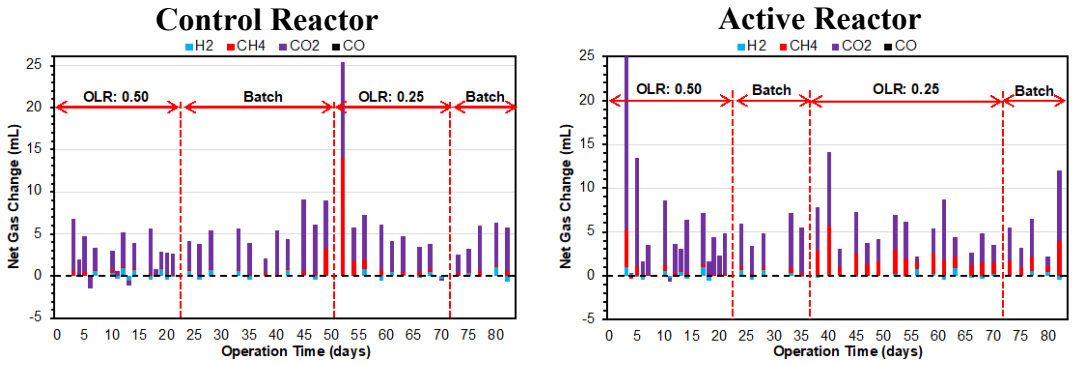

Figure 3.9: Produced and consumed net gas amounts at WS fermentation test.

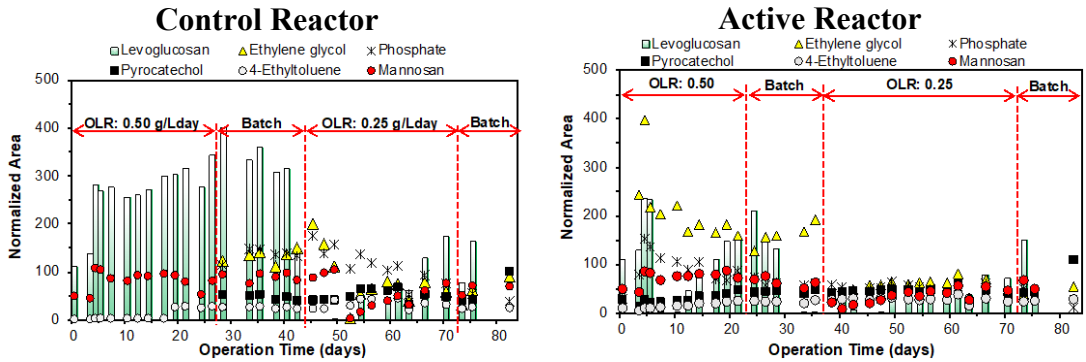

Figure 3.10: Effluent profile of the selected PyP molecules via silylation analysis.

In case of the experiments without biochar (control), a similar situation was observed in terms of general trend of overall VFA amounts. However, considerably lower VFA values were monitored throughout the experiments as compared to active reactor (Figure 3.7). In addition, levoglucosan levels were higher during Phase-I with higher OLR. In contrast to the active reactor detoxification of MMC appearing in the control reactor has taken longer times during the first batch period (Figure 3.10). In Table 3.5, COD based estimations were presented to reveal an overall performance of the mono-substrate tests. COD recovery parameter (3.8) was found critical for this closed loop anaerobic system where all input and output materials should be identical in terms of total COD since there is no oxidative agent that can consume COD. In this matter, both tests were shown an extraordinary performance and resulted in COD recoveries over 95%. In case of VFA production performances, active reactor with biochar has ended up with a double V_P and considerably higher ε_{VFA} values.

The efficacy of biochar as packing material for WS fermentation was verified by this WS mono-substrate fermentation tests (Figure 3.11). Biochar-packed reactor resulted more effective and less prone to intoxication than the glass balls packed

reactor, nonetheless, MMC could not address a continuous WS biodegradation at a significant level without inhibition (>0.25 gCOD/L-d). The inhibition was reversible with a total recovery of the process, testified by the disappearance of the main pyrolysis products (e.g. levoglucosan) after the stop of WS addition. The microbial inoculum could grow on PyP, therefore it contained pyrotrophic microbes [7], which are positively influenced by biochar interaction, but the inhibition of biological activity occurred at a lower OLR than that demonstrated for stable biomethanation with a similar WS substrate [44]. These observations suggest a key role in the combined toxicity of WS and acidogenic fermentation products (namely, VFA) and imply that the amount of VFA tolerant *pyrotrophs* should be drastically increased to obtain an acceptable volumetric productivity.

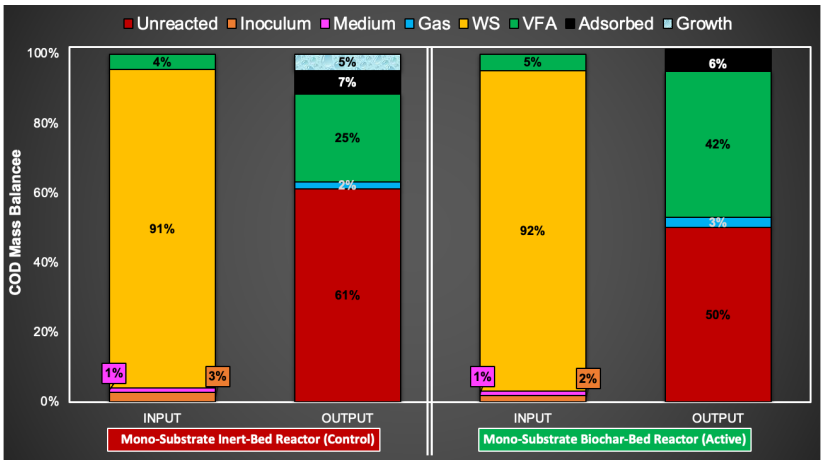

Figure 3.11: Overall COD balance by percentage for mono-substrate tests.

Table 3.5: Overall balances and product yields of WS mono-substrate test.

Parameters	**Units**	**Control Reactor**		**Active Reactor**	
		Phase I	Phase II	Phase I	Phase II
Total Input [M_{IN}]	*gCOD*	3,0	1,1	3,0	1,8
Total Output [M_{OUT}]	*gCOD*	2,8	1,1	2,8	2,0
COD Recovery	*%*	95%		101%	
Produced VFA [M_{VFA}]	*gCOD*	1,0		2,0	
VFA Productivity [V_P]	*gCOD-L^{-1}-day^{-1}*	0,06		0,12	
VFA Yield [ε_{VFA}]	*%*	27%		41%	

3.5.2. PyP Co-Fermentation Experiment

To increase the VFA tolerating *pyrotrophs*, a gradual bioaugmentation approach based on glucose/WS co-feeding and pH control was followed. Ideal pH condition for acidogenic fermentation is known to be between 5.0 – 6.5 and lowering pH has a negative impact on cell growth [80], [81]. For this reason, target pH value was 6.0 (Figure 3.13) for this test aiming to firstly enrich a VFA tolerant MMC consortium and then select/acclimatize the *pyrotrophs* without the early intoxication phenomena observed for WS fermentation. Finally, to create a selective pressure towards a complete pyrotrophic MMC, syngas rich in CO (as an additional inhibitor) was added to the reactor headspace, providing a constant input of about 10% of the input COD. The operational conditions including the OLR (1.0 gCOD L^{-1} d^{-1}) were kept constant throughout the experiment except for the input ratio between the co-substrates. Different ratios of input materials were applied in six sequential operational phases with a gradual increase in WS/glucose ratio. The biochar-packed bioreactor was operated in continuous mode operation with 20 days of HRT, except for a short period (hereinafter batch period) between the 11^{th} and 18^{th} days when the feeding was stopped.

3.5.2.1. Phase I (GLU 75% : WS 15%)

Minimal biological activity was observed during the first 15 d of the experiment, afterwhile a sharp increase in acetic acid concentration was observed (Figure 3.12) together with a large production of CO_2 and a detectable CO consumption. The delay at the beginning of the fermentation was comparable to the typical lag phase observed in presence of WS [44], even if the stop in feeding between day 11 and day 18, which was due to operational issues, could have triggered the fermentation start, as previously observed in WS mono-substrate fermentation tests (Figure 3.10). After the stop in feeding, acidogenesis improved over time, with VFA concentration that linearly increased from 3 to 7.5 gCOD L^{-1}. At the beginning of the experiment, acetic acid was the main VFA, while after 25 days butyric, propionic and valeric acids were higher. The final amounts of acetic, propionic, butyric, valeric and caproic acids at day 32 were 1.9, 0.8, 3.4, 1.2, and 0.2 gCOD L^{-1} respectively.

Glucose and levoglucosan had a similar trend in the first phase of fermentation. Both started to be consumed after 15 days, gradually (glucose) or instantaneously

(levoglucosan) reaching negligible concentrations in output solution. Mannosan, the main marker of hemicellulose pyrolysis, was consumed a few days later than levoglucosan and glucose, reaching a negligible amount in the solution in output on day 25 (Figure 3.14). This finding suggested a similar degradation rate for all hexoses.

Ethanediol, a compound that can be formed during hydroxy acetaldehyde fermentation [82], had a quite peculiar trend, with a gradual increase during the lag phase, followed by a sharp peak within the beginning of the acidogenic activity and a drop similar to that observed for sugars. Such a trend was similarly observed for phosphate, suggesting that both compounds can be considered as markers for MMC activity, which was characterized by an incomplete adaptation during the initial phase of WS degradation. The concentration of WS derived from lignin (catechol and 4-methylcatechol) slightly increased along with the WS input, suggesting an incomplete degradation of phenolics.

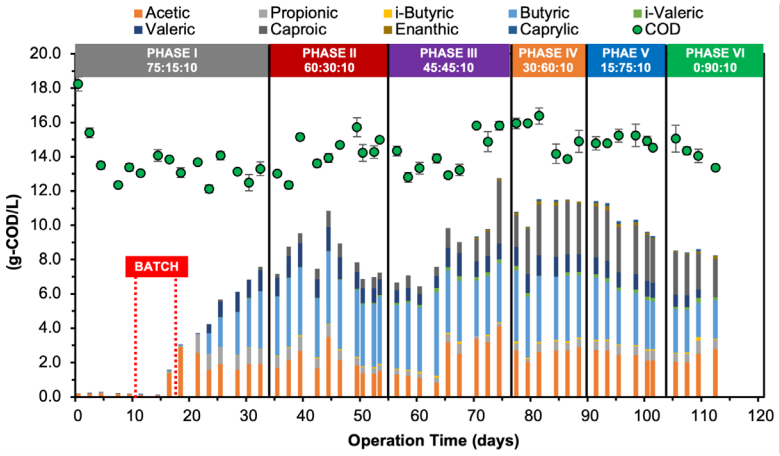

Figure 3.12: VFA and COD profile of the co-fermentation effluents.

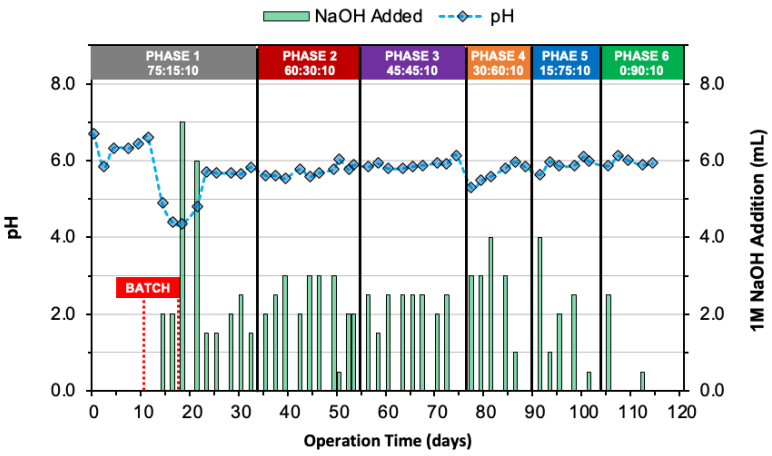

Figure 3.13: Alkaline additions and pH profile of the co-fermentation effluents.

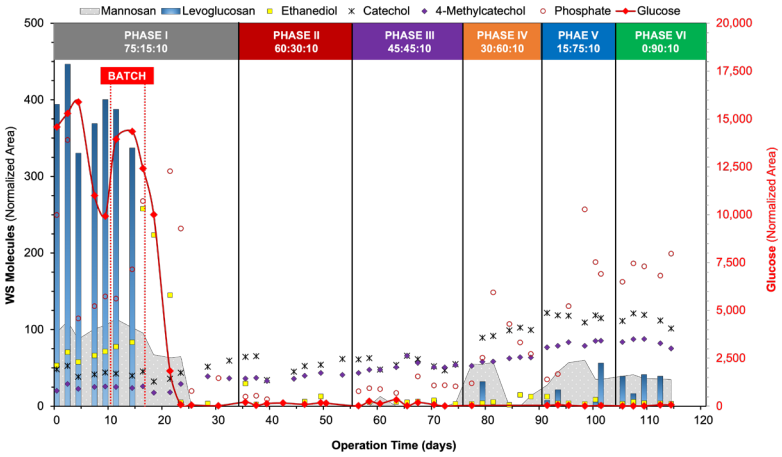

Figure 3.14: Profiles of normalized integrated area of selected GC-MS detectable compounds in the co-fermentation effluents.

3.5.2.2. Phase II (GLU 60% : WS 30%)

During the second phase of operation (+15% of WS in input, - 15% glucose), VFA concentration ranged between 6 and 11 gCOD L^{-1} (Figure 3.12) and their profile was stable (24% acetic, 7% propionic, 47% butyric, 14% valeric and 7% caproic acid), in contrast to what happened in Phase I. A significant increase in the production of CH_4 was observed in the gas in output (Figure 3.15); like the end of Phase I, all sugars and ethanediol were not detected in the solution in output, whereas an almost constant concentration of catechol and 4-methylcatechol was observed. Phosphate which had been provided with the influent (3.1) was completely consumed, probably due to microbial growth.

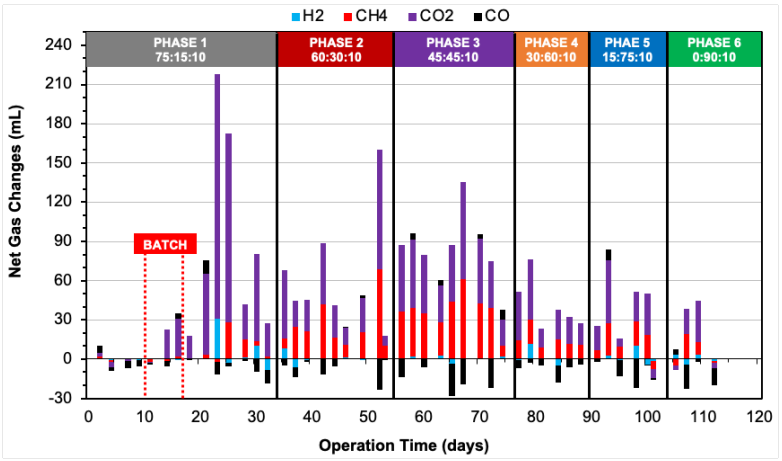

Figure 3.15: Net gas amounts at PyP co-fermentation experiment.

3.5.2.3. Phase III (GLU 45% : WS 45%)

Given the pyrotrophic activity reached during Phase II, the substrate composition was furtherly changed on day 56, providing the same amount of WS and glucose (45%) under the same operational conditions applied before. As result of time and feedstock change, VFA concentration markedly increased to a final value of 12.8 gCOD L^{-1} (Figure 3.12) corresponding to 80% of the soluble COD of the solution in output. VFA profile steeply changed as well, with a relative content of acetic, propionic, butyric, valeric, and caproic acids of 32, 1, 27, 7, and 29%. The production of CH_4 and CO_2 was slightly higher than that of Phase II (Figure 3.15) and higher consumption of CO was observed (2.2 mgCOD d^{-1}). GC-MS analyses of the solution in output showed a total consumption of all holocellulose derivatives analyzed and a slight increase of catechol and 4-methylcatechol almost proportional to the increase in WS share in the feeding (Figure 3.14). Phosphate concentration was slightly higher than what measured in Phase II, suggesting a decreased biofilm formation rate that could be related to some stabilization of MMC.

3.5.2.4. Phase IV (GLU 30% : WS 60%)

WS concentration in the input solution was further increased during Phase IV (12.0 gCOD L^{-1}). Even at a such high concentration of WS input, which was more than twice as compared as the previously tested concentrations in the mono-substrate fermentation test {Chapter 3.5.1}, VFA concentrations in the solution in output were high and stable (11.5 gCOD L^{-1}), and VFA became the main soluble substances (≈80% of COD). As previously observed after each feedstock change, the VFA profile changed (Figure 3.12), with a further chain elongation: detectable amounts of enanthic and caprylic acids (C_7 and C_8) were observed, while caproic acid, which was almost absent using glucose-rich feedstock, became the second most dominant VFA type after butyric acid on COD basis. CH_4 and CO_2 production decreased (Figure 3.15) whereas CO uptake was similar to the previous phase. The decreased *methanogenesis* activity can suggest that glucose was the preferential source for the residual methanogenic activity and/or WS products selectively inhibited the residual methanogens. The decrease in CO_2 production could be expected by the fact that the COD/C ratio was higher for WS than for glucose.

Levoglucosan was almost completely biodegraded (with a minor presence during day 79), while after more than 50 days without detecting holocellulose PyP, about 20% of the input concentration of mannosan was detected at the beginning of Phase IV (Figure 3.14). Concentrations of phenols increased again similarly with the increase of WS provided to the system.

Considering that most of COD during Phase IV came from WS, the observed data trend suggested the end of biochar colonization and the appearance of phenomena more related to adaptation to inhibitors which, according to the higher feeding concentrations of WS, were well in the range for exerting toxicity. It was possible to identify a sort of "shock" on days 77-81 after the feedstock change, followed by another equilibrium (with a higher VFA concentration and lower levoglucosan and mannosan amounts) observed between day 81 and day 91.

3.5.2.5. Phase V (GLU 15% : WS 75%)

WS concentration in the inlet was further increased to 17 gCOD L^{-1} during Phase V, a much higher concentration than the highest concentration of non-treated/raw WS ever fermented (to the best of the authors' knowledge). Consequentially to the change in the substrate composition, VFA yield, and concentration gradually decreased to 9.5 gCOD L^{-1} (Figure 3.12), while their profile did not change in comparison to Phase IV. Given that just negligible amounts of AS (levoglucosan on certain days, and mannosan steadily) were detected in the solution in output, the decrease in VFA yield can be probably related to WS overload that mainly involved the conversion of GC detectable organics. Concerning lignin derivatives, 4-methylcatechol increased along with the increase of WS input, whereas catechol had a constant concentration, suggesting a minimal degree of biodegradation.

3.5.2.6. Phase VI (GLU 0% : WS 90%)

In the last phase, 17 gCOD L^{-1} as WS (90%) and syngas (10%) were the only feedstock provided to the bioreactor. VFA concentration (8.5 gCOD L^{-1}) stabilized on the value obtained at the end of Phase V, whereas a decrease of total COD from 15 gCOD L^{-1} to 13 gCOD L^{-1} of the outlet solution was observed as a consequence of glucose removal. Methane production was not increased, and CO uptake was slightly improved to 2.3 mgCOD d^{-1}. Residual levoglucosan and mannosan were steadily detected by GC-MS by still achieving a highly-efficient consumption of more than

95% of both AS. On the other hand, both catechol and 4-methylcatechol had a decreasing trend soon after the phase switching. Although minimal, such an effect suggested that after long bioaugmentation, pyrotrophic MMC can also biodegrade the water-soluble phenols. Yet, a highlight should be given to the biodegradability of WS phenols in longer-term studies.

3.5.2.7. SEC-RID analysis of effluent

To obtain a general description of GC-MS detectable WS and non-analyzed constituents in terms of MWD, the solution in output to the fermentation process was subjected to size exclusion chromatography (SEC) coupled with index of refraction detection (RID). SEC-RID did not reveal VFA and gave MWD of sugar-like organics (e.g. hydroxy acetaldehyde, anhydrosugars sugar oligomers) and other water-soluble compounds (e.g. ethanediol, hydroxy-acids) with an index of refraction higher than water. Therefore, the comparison of MWD of WS in input and the solution in output to the fermentation process is particularly useful to have information about WS constituents without the limitation of GC-MS analysis.

MW distribution during the lag-phase showed 80-90% relative content of LMW mainly due to the unreacted glucose (Figure 3.16). Just after the lag-phase (day 18) and glucose consumption, the solution in output consisted mainly of high molecular weight (HMW) compounds (HMW>1450 Da), suggesting a preferential consumption of glucose and lighter WS organics in the beginning of the experiment (Figure 3.14).

Since glucose was never detected after day 25 and VFA were not revealed by RID, the MWD can be mostly related to the unconverted portion of WS or polar constituents (e.g. ethanediol) arising from the fermentative activity.

A clear and smooth transition toward HMW was observed during the experiment (Figure 3.16). In the beginning, roughly a half of RID detectable constituents was characterized by LMW organics, 30% by compounds with MW between 1.45 and 10 kDa and only 20% by HMW compounds. Such a distribution was close to that of input WS, with partial removal of lighter compounds. Afterwhile, it was possible to see a decrease of LMW concentration, an almost constant amount for organics with MW between 1.45 and 10 kDa, and a relative increase for MW>10 kDa. At the end of Phase VI, a mass distribution enriched in HMW organics (70% relative content) was observed. Since 70% of RID detectable organics in the solution in output had MW>1.45 kDa , assuming that SEC-RID was representative of non-VFA organics in

the solution in output (≈5 gCOD L^{-1} from Figure 3.12) and that all organics detected had a comparable COD, the final expected concentration of such compounds in the solution in output was about 3.5 gCOD L^{-1}. Such a value is very close to the expected inlet concentration of HMW, being 15% (Figure 3.12) of 17 gCOD L^{-1} provided as WS. Even if some changes in the relative distribution of HMW (enrichment of organics with MW between 1.45-10 kDa MW) occurred, the HMW seemed to enter the reactor without being consumed. The time trend of MW distribution observed during the experiment suggested that most of the compounds with MW<1.45 kDa was increasingly converted during adaptation, whereas larger WS organics were not effectively converted by pyrotrophs. Such phenomena were not surprising considering that larger WS organics are characterized by chemical structures that are more challenging for biodegradation or, in some cases, known to be not biodegradable [83].

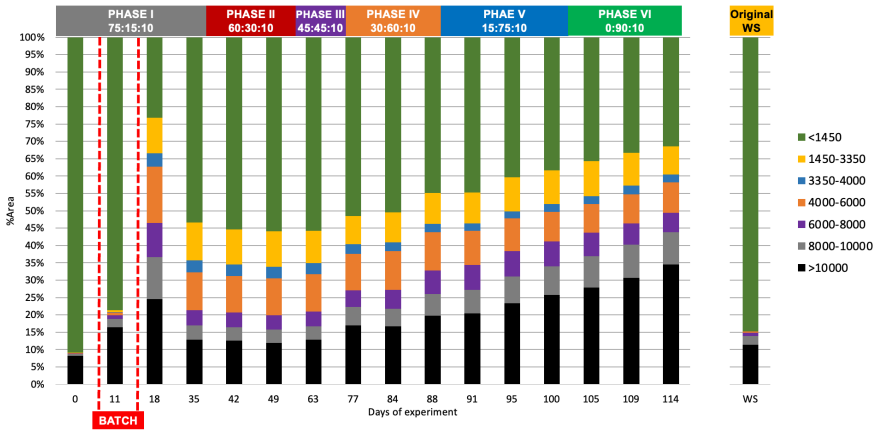

Figure 3.16: Molecular size distribution profile the co-fermentation effluents, obtained by HPLC-SEC (as in percentage area of RID detectable compounds).

3.5.2.8. Overall Performance Evaluation

To prove the consistency of the experimental results and to highlight the effectiveness of WS conversion along the bioaugmentation, a COD balance was performed for all the operational phases. A glance at COD input, namely glucose/WS/syngas, and outputs, namely gas, VFA, other soluble organics, adsorbed organics and microbial growth was reported in Figure 3.17.

Product recovery rates on COD basis were acceptable all through the phases (Figure 3.17). The lowest COD recovery was obtained in Phase I, when 14% of COD

input was consumed for microbial growth (Eq. (3.14). After the microbial enrichment phase, COD recoveries (COD_{out}/COD_{in}) were always above 90%.

Being the syngas added to evaluate co-fermentation in a realistic system, most of the fermentation phenomena involved WS and glucose. Nonetheless, it was worth noticing that above 46% of fed CO was used: this was a quite promising performance for this bioreactor set-up that was even not fully optimized for gas fermentation.

During Phase I, in which most of the COD provided was from glucose, the main feature was an incomplete conversion of the COD in input (yield of unreacted was 25%, mainly unconverted glucose). The yield of unreacted compounds apparently increased to 37% during Phase II, even if glucose and GC-MS detectable WS compounds were totally consumed. Given the limited information about non-GC-MS detectable WS, it was not possible to determine if such increase was just due to a minimal biodegradation of the latter portion of WS (roughly 28% of the input), to the production of non-VFA fermentation products (e.g. ethanol, accounted as "unreacted") or to the combination of both.

The clearest improvement for unreacted portion conversion was observed during Phase III, when still half of the soluble COD was provided as glucose; 50% VFA yield was obtained the minimum amount (25%) of unreacted compounds in the solution in output was observed and a significant (33%) yield of methane was achieved.

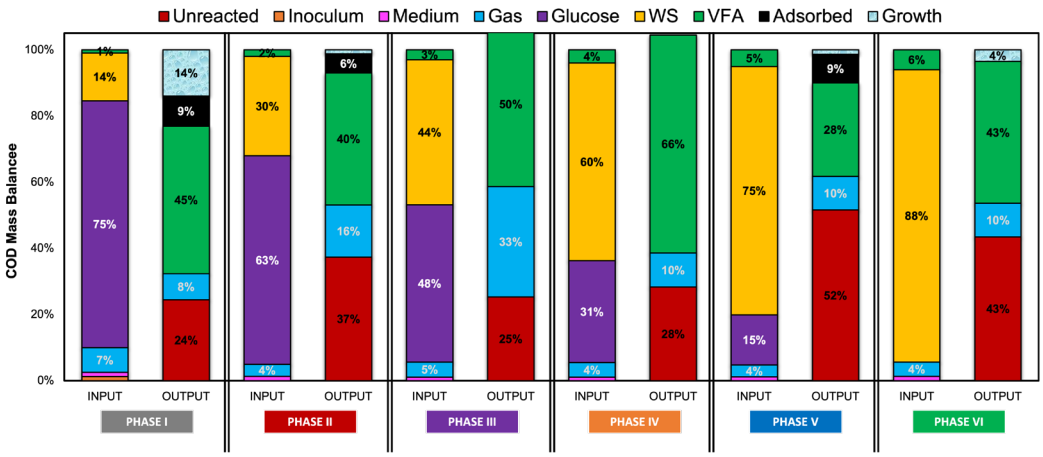

Figure 3.17: COD balance for various phases of the co-fermentation experiment.

The switch from Phase III and Phase IV (60% WS) steered the fermentation path from methanogenesis toward acidogenesis. Methane-rich off-gas yield settled at 10% and the reactor provided the best VFA yield (66%) with just 28% yield of unreacted

substances. According to OLR used, the performance observed during Phase IV corresponded to the best volumetric productivity of VFA obtained, equal to 560 mgCOD L^{-1} d^{-1}. Phase V showed a decrease in VFA yield (to 28%) and an increase of unreacted material (52%) that can be interpreted as a sort of shock due to the increase in WS provided. Nonetheless, even if the subsequent Phase VI involved pure WS feedstock, such shock was overcome by the MMC with a VFA yield of 43%, with unreacted compounds that decreased to 43%.

Table 3.6: Operational conditions, overall balances, and product yields of the PyP co-fermentation experiment.

Parameters	Units	Phase I	Phase II	Phase III	Phase IV	Phase V	Phase VI	Overall
$Feed_{GLU:WS:GAS}$	$\%_{COD}$	75:15:10	60:30:10	45:45:10	30:60:10	15:75:10	0:90:10	48:42:10
$C_{SUBSTRATE}$	g_{COD}/L	15+3+2	12+6+2	9+9+2	6+12+2	3+15+2	0+15+2	18.5
OLR	$g_{COD}/L\text{-}d$	1,0	1,0	1,0	1,0	1,0	0.8	0,98
HRT	*days*	20	20	20	20	20	20	20
Duration	*days*	35*	21	21	14	14	9	114
Total Input	g_{COD}	5,0	3,9	3,5	2,2	2,6	1,1	24,1
Total Output	g_{COD}	3,9	3,7	3,8	2,3	2,4	1,1	19,8
COD Recovery	%	77%	93%	108%	104%	90%	96%	82%
Produced VFA	g_{COD}	2,2	1,6	1,8	1,5	0,7	0,5	8,9
Productivity	$g_{COD}/L\text{-}d$	0,35	0,39	0,49	0,56	0,28	0,34	0,39
VFA Yield	%	58%	43%	46%	63%	31%	44%	45%

Considering that residual glucose was negligible after day 25, it can be assumed that the unreacted components of Phase II and Phase VI mainly came from WS. Using that assumption and comparing the unreacted amount with the WS input, it was possible to highlight that during Phase II the unreacted COD was close to that of WS provided. This meant that, even if the GC-MS detectable compounds of WS were completely degraded, the overall pyrotrophic activity (utilization of WS/syngas) was not relevant for the COD balance.

The transition towards pyrotrophy occurred during Phase III when the unreacted COD become just a half of the WS provided. The ratio between unreacted compounds and WS remained stable during Phase IV, and increased during Phase V, probably due to the aforementioned shock, and finally settled around 49% during the last phase in which WS and syngas were the only feedstock provided. Considering that the unreacted portion included also some non-VFA byproducts, such value was not so far from what was expected considering the biodegradable fraction of WS [40] [41]. This suggests that the long-term enrichment procedure here used, where a gradually increasing ratio of PyP input was applied together with an easily biodegradable co-substrate (glucose), allowed a reproducible selection of a biologically-efficient pyrotrophic community, able to produce VFA with significant concentration. From GC-MS and SEC-RID analysis, such *pyrotrophs* mainly addressed the lighter constituents of WS (MW<1.45 kDa) with negligible activity towards HMW (>1.45 kDa) constituents of WS. It is worth noticing that the Phase V condition was qualitatively identical to that tested in mono-substrate WS fermentation experiments {Chapter 3.5.1}, therefore it can be stated that the long bioaugmentation procedure allowed to culture *pyrotrophs* that can tolerate high concentrations of both WS (as inhibitory substrates) and VFA (as inhibitory products).

3.5.3. Microbial Community Analysis: *Pyrotrophs*

Changes in the composition of the MMC were investigated by next generation sequencing (NGS) method. Only phyla with a r.a. > 0.5% in at least 1 sample and families or genus with a r.a. > 1% in at least 1 sample were showed in Figure 3.18. The relative abundance at the phylum level is showing that Firmicutes was the predominant type for all cases including the original seed sludge (inoculum), followed by Actinobacteria. The main difference obtained at the phylum level between reactors were for the third most dominant, which was Bacteroidetes for all the experiment except the co-fermentation experiment. On the other hand, the microbial abundance profiles were quite dissociated at the family level as compared to the phylum level, except for the mono-substrate tests which were quite similar to each other. The most dominant microbial family for the inoculum sludge was *Clostridiaceae 1* with 42% relative abundance (r.a.). While *Streptococcaceae* with a 25% r.a. was dominating the sample from the co-fermentation experiment. In the case of samples from the mono-

substrate tests having a large portion of other unclassified families, followed by *Clostridiaceae-1* as the most dominant classified family.

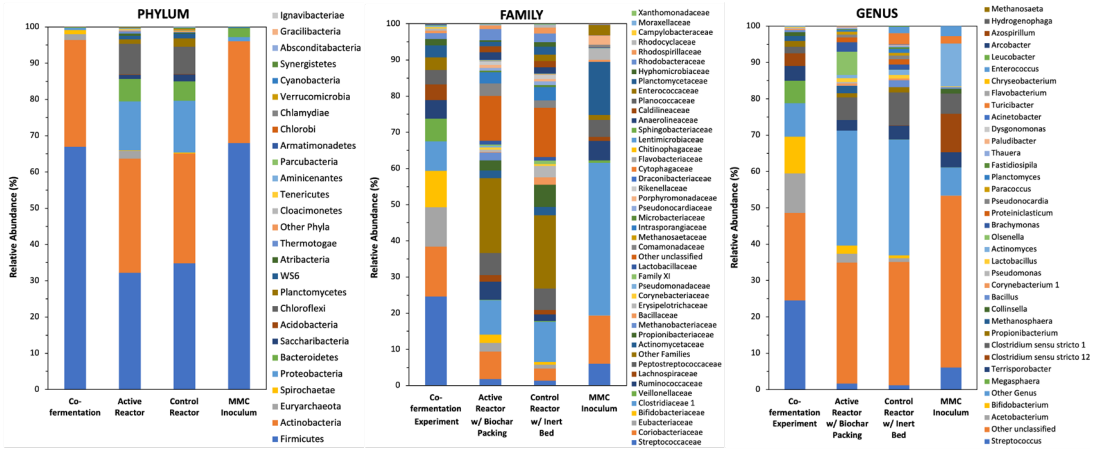

Figure 3.18: Taxonomic composition and relative abundance of MMC samples.

Total numbers of identified different genus types for co-fermentation, active reactor, control reactor and inoculum that had a r.a. > 1% in at least 1 sample, were 15, 26, 29, and 13 respectively. Moreover, a significantly lower percentage of 'other genus' and 'other unclassified' groups in the co-fermentation experiment (r.a. 33%) versus mono-substrate tests (r.a. ≈65%) were determined. Both these indications were implying a better microbial enrichment with a livelier pyrotrophic consortia has been achieved in the co-fermentation approach where glucose, WS and syngas have been provided together to the biochar-packed bioreactor. *Streptococcus* was the most dominant genus type (r.a. 25%) in co-fermentation experiment followed by *Acetobacterium* (r.a. 11%), *Bifidobacterium* (r.a. 10%), and *Megasphaera* (r.a. 6%). In the case of mono-substrate tests, most dominant genus types were varying from the co-fermentation experiment and also each other. For instance, *Olsenella* and *Clostridium sensu stricto 1* with 6% of relative abundance ratios were the most dominant types in the active reactor (biochar-packed), while in the control reactor without biochar anaerobic spore-forming *Clostridium sensu stricto 1* was the most dominant and only genus type with a relative abundance of over 5%. This issue was implying that the fatty acid producer *Clostridium sensu stricto 1* can be the most robust pyrotrophic microbe with the capability of metabolizing a wide range of compounds including carbohydrates, amino acids, and some aromatics[84]. This particular genus could survive with WS as a single energy source regardless of the presence of biochar

as a microbial enhancement tool, while the case of non-spore forming anaerobic *Olsenella* (a dominant genus only in biochar-packed active reactor of the mono-substrate test) can be given as an example of the biochar selectivity on pyrotrophic communities.

Biochar is known as a highly porous conductive material and several works reported that microorganisms, such as methanogenic archaea and hydrophobic microbiota, could colonize the biochar microporosities [64], [85]–[87] as those shown with 1000 and 250 magnifications (Figure 3.19). SEM images of biochar bed samples demonstrated the presence of coccus and bacillus with 0.5 and 6.5 µm lengths on the outer and inner (e.g. carbonized wood vessels) surfaces of biochar. Geometrical shapes of SEM-detected microbes were consistent with those of the 10 most abundant genus identified using the microbial community analysis (Figure 3.18).

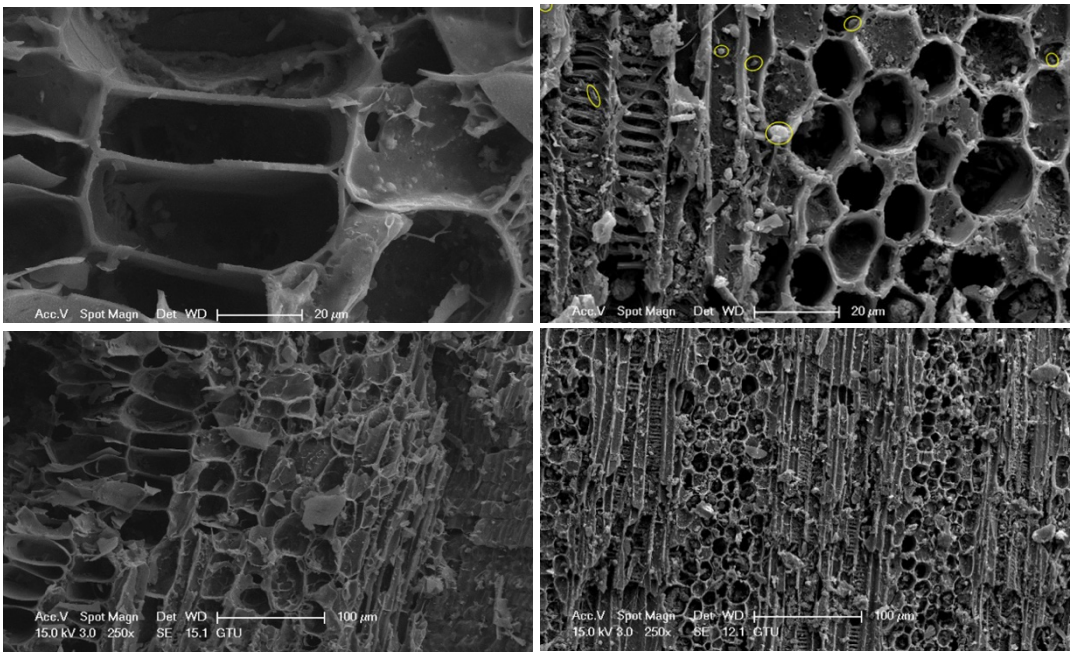

Figure 3.19: SEM of biochar grains: Images before experiment (clean) on the left, and images after experiment (microbially-dirtied) as a packing material on the right

3.6. Conclusion

Previous works already demonstrated the existence of *pyrotrophs*, namely an MMC able to use pyrolysis products as carbon source, that can be used to funnel the complex mixture released by pyrolysis to obtain utilizable chemicals.

The aim of this chapter of the thesis, was to establish if it is possible to obtain and exploit a pyrotrophic acidogenic consortia, able to produce VFA starting from whole, non-pretreated, mixture of pyrolysis product.

Preliminary experiments were previously confirmed that biochar boost MMC growth, especially when dealing with PyP, but mono-substrate fermentation for production of VFA was not successful with direct WS fermentation and natural inoculum. Even at OLR as low as 0.25 gCOD-L^{-1}-d^{-1} WS fermentation failed to provide a stable VFA production, showing a reversible intoxication phenomenon which was attributed to the combined effect of product (VFA) and substate (WS) inhibition. Searching for new VFA tolerant pyrotrophic consortium, the MMC was bioaugmented through co-fermentation with glucose. A new type of reactor, based on packed biochar, and a new acclimatization procedure, consisting in co-feeding WS and glucose and constant amount of syngas were developed and tested.

Although the achieved volumetric productivity was low (<0.6 g-COD L^{-1} d^{-1}), bioaugmented *pyrotrophs* demonstrated to be able to convert most of GC-MS detectable constituents (e.g. anhydrosugars) of WS, a significant portion of non GC-MS detectable constituents (e.g. oligomers with MW<1.45 Da) together with headspace CO. Even without selective inhibition of methanogen, the main fermentation products were VFA, whose profile was a function of the WS/glucose ratio.

Looking to whole results, this chapter provided a novel way for the simultaneous utilization of gas (syngas), liquid (WS) and solid (biochar) products of intermediate pyrolysis through original biochar-packed anaerobic bioreactor. Such approach can already be applied for the valorization of various toxic aqueous effluents of thermochemical processes (e.g. pyrolysis, gasification, hydrothermal liquefaction) and, in a broader prospective, it could be a useful tool to circumvent the lignocellulose hydrolysis step. Nonetheless, it should be pointed out that the absolute yield of VFA and productivity are lower than those observed with compounds obtainable from hydrolysis (e.g. glucose). The performances of Biochar-Packed bioreactor should be improved considering the following issues:

- MMC improved their performances over the time, mainly due to an improved colonization of the biochar bed with increasingly adapted microorganisms.

Therefore, longer adaptation and acclimatization/bioaugmentation procedures with increasing OLR could further improve the volumetric productivity.

- Being 9% of input converted into CH_4, the selective inhibition of methanogenic archaea with chemicals or suitable experimental conditions could increase VFA yields [88].
- Most of the yield loss was caused by a scarce conversion of HMW organics, therefore pyrolysis can be optimized to decrease the yield of such compounds and increase the yield of lighter bioavailable molecules.

4. SYNGAS FERMENTATION

The most common target products from syngas fermentation process are liquid (e.g. ethanol) and gas (methane) fuels. However, those fuels are emitting greenhouse gasses during the conversion into energy. On the other hand, biomass originated C1-rich syngas can also be converted into acetate and some other VFA, which are value-added materials and commonly considered as building block chemicals. However, aqueous organic acids present in the syngas fermentation effluent, are requiring high energy demanding extraction process, to be sold as a commercial commodity. On the other hand, the benefits can be achieved from acetogenic syngas biorefinery, should not be limited to the economic value of extracted VFA. In this study, VFA-rich effluents from syngas fermentation are proposed to be used as a direct feeding material for PHA producing microorganisms which bacteria preferring VFA as a carbon source for intracellular PHA accumulation (Figure 4.1). For this purpose, real syngas materials originating from the pyrolysis of lignocellulosic biomass, has been used as a feedstock for the attached-grown MMC within a CBSR under continuous operation. Two operational phases with different HRT were applied during the total experimental period of 75 days. During the first high HRT (50 d) regime resulted in high VFA concentration (≈10,000 ppm_{COD}), 89% of gaseous CO was fixed by CBSR, and 67% of it bioconverted into VFA at 2,720 mg-COD/L-day rate. While the subsequent low HRT (9 d) regime was provided a better performance, with 9,760 mg-COD/L-day productivity and 95% of VFA yield. The concentration of mature fermentation effluents was dominantly originated from target products (VFA:COD ≥ 90%) and free-from suspended matters (≤ 2%) with a slightly alkaline pH (8.8), making them a highly suitable carbon source for the latter PHA accumulation process.

4.1. Introduction to Syngas Fermentation

Biomass is a renewable organic material originated from plants and animals (e.g. forestry residuals, food-waste, sewage sludge, animal waste). Especially lignocellulosic biomass originated from plants, preferably not included in the food chain, is an abundant sustainable source to be used for obtaining energy and various kinds of valuable materials such as gas fuels (e.g. CH_4, H_2), liquid fuels (e.g. bio-oil, ethanol) and carbonous biochar. Furthermore, due to its rich, yet physiochemically

complex and heterogenous composition, several alternative processes have been developed to utilize the lignocellulosic biomass for non-energy purposes. Thermochemical methods such as gasification and pyrolysis, are conducted in limited or extinct oxygen environment under high temperatures (400-1200 °C) for upgrading lignocellulosic biomass. Pyrolysis and gasification end up with a high yield of C1-rich gasses (CO, CO_2, CH_4) with some recessive amounts of H_2, namely syngas (alternatively synthesis gas) which corresponds 10-60%$_{COD_{eq}}$ chemical energy of the input biomass [3] depending on the operational conditions (e.g., temperature, residence time, reactor bed-type, oxidant type/amount, flowrate, etc.). Methane with a 55-60 MJ/kg heating value is a widely-used gas fuel, while carbon monoxide has much lower heating value (10 MJ/kg). Moreover, thermal oxidation of both gasses ends up with CO_2, as the major greenhouse gas in our atmosphere, that is accepted as the main responsible for global climate change.

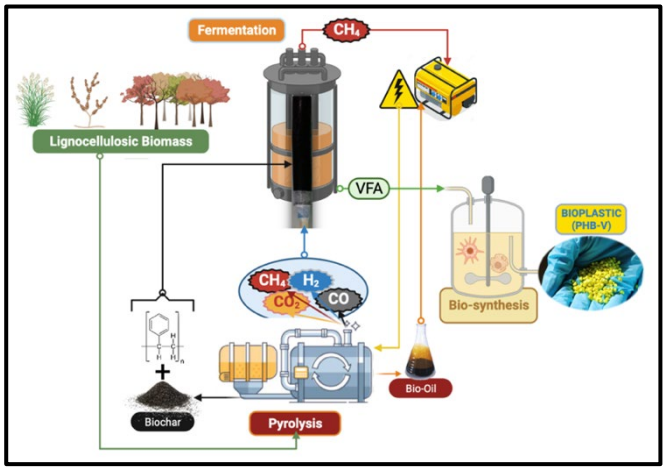

Figure 4.1: Simplified flow-diagram of the syngas fermentation biorefinery for obtaining PHA from lignocellulosic biomass resources.

Conversion of syngas into chemicals and fuels can be done either chemically (e.g. Fischer-tropsch process, FTP) or biologically (e.g. biomethanization, anaerobic fermentation). While FTP was theorized and started to be tested in early 20s and have been already applied in industrial levels since 1936 [89], biological approach is much newer [90], yet could be more widely-applied in the near future due to its more robust nature as compared to the catalyst driven processes. Biomass derived syngas contains some impurities such as volatile tars, trace organics (benzene, ethane, ethylene, acetylene), sulphury molecules (H_2S, SO_2, COS) ammonia (NH_3), and varying ratios

of $CO:CO_2:H_2$, due to the heterogenic composition of the lignocellulosic input and thermochemical conversion technique. For this reason, it is very challenging to apply chemical catalysis methods directly for upgrading biomass originated syngas, without a complete gas-treatment and conditioning unit which corresponds a significant cost for thermochemical conversion plants [91]. On the other hand, biological processes are more tolerant to varying compositions of non-treated syngas materials naturally containing impurities [92].

Syngas can be biologically converted into; methane by anaerobic digestion [93], VFA (e.g. acetate, butyrate, lactate) by acetogenic fermentation [94], or liquid fuels (e.g. ethanol) by solventogenic bioconversion [95] in a HTB biorefinery perspective [3]. One another recent approach was to bio-utilization of syngas for obtaining PHA. PHAs are biodegradable polymeric materials, accumulated in microbial cells of peculiar bacteria. Intracellularly accumulated PHA granules can be re-used as a carbon and energy source for microbial growth in the absence of extracellular organic carbon, if required [96]. Most of the studies has shown that the bacteria are generally desired the existence of VFA during the intracellular PHA production [97].

Strictly anaerobic *R. Rubrum* bacteria has a quite unique metabolism for converting CO directly into PHA [98], [99]. However, the productivities are relatively low and the proposed process requiring an additional organic carbon source preferably an organic fatty acid such as acetate. On the other hand, acetogenic and solventogenic fermentation of syngas is widely tested method even with some preliminary commercialization attempts mainly for ethanol production [100].

Coupling of two mature biological processes with MMC, namely, acetogenic syngas fermentation and VFA-to-PHA bioconversion, are appearing as a promising alternative way for PHA obtainment from biomass derived syngas. To the best of our knowledge, nobody has followed such kind of integrated trilogy process, where biomass is first converted into C1-rich syngas, followed by anaerobic fermentation for VFA obtainment, and lastly PHA accumulation through syngas originated VFAs.

Here, a three-step hybrid biorefinery approach was proposed; (I) biomass-to-syngas via thermochemistry; (II) syngas-to-VFA via anaerobic fermentation, and (III) VFA-to-PHA via a secondary microbial conversion. For this purpose, C1-rich raw syngas materials (without a complete gas treatment) obtained through the batch pyrolyzes of lignocellulosic biomass, were tested as a feedstock for attached grown

acetogenic MMC within a char-based biofilm sparger reactor (CBSR), for obtaining VFA-rich effluents.

4.2. Methodology

4.2.1. Syngas characteristics

Syngas samples used in this study were obtained by pyrolysis of fir sawdust as a representative lignocellulosic biomass. More specifically, 30g biomass was pyrolyzed at constant temperature (650 °C) for 15 minutes residence time under N_2 environment. Numerous batch pyrolyzes were conducted by a bench-scale pyrolizer set-up was previously detailed elsewhere [101]. Briefly, a horizontal tubular furnace equipped with a quartz reactor was used, following by; a 4°C water-trap for aqueous products, a glass-ware cyclone unit to precipitate tars, and a cotton trap for adsorbing the residual noncondensables. Produced syngas had a 632 mg-COD/L concentration, and containing 45.7% (±1) of CO, 19.2% (±5) of CO_2, 11.7% (±0) of CH_4, and 2.4% (±2) of H_2 with a balance of N_2. Gas samples were stored in 10-liter sized air-tight gas bags (Supel™ Inert Foil, 10L) under room temperature, during the continues mode gas fermentation experiment.

4.2.2. Preparation of Biochar-Polystyrene Monolith

The manufacturing process of the novel biochar-made monolith was previously optimized prior to this study with dozens of different trials which provided different porosity, mechanical resistance, homogeneity, and durability {Appendix D}.

Around 30g biochar obtained from the slow pyrolysis of wooden biomass (orchard pruning) was grinded and dry sieved to 1.0 mm to obtain powdered biochar with an approximately homogenous particle-size distribution. Around 15g of polystyrene (PS) foam was softened with acetone (≈1-2 ml per g of PS foam) and mixed with grinded and sieved biochar. The heterogenous biochar and PS mixture was harsh kneading with subsequent additions of acetone till the obtainment of a dough-like material. The latter was casted into a conical 50 ml Falcon™ test tube to provide the external shape and a cylindrical glass rod was replaced into the center, which provide the internal channel for gas delivery. The entire assembly was then dried at 80°C for 2 hours, after that monolith was removed from cavity. Finally, the inner glass

tube was removed from monolith and substituted with 8 mm polyamide tubing, that was sealed with fresh biochar-PS dough, and dried again (Figure 4.2). Geometrical details of the char-based sparger monolith were as follows; 11 cm of total length, 27 mm of outer diameter, 6 mm of inner diameter, 61 mL bulk volume, and around 40% of porosity.

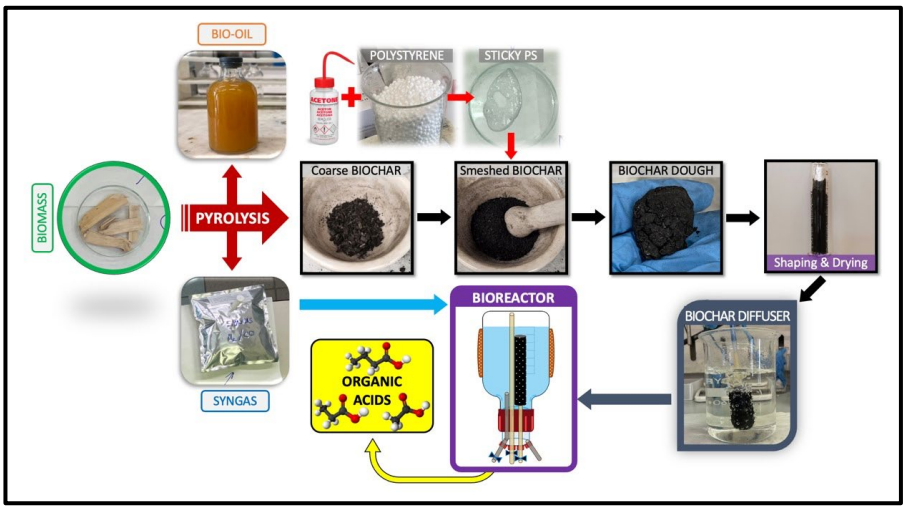

Figure 4.2: The manufacturing steps of the developed biochar-diffuser.

4.2.3. Char-based biofilm sparger reactor (CBSR)

To overcome the challenges of acetogenic syngas fermentation, which are depending on mainly; existence of toxifying impurities [34], [102], and also both substrate (CO) and product (VFA) inhibition, a novel gas fixation tool made by biochar was proposed and tested with clean gas mixtures (H_2/CO_2). The tailor-made bioreactor system equipped with the novel biochar-made sparger, was manufactured for this study to investigate the performance under real raw syngas feeding.

The CBSR system constructed for this study (Figure 4.3), was comprising of mainly; an upside-down positioned 500mL glass bottle with a four ported cap and external heating pads, a syngas feeding line (gasbag and gas pump), a hydraulic compensator bottle (to minimize water vapor loss), a gas circulation line and liquid feeding/discharging line, which all regulated by an Arduino microprocessor as a cost-efficient automation system, as detailed elsewhere [25].

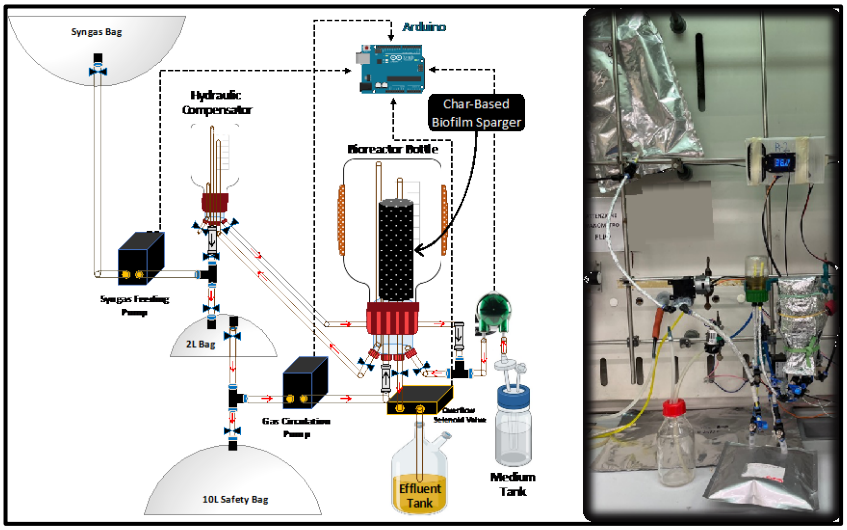

Figure 4.3: Char-based biofilm sparger reactor (CBSR) set-up for syngas fermentation.

4.2.4. Inoculation, start-up, and operation of CBSR

After the CBSR set-up was constructed and all connections are sealed, all system is flushed with excess amount of Helium gas to purge away the existing internal air. Later, a 450 mL of start-up mixture which compromise of; %10 (v:v) of anaerobic digestate (details in [14]), 40 g/L $NaHCO_3$ as an slightly alkali buffer and 7% of basal medium (according to [14]), was injected. A secondary Helium flushing was made into the wetted system to minimize the available soluble oxygen.

After the inoculation with an anaerobic digestate obtained from an industrial wastewater treatment plant of a wine industry (Caviro Extra S.p.A), continuous mode of operation was started. Gas and liquid feeding and discharging cycles were made periodically (mostly in daily basis) during the operation. For liquid feeding, distilled water containing 7% (v:v) bicarbonated basal medium was used to sustain a constant nutrient and buffer conditions throughout the experiment. The amount of continuous liquid feeding was made according to the two different HRT regimes, which were 9 mL/day and 50 mL/day for 50 and 9 days of HRT respectively. Bioreactor was operated under mesophilic temperature conditions (36.2 °C ± 2.0). While biomass originated real syngas feeding was kept in excess amount in the system, and periodical syngas feeding amounts were tuned according to the gas consumption rates. Non-converted portion of syngas (mainly CH_4) stayed inside the gasbags of the CBSR (with total 12 liters capacity) were measured by volume, analyzed by its composition and

removed from the system periodically. No chemical inhibitor was used throughout the study, since CH_4 production was in negligible amounts.

4.2.5. Analytical methods and formulas

Fermentation liquids were centrifuged at 5000 rpm for 10 minutes prior to the measurement of soluble COD content, which is conducted by a Quick-COD Analyzer according to the ASTM D6238-98 method. The pH measurements were conducted with a bench type multiparameter device (SI Analytics Lab 845). VFA were analyzed quantitively in a gas GC-MS (Agilent 6850 gas chromatography with 5975 quadrupole mass spectrometer) followed by a solvent (dimethyl carbonate) extraction method [27]. Ammonia nitrogen (NH_4-N^+) and phosphate (PO_4^{3-}) were measured by the procedures of Hach test kits, using a spectrophotometer device (Hach DR/2010, Germany), which are based on the standard methods for the examination of water and wastewater [103]. Gas compositions of both input syngas and off-gasses from the fermentation experiment, were measured in a GC system equipped with a thermal conductivity detector (GC-TCD, Agilent 7820A) following by the procedure described elsewhere [51].

The estimations based on the experimental data were done according to developed suitable formulas, which can be used as a direct measurement unit of chemical energy flows in this kind of HTB processes, as proposed and discussed in detail elsewhere [3]. Total 'fermentable syngas feed' is a definition which implies the total bioconvertible chemical energy provided into system (4.1). Gas fixation ratio as in percentage basis, were estimated based on the difference between total fed and total removed CO and H_2 gas volumes (4.2). Total amount of produced VFA is expressed in mg-COD was calculated by the sum of daily VFA outputs and total VFA mass presented in the final day (4.3). Another critical parameter to assess the performance is the product (VFA) yield, that was calculated by the percentage ratio of produced VFA mass and total COD mass of fixed fermentable gases (4.4). Volumetric productivity (V_P) of the CBSR system was estimated accordingly to the total produced VFA mass, for unit of time (HRT), per total biologically active volume of the system that is equal to the biofilm spargers bulk volume (V_{CBS}) in the CBSR (4.5).

$$\sum_{Day\,0}^{Day} V_{SyngasFed}\; x\; [CO\% + H_2\%] \tag{4.1}$$

$$\frac{(Eq.1)-\sum\left[(V_{H_2removed}+V_{COremoved})x0.67\frac{mg_{COD}}{mL}\right]}{(Eq.1)}\ x\ 100 \quad (4.2)$$

$$\left(\sum_{Day\ 0}^{Day\ 54} V_{Effluent} x C_{VFA}\right) + \left(V_{Tot}\ x\ C^{Day54}{}_{VFA}\right) \quad (4.3)$$

$$\frac{(Eq.3)}{(Eq.1)x(Eq.2)} x100 \quad (4.4)$$

$$\frac{(Eq.4)}{HRT\ x\ V_{CBS}} \quad (4.5)$$

4.3. Results and Discussion

Biomass originated real syngas materials, which are rich in inorganic mono carbon gasses (C1) were fermented into VFA by CBSR under continuous gas and liquid feed mode for 54 days long. Until the second week of operation, soluble COD values were under 1000 ppm and no VFA were detected, which period can be called as lag-phase, when the acetogenic microbes were being selected and colonizing onto the sparger. Later, adapted acetogenic biofilm has shown a logarithmic increase (350-450 mg-VFA/day) by performance until the 50th days of operation, when the microbial enrichment phase would be occurred. Later on, during the first operational phase (50d HRT), CBSR system has reached a steady soluble COD concentrations up to 10,000ppm levels (Figure 4.4), with a more than 90% of VFA:COD ratio at the end. Very high VFA proportion in the solubilized COD implying that char-based sparger was successfully colonized by mostly acetogenic microbes, who are capable of converting syngas constituents (CO, CO_2, H_2) into mainly acetic acid and so on. Then, HRT was decreased down to the 9 days, to reveal the productivity of CBSR at lower inhibition stress from VFA under syngas feeding.

In the beginning period of the enrichment phase, colonized consortia on the biofilm sparger, were producing acetic acid most dominantly, later the proportion of other VFAs (mainly propionic and butyric acid) were become more apparent in the effluent (Figure 4.5). Yet, acetic acid was always most dominant VFA type with an average 82% (±3%) of dominance ratio in COD basis. This syngas fermentation test was conducted without an automated pH control approach, which is an additional

investment and operational cost for plants, yet sufficiently stable pH conditions was achieved throughout the 54 days long continuous mode operation of CBSR, thanks to the bicarbonate addition as a chemical buffer (Figure 4.5). Maximum and minimum pH values were recorded as 9.1 and 8.0 respectively, while overall average pH was calculated as 8.6 (±0.3). Our results were confirming that syngas fermentation can be applicable in slightly alkaline conditions, without the requirement of an active pH control system, even at high VFA concentrations around 10,000ppm.

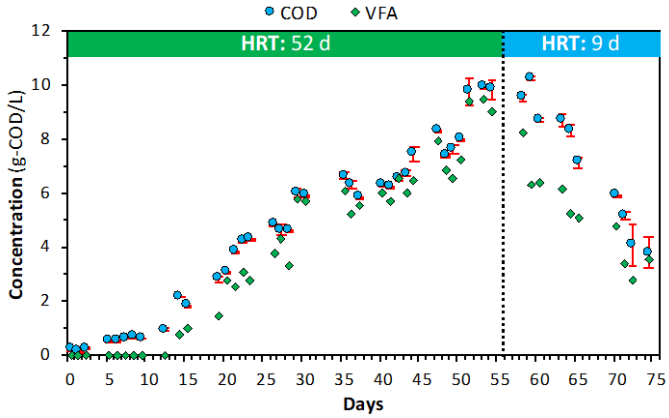

Figure 4.4: Soluble COD and total VFA profile of the fermentation effluents.

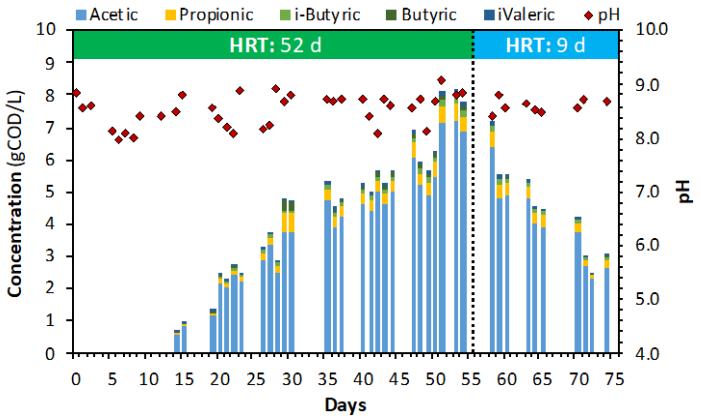

Figure 4.5: VFA composition and pH profile of the fermentation effluents.

In Table 4.1, general performance criteria of the syngas fermentation test by CBSR were listed. In real scale operation, it is critical to achieve a high conversion rate (fixation rate), which was calculated as 87% and 81% for the subsequent phases. This means that, approximately 10,000 mg-COD out of 11,510 mg-COD coming from the fermentable portion (CO, CO_2, H_2) of fed syngas, was fixed by CBSR for initial phase (50d HRT). On the other hand, 6739 mg-COD of it has been bioconverted into

the VFA, which was corresponding a 67% of product yield. Moreover, char-based sparger as a biological gas fixation tool, was offered a quite promising productivity as 2107 mg-COD/L-day at high VFA concentration, and 6857 mg-COD/L-day under the lower VFA level. Productivity estimation was depended on the net VFA production, HRT, and the volume of the biologically active sparger volume.

Table 4.1: Performance summary and critical results of the syngas fermentation test.

Parameter	Unit	HRT 52d	HRT 9d
Fermentable Syngas Feed	mg_{COD}	11,510	7,036
Gas Fixation Rate	$\%_{COD}$	87%	81%
Effluent COD	mg_{COD}/L	9,800	3,800
VFA Produced	mg_{COD}	6,739	3,778
VFA Yield	%	67%	67%
CBSR V_P	mg_{COD}/L-day	2,107	6,857

4.4. Conclusion

75 days long acetogenic fermentation of biomass originated syngas experiment was conducted, within a peculiar CBSR system whose working principle was dependent on MMC biofilm attached to porous and conductive biochar. Two different HRT regimes were performed, which were 50d and 9d, respectively, to reveal the significance of operating VFA concentration level that has an inhibitory effect on microbial cultures. According to the experimental results, low HRT (9 d) regime with lower VFA level, was revealed a much better performance in terms of both the V_P (3.6 times higher) based on the char-monolith biologically active volume, as compared to the high HRT (50 d) regime. Even though, there are some few studies investigated the solventogenic microbial conversion of real syngas into alcohols (e.g. ethanol) by single strains [34], [102], [104]–[109], there is no study about acidogenic fermentation of biomass originated syngas neither with single strain nor MMC, to the best of our knowledge. For this reason, the main importance of such experiment is, to showing that anaerobic MMC can efficiently convert the biomass originated raw syngas materials into VFA by the help of CBSR system without a severe toxification effect, which may have been observed due to either product (VFA), or substrate (toxic impurities and CO itself) inhibition.

5. H_2/CO_2 FERMENTATION

Homoacetogenic fermentation of CO_2 and H_2 allows to produce renewable VFA through a sustainable and mild pathway. Nonetheless, low mass transfer rate of H_2 and product inhibition rows against process feasibility. To address this key aspect, biomass derived biochar was used to manufacture a highly porous and moldable composite. This material was shaped into a monolith, which was proposed as supporting growth media for attached-grown microbial mixed cultures within a CBSR. This novel device was tested for acetogenic fermentation of H_2/CO_2 changing hydraulic residence times (HRT; 2, 5.5, 10, 60 days). As most striking results, 60 days HRT provided the highest VFA concentration ever obtained (58 $gCOD_{VFA}$ L^{-1} and 52 g L^{-1} acetic acid). Such result suggests that biochar could enhance mass transfer rate, shield from product inhibition and/or improve the growth of biofilm.

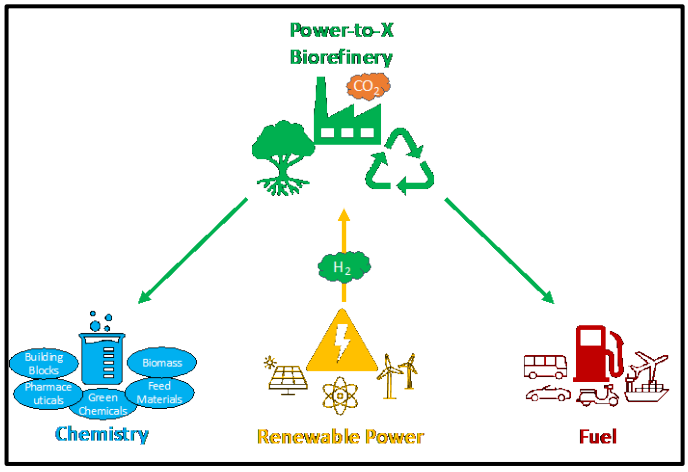

Figure 5.1: Power-to-X biorefineries hypothetical schema.

5.1. Introduction to Power-to-X Approach

Power-to-X concept proposes the use of renewable power (e.g., photovoltaic, wind, hydropower, geothermal, etc.) to produce commodity chemicals, materials, feed, and food (Figure 5.1) [110].

Water-electrolysis derived green H_2, and CO_2 obtained by either, carbon capture technologies, or biogas plants, or industrial off-gasses (e.g. emissions of steel and cement factories, biomass incineration), can be transformed by strictly anaerobic acetogenesis, which are capable autotrophic assimilation of inorganic H_2/CO_2 and CO

and ferment them into acetic acid (CH_3COOH) and other VFA [111]. A genuine group of acetogenesis are known as "homoacetogens", who are capable of converting two 4 moles of H_2 and 2 moles of CO_2 into acetic acid (5.1) as almost single fermentation product (Figure 5.2) [25]. Given that homoacetogens are almost ubiquitarian in natural occurring anaerobic consortia [112], MMC could provide a consistent path for production of renewable organic acids, with reliable setup (simple, non-sterile reactor), mild operating conditions (e.g. low temperature and pressure) and with potential feedstock flexibility (e.g. H_2/CO_2 from various sources).

$$2CO_2 + 4H_2 \rightarrow CH_3COOH + 2H_2O \quad \Delta G^0 = -95 \frac{kJ}{mol} \tag{5.1}$$

Several gas fermentation tests, in different sizes varying from bench-scale to industrial plants, have been conducted in the last few decades, mostly focused on C1-rich syngas fermentation derived from biomass, and correspondingly many review papers and book chapters, have been continuously published to refresh the available data in the literature on this regard [92], [113]. The largest technical challenge for gas fermentation is the low (in comparison to chemical catalysis) volumetric productivity (V_P) and/or the low concentration of VFA [100].

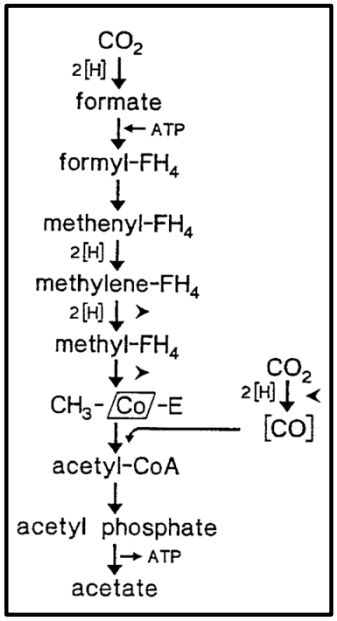

Figure 5.2: Metabolic pathway of homoacetogenic CO_2 fixation into acetate.

Given the low water solubility of H_2 (C_{aq}^*: 1.62 mg/L at 21°C and 1 bar) [114], [115] and toxicity of VFA (50% inhibition concentration, IC_{50}, of acetic acid is between 5 and 12 g/L [7]the obtainment of acceptable V_P requires an extremely high mass transfer coefficient (K_La), high density of VFA-tolerant microbes or combination of thereof.

Several studies demonstrated that methanogens-deprived MMC are able to convert H_2/CO_2 mixture into VFA. *Omar et al.* tested the capability of MMC (mesophilic digestate treated with bromoethanesulfonate, BES) for conversions of H_2/CO_2, showing a minimal (<1 gCOD/L) accumulation of VFA at batch test performed with serum bottles [116]. Same configuration was tested by *He et al*., who used thermally treated anaerobic sludge as inoculum, achieving a production of 8.5 gCOD/L from H_2/CO_2 and V_P equal to 0.5 gCOD L^{-1} d^{-1} [117].

Modestra et al. and *Katakojwala et al.* evaluated the effect of increased pressure (respectively to 2 bar and to 15 bars) onto performance of similar system (CSTR with mixing at 100 rpm) obtaining an increased V_P and/or VFA concentration at higher pressure [118] [119]. As expected by the increase in H_2 solubility with increased pressure, the maximum performance obtained with CSTR, was achieved with highest pressure, was 4.5 gCOD/L of VFA with a V_P 1.1 gCOD/L-day.

The largest improvement in VFA concentration and V_P was certainly achieved by *Wang et al*. [120], [121] and *Zhang et al*. [122], [123] which both used an innovative hollow fiber membrane reactor, already tested for syngas fermentation, achieving an increase of both VFA concentration and productivities of one order of magnitude above any previous study. The best performance achieved with such system allowed to produce 48-44 COD L^{-1} of VFA with 0.8-2.1 COD $L^{-1}d^{-1}$ [121] . Such outstanding results suggested that a way to increase both K_La and overall V_P is to provide the gas onto a large and bacterially colonizable area, thus combining the effect of increased mass transfer (due to small-semipermeable channels) and prompt gas fermentation. In principle, such features can be obtained with microtrickle bed, microstructured monolith or bio-film supporting gas sparger. Starting from this idea and considering the natural tendency of gas sparger to be colonized by biofilm, we designed a new type or reactor, namely an CBSR equipped with a monolith made of biochar/polystyrene composite. Indeed, the latter possess several features, like porosity electron conductivity, redox activity, and adsorption capability, which could be beneficial to gas transfer [124], microbial activity [125] [126] [127] and acidogenic performance

[44], [64], [101]. Aim of this work was to test such device and evaluate the performance (yield, concentration of VFA and V_P) of thereof within a reliable Power-to-VFA path based on MMC fermentation of H_2/CO_2.

5.2. Methodology

5.2.1. Char-Based Biofilm Sparger Reactor (CBSR) Manufacturing

As mentioned in the introduction, a new type of CBSR was developed and tested. The system was designed on the basis of the Biochar-Packed Anaerobic Bioreactor previously developed [25], with several modifications which were related to the specific requirements for gas fermentation at bench scale.

The char-based new sparging device consisted in cylinder with coaxial cavity which was obtained from about 30 g biochar and 15 g of polystyrene with a procedure that was detailed (Figure 4.2). The resulting monolith consisted in a cylinder with truncated cone-head with the following geometrical-physical characteristics; 11 cm of total length, 27.0 mm of outer diameter (OD), 21.0 (±2.0) mm of wall thickness, 63 cm^3 bulk volume, and 50% of porosity (Figure 5.3).

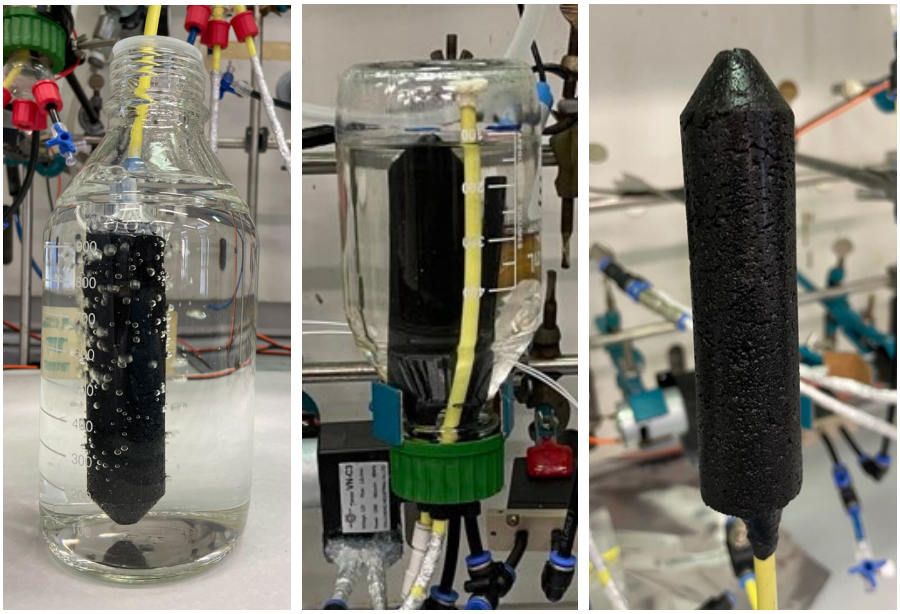

Figure 5.3: The biochar-polystyrene monolith used in this study during the initial tests (left), prior to the fermentation test inside the bioreactor (left, middle) and after the 100-days of continuous operation (right).

Briefly describing the system, the system consists in three main volumes, namely bioreactor (500 mL sized Pyrex bottle), hydraulic compensator (100 mL Pyrex bottle) and gas bags (2- and 5-liters multi-layer foil sampling bags), connected with gas and liquid pumps between each other as described in Figure 5.5**.** The bioreactor bottle was positioned upside down and equipped with a four-ported cap (submerged for minimizing gas-leaking) kept at 36 ± 0.3 °C by external heating pads. Two ports of the bioreactor cap connected to liquid input and output pipes. Other two ports were equipped with two polyamides pipes, one pipe connects the headspace of bioreactor and hydraulic compensator whereas the gas pumping pipe come from gas pump and, entering in the reactor, was tightly connected to the inner pipe of the biofilm sparger.

Given the limited size of the system, in order to hydraulically manage the change in volume of gas during gas pumping, a 100 mL, hydraulic compensation bottle was connected with the bottom bioreactor bottle. Such device, kept at room temperature, also drain the condensate and aerosols in pumped gas, thus avoids the transfer of liquid to gas bags and prevent the wearing of gas pump. H_2 was produced by means of alkaline electrolyzer and delivered to the reactor gas bags through pressure regulator (set to 0.6 bar relative pressure) and solenoid valve. A mini vacuum pump (previously tested for gas-tightness) was used to deliver CO_2 from an intermediate storage bag into the reactor gas bags. Liquid input and output were respectively provided by means of peristaltic pump and overflow. pH monitoring, remote control and reactor automation was performed by means of an Arduino board connected to a PC [25].

As above mentioned, gas fermentation was performed by means of newly developed CBSR which aims to obtain a microporous sparger colonized with a biofilm that directly convert H_2 and CO_2 into VFA, which are released into the liquid surrounding the sparger.

To maximize the rate of conversion and provide the right environment for fermentation inside the sparger, the device was operated through 3 consecutive phases, named as (i) squeezing, (ii) gas-sparging and (iii) soaking which are detailed in (Figure 5.4). Squeezing phase start when the gas circulation pump delivers a positive pressure to the liquid-filled sparger, causing the expulsion of liquid from the channels of thereof to the bulk of bioreactor. Subsequent gas-sparging phase starts as soon as the liquid is removed from the channels, and the gas fill the sparger and direct contact the microbial biofilm, until it bubbles on the external wall. Finally, the gas recirculation pump is stopped, causing the soaking of monolith channels by the surrounding broth. Such

cycling was obtained by means on-off 2.5-7.5 sec timer controlling a 1 L min^{-1} mini gas pump.

For liquid and gas inputs, which were provided every three hours, the gas pump was temporary paused to guarantee communicating vessel equilibration. Then, a set amount of liquid and gas were provided by peristaltic pumps, and overflow valve opens for 1 min, allowing an equivalent amount of fermented liquid has been discharged automatically through overflow pipe.

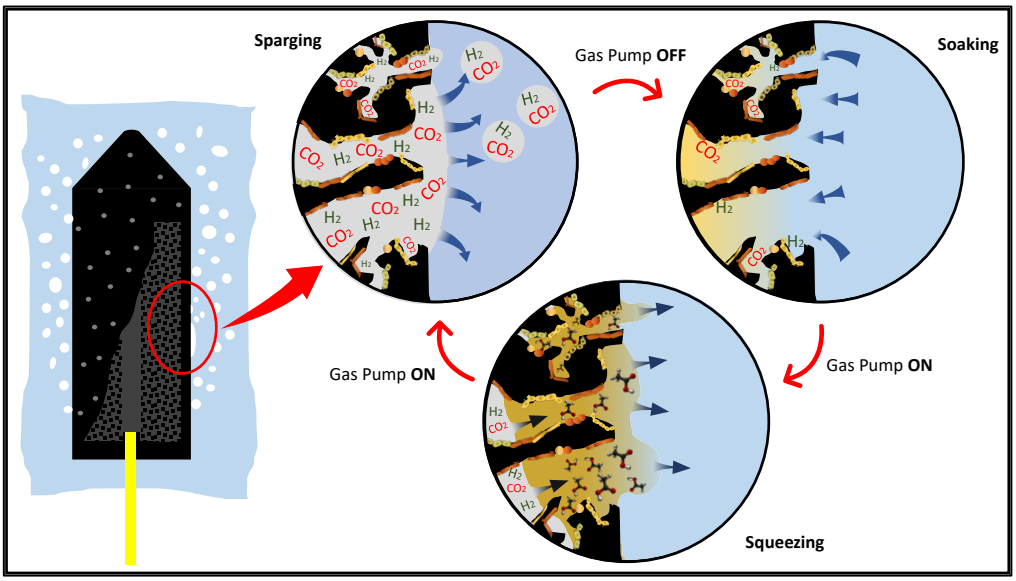

Figure 5.4: Visual description of cyclic operating principle of the char-based biofilm sparger for H_2/CO_2 fermentation into acetic acid.

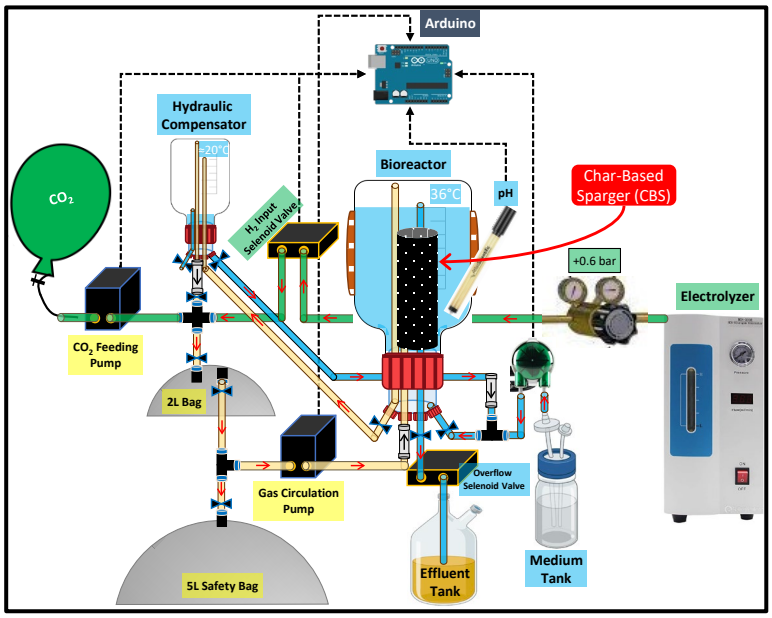

Figure 5.5: Methodological scheme of CBSR setup and connected apparatus.

5.2.2. Gas Fermentation

CBSR was inoculated with 50 ml of digestate from an industrial anaerobic digester (details in [101]), 50 ml of basal medium (Table 3.3), 20 g $NaHCO_3$ and 400 ml of distilled water. pH of this suspension was 8.5 and total and soluble COD were 5.4 ± 0.3 gCOD L^{-1} and 0.33 ± 0.02 gCOD L^{-1}.

For all the experiment, the liquid input consisted in distilled water containing 40 g L^{-1} $NaHCO_3$ (as buffer and additional carbon source) and 10% v/v basal medium (as nutrient source for microbial growth). Such composition provided a stable pH within the target slightly alkaline conditions (between 7-8 depending by partial pressure of CO_2 within the reactor) without active pH control, as previously shown by *Katakojwala et al* [119]. According to the stoichiometry of homoacetogens, H_2 : CO_2 $_{(mole:mole)}$ ratio in the feeding was kept around a stable level, which is 2.4 ± 0.5, during the whole experimental period. Excess CO_2 and H_2 (stored in the gas bags) were provided accordingly to gas consumption, and non-converted H_2/CO_2 and produced (and eventual CH_4) inside the bioreactor's gasbags were measured, analyzed and manually removed et the end of each experiment day. To suppress methanogenic activity, when more than 1% methane was detected, the liquid input was added with 25 mM of sodium 2-bromoethanesulfonate (BES) as for methanogenesis suppression.

Quantitation of H_2, CO_2 and CH_4 were performed with GC-TCD (7820A, Agilent Technologies) as previously described [128]. COD and VFA content of fermentation effluents were obtained on working daily basis. COD has been quantified by Quick-COD analyzer following the ASTM D6238-98 method based on thermal oxidation at 1200 °C. VFAs were quantified by means of solvent extraction and GC-MS through previously published method [27].

To validate the system, as well to obtain a control of gas fermenting microbiota, a twin test was performed using a reactor and reaction condition identical to that aforementioned but equipped with a commercial, aquarium-like, porous stone for gas delivery {Appendix D}.

5.2.3. DNA Extraction, Microbial Analysis (16S rRNA) and SEM

At the end of experiment, all available VFA-rich bioliquids of CBSRs and control reactor with an inert gas-diffuser were removed. Later, the bioreactors were

rinsed with an excess amount of distilled water two times and all the washing liquid was collected. Subsequently, the washing liquids and bioliquids were centrifuged for 15 min at 5000 RPM, the supernatants were discharged, and the precipitated sludges were collected separately. In addition, a representative portion of the microbially dirtied diffusers were cut. All microbial samples (suspended cakes and biofilm onto diffusers) were freeze-dried at -65 °C and 1.0 mbar vacuum conditions before the biological assays and SEM analysis. Biochar samples were gold-coated before to SEM and photographed by Philips XL30S-FEG.

Total DNA was extracted from about 500 mg of freeze-dried samples using the E.Z.N.A.® SOIL DNA KiT (Omega Bio-Tek) following the manufacturer's instructions. DNA extractions from negative controls based on laboratory aerosol (Eppendorf opened on the workbench during the extraction procedure) were conducted at the end of each extraction following the same procedure as the real samples. DNA yield was assessed using the Qubit dsDNA HS Assay Kit with a Qubit 2.0 fluorometer (Invitrogen).

16S sequencing libraries were generated using the 16S Barcoding Kit (SQK-16S024) from Oxford Nanopore Technologies (ONT), Oxford, UK, following the manufacturer's instructions. 10 ng of DNA were employed for PCR amplification, where 30 PCR cycles were chosen instead of 25 to increase reaction yield. The entire PCR process was composed of initial denaturation at 95 °C for 1 min, denaturation at 95 °C, annealing at 55 °C and extension at 65 °C for 30 cycles, followed by a final extension at 65 °C for 1 min. Negative PCR controls were also included for each batch of PCRs. Targeted samples were pooled in equimolar ratios and the pooled sample were loaded onto a MinION flow cell (R10.3, FLO- MIN111). The flow cell was placed into the MinION for the sequencing and controlled using ONT's MinKNOW 4.3.12 (Oxford Nanopore Technologies, Oxford, UK) software. The use of long-reads 16S rRNA amplicon in Nanopore MinION brings the accuracy in taxa identification to ~95 % [129].

The base-called data (fastq) were further processed using the 16S- workflow available in the cloud-based data analysis platform EPI2ME with "Fastq 16S Analysis" and the average quality of about 85 %, for demultiplexing. The reads were clustered at different taxa levels. The relative abundance of each taxa within each sample was calculated, and the taxa were sorted in descending order by relative abundance

retaining only the taxa with a relative abundance higher than 0.1 %. Microbial compositional analysis was performed using Primer v. 7 [130].

5.3. Results and discussion

5.3.1. Substrate consumption rate (H_2) and product (VFA) profiles

As described in the introduction, H_2/CO_2 fermentation test was set up in order to achieve three main targets:

- Inoculate the CBSR with natural microbial mixed culture, seed and enhance and acclimatize the bacterial biofilm within the biochar/PS sparger.
- Evaluate the performance of CBSR at different HRT (30, 60, 5.5 and 2 days), through analysis of VFA concentration/profile in liquid output, H_2 fixation rate and resulting VP.
- Evaluate the effect of HRT and resulting concentration of VFA on performance of CBSR.

Figure 5.6 shows the trend in soluble COD, which is a measure of overall gas fixation and include all soluble products of fermentation. VFA profile of the fermentation is shown in Figure 5.7. After the inoculation, the reactor was fed with 50 ml/d, which corresponds to 10 days of HRT. H_2/CO_2 conversion started almost immediately, with an increase of H_2 fixation rate (3.6 gCOD L^{-1} d^{-1} at day three) and a sharp increase in VFA (almost exclusively, namely 98%, acetic acid) concentration. Given the relatively large amount of volume that surrounds the sparger and the amount of inoculum used, such prompt start of fermentation could be due to both initial biofilm formation as well as activity of suspended biomass. To highlight more clearly the performance of biochar attached biofilm, after 5 days, the inoculated suspended biomass was removed, by centrifuging the entire liquid of the reactor for 10 minutes at 5000 RPM (≈4000 g). This operation produces a clear liquid that, interestingly shown a negligible suspended material until the end of the entire experiment. For this reason we could assume that, after day 5, biological activity was in the biofilm attached to the sparger.

After removal of suspended biomass H_2 fixation rate first slightly decreased, subsequently becomes quite variable (1.0 to 6 gCOD L^{-1} d^{-1}), and finally steadily

increases. VFA (mainly acetic acid) concentration showed roughly similar trend, with a variable concentration (12-20 $gCOD_{VFA}$ L^{-1}) that finally increased to 26.1 $gCOD_{VFA}$ L^{-1} at the end.

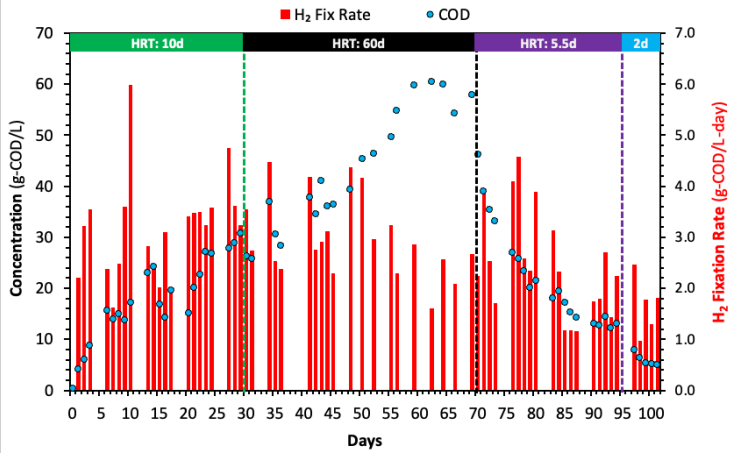

Figure 5.6: Substrate (H2) consumption rate and soluble COD profiles.

During this first stage of experiment average H_2 fixation rate were estimated as 3.2 gCOD $L^{-1}d^{-1}$, whereas volumetric productivities for soluble substances and VFA were equal to 2.8 gCOD $L^{-1}d^{-1}$ and 2.3 $gCOD_{VFA}$ $L^{-1}d^{-1}$, respectively. No significant methane production was observed, suggesting an adequate suppression of methanogens by means of the on-demand BES addition detailed in methods section. COD balance showed an average difference between H_2 fixed and soluble products generated equal to 0.4 gCOD $L^{-1}d^{-1}$, which would suggest a significant biofilm formation during this stage.

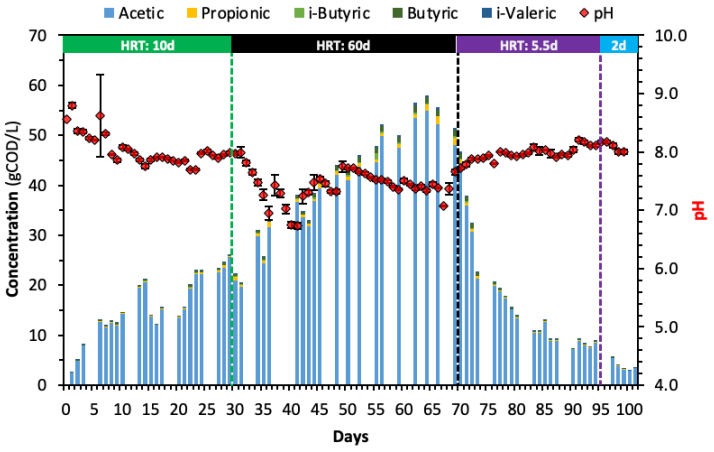

Figure 5.7: VFA and pH profile.

Even if it is difficult to establish the extent of biofilm formation, the fact that H_2 fixation rate plateaued to an average 3.5 gCOD L^{-1} d^{-1} suggested a complete colonization of the biochar-based sparger. To explore the potential of obtaining higher acetic acid titer and explore the tolerance of biofilm to VFA, the HRT was increased to 60 days. Such approach aimed to push for adaptation to higher VFA concentration (and consequential higher inhibition) as well to establish when product inhibition becomes unsustainable for the CBSR microorganisms.

After the increase of HRT, the linear increase in VFA concentration continued, suggesting a further improvement in biofilm amount and/or adaptation to higher VFA concentration. Soluble COD and VFA peaked after day 60 and reached 58 $gCOD_{VFA}$ L^{-1} d^{-1} and 60 ± 2 gCOD L^{-1} d^{-1} as highest values obtained during the study. At such point VFA consisted almost exclusively in 53 g L^{-1} of acetic acid (55 gCOD L^{-1}) with minor amount of propionic and butyric acid (both between 1.3 – 1.6 gCOD L^{-1}).

Indeed, the maximum VFA concentration achieved at such stage, at the best of author knowledge, it is the highest VFA concentration ever achieved by anaerobic acidogenic MMC [131], and almost comparable to the highest levels (70-80 gCOD L^{-1}) that can be obtained by ethanol oxidizer bacteria (e.g. *acetobacter*) [132]. Such striking results suggests a large improvement of the rate of H_2/CO_2 fermentation together with a marked mitigation of VFA toxicity. Such phenomena, whose reasons will be discussed in detail in subsequent sections, was previously reported for biochar supported microorganism within anaerobic digestion environment [133].

To relief the VFA inhibition, as well to evaluate the actual relationship between V_P and VFA concentration for the biochar-attached biofilm the value HRT was stepwise decreased to 5.5 and 2 days. Such change in HRT lower VFA concentration by dilution and should obtain, in principle, higher VP with lower VFA concentration. As expected, upon decreasing HRT, VFA concentration decreased to 13 gCOD L^{-1} in 15 days (3 x HRT). Nonetheless, as results of lower concentration of inhibitory VFA, actual V_P values remained quite low in comparison with that observed with 10 d of HRT, until HRT was decreased further to 2 d and VFA concentration became 5 gCOD/L. After that further dilution, V_P raised back to 1.8 $gCOD_{VFA}$ L^{-1} d^{-1} with subsequent increasing trend.

Looking more in detail to the relationship between 7-days-average V_P and actual VFA concentration of each week, comparable results were found in the 0-40 gCOD L^{-1} range, whereas V_P halved at around 50 gCOD L^{-1} and becomes negligible at more

than 55 gCOD L^{-1}. Overall, the V_P was mainly related to VFA concentration and, more specifically, on the level of exposure to VFA in the 10 days before. In practice the biofilm has shown consistent performance when the VFA concentration was less than 40 gCOD L^{-1} (before day 48 and after day 70) with lower performance when the VFA concentration has been above that concentration and shortly thereafter such VFA peaking event (up to 10 days after).

Noticeably, this means that 100% inhibition concentration (IC_{100}) for biochar supported biofilm would be at least one order of magnitude higher than that reported for anaerobic and aerobic microorganisms [7]. Such noticeable tolerance of biochar-attached biofilm could be due to some specific feature of biochar supported microbiota [125] and, together with an increase of K_La from CBSR configuration, could explain the outstanding VFA concentration as well as the high V_P obtained.

5.3.2. Comparative Performance Evaluation

Table 5.1 provide a summary of the average results obtained along the study, highlighting some performance indicators for CBSR. Achieved products (VFA and other soluble products) concentration and V_P were mainly related to HRT of the system. VFA were the main fermentation products irrespective to the HRT used, as expected by the higher thermodynamic stability of such compounds within pH and H_2 pressure here used [5]. Nonetheless, a significant production of other soluble products (e.g. ethanol and other non-analyzed soluble substances) was observed during operation at shorter HRT (1, 5.5. and 10 d), suggesting a non-equilibrium stage at the beginning of the experiment and after steep changes of HRT.

Average V_P ranged between a minimum of 0.8 $gCOD_{VFA}$ L^{-1} d^{-1}, obtained in correspondence of 60 days HRT and with an average VFA concentration equal to 55 $gCOD_{VFA}$ L^{-1}, and a maximum of 2.3 $gCOD_{VFA}$ L^{-1} d-1, obtained during the first phase of operations performed at 10 days HRT.

As mentioned in previous paragraph, V_P was influenced by VFA concentrations (in turn influenced by HRT) but in a relatively complex way. In instance, when the HRT were changed to 5.5 d, and VFA concentration halved, V_P stay sticked to the relatively low values observed with 60 d HRT, with an increase that re-started only after further decrease of HRT to 2 d.

Table 5.1: Performance parameters for CBSR operations with different HRT.

Days	**1-30**	**31-70**	**60-70**	**70-94**	**95-100**
HRT	10	60	60	5.5	2
Solubles ($gCOD_{SOL}\ L^{-1}$)	19	45	59	22	5.8
VFA ($gCOD_{VFA}\ L^{-1}$)	15	42	55	17	3.8
COD_{VFA}/COD_{SOL}	85%	96%	95%	72%	66%
V_P ($gCOD_{VFA}\ L^{-1}\ d^{-1}$)	2.3	1.6	0.8	1.4	1.8
V_P ($gCOD\ L^{-1}_{sparger}\ d^{-1}$)	18.2	12.7	6.3	11.1	14.3

When considering absolute value of V_P, it is important to notice that, given the practical limitations we faced for this study (standard glass bottle and non-optimized sparger shape), such data were obtained with a large amount of the reactor (88%) that was actually non-biologically active. This means that the CBSR reactor could be drastically improved just by reducing the amount of liquid around the sparger or by an optimization of reactor geometry. Given that optimization would be trivial to made at higher reactor scale, it can be useful to calculate a "corrected" V_P, taking into account just the sparger volume. This V_P, hereafter named optimized V_P, corresponds to the V_P obtainable with an optimized CBSR reactor which is completely filled with the sparger. On the basis of this calculation, the optimized V_P (fifth row of Table 5.1) would be between a minimum of 6.3 $gCOD_{VFA}\ L^{-1}\ d^{-1}$, when delivering a 59 $gCOD\ L^{-1}\ d^{-1}$ solution with 55 $gCOD_{VFA}\ L^{-1}$ VFA content, and a maximum equal to 18.2 $gCOD_{VFA}\ L^{-1}\ d^{-1}$, when delivering VFA at 15 $gCOD_{VFA}\ L^{-1}$. Table 5.2 provides the comparison of such VPs and optimized VPs (at high and low VFA concentration) with the available literature related to H_2/CO_2 fermentation with MMC. Looking to actual V_P, as $gCOD_{VFA}\ L^{-1}\ d^{-1}$, CBSR performance was actually between the data obtained with standard CSTR (or similar systems) and high performing HfMBR, with absolute V_P similar to that obtained with pressurized CSTR. On the other hand, the optimized V_P ($gCOD_{VFA}\ L_{sparger}^{-1}\ d^{-1}$) is actually the highest V_P ever obtained in conversion of H_2/CO_2 to VFA with MMC, with absolute values that are close to that obtained in high performance industrial fermentation process (e.g. glucose fermentation to ethanol [134]).

Table 5.2: Comparison of H_2/CO_2 fermentation performance between CBSR and the literature studies based on MMC.

Reactor Type	**T** *°C*	**pH** -	**HRT** *d*	**C_{VFA}** *gCOD L^{-1}*	**V_P** *gCOD L^{-1} d^{-1}*	**Reference** -
HfMBR	35	*4.5-4.8*[a]	27	13.6	0.5	[135]
HfMBR	35	4.5-4.8[a]	9	3.9	0.5	[135]
HfMBR	35	6.0[a]	64	11.2	0.2	[135]
HfMBR	55	6.0[a]	46	42.8	2.1	[121]
HfMBR	55	6.0[a]	110	44.9	2.1	[121]
HfMBR	55	6.0[a]	2.5	20.7	8.2	[121]
HfMBR	55	6.0[a]	1.0	11.2	11.2	[121]
HfMBR	55	6.0[a]	0.5	4.5	9.0	[121]
HfMBR	55	6.0	0.5	4.5	9.0	[121]
HfMBR	55	6.0	1.0	11.2	11.2	[121]
HfMBR	55	6.0	2.0	2.1	10.3	[121]
HfMBR	25	6.0[a]	98	46.2	0.5	[120]
HfMBR	25	6.0[a]	58	48.2	0.8	[120]
Serum bottle	37	6.0	10	0.2	< 0.1	[116]
Serum bottle	37	6.0	10	0.3	< 0.1	[116]
Serum bottle	37	6.0	10	0.2	< 0.1	[116]
Serum bottle	37	6.0	10	0.3	< 0.1	[116]
P-CSTR[b]	30	6.5	2	1.0	0.5	[118]
P-CSTR[b]	30	6.5	2	1.0	0.5	[118]
P-CSTR[b]	30	6.5	2	1.3	0.7	[118]
P-CSTR[b]	30	6.5	2	0.6	0.3	[118]
P-CSTR[b]	30	6.5	3	2.5	0.8	[118]
P-CSTR[b]	30	6.5	3	1.1	0.4	[118]
Serum bottle	25	6.0	17	8.4	0.5	[117]
HfMBR	25	7.5-8.0[a]	23.7	6.9	0.3	[136]
P-CSTR[b]	28	6.5	4.0	3.7	0.9	[119]
P-CSTR[b]	28	7.5	4.0	4.0	1.0	[119]
P-CSTR[b]	28	8.5	4.0	4.5	1.1	[119]
CBSR	36	8.5	10	15	2.3	This study
CBSR	36	8.5	10	15	18.2	This study
CBSR	36	8.5	60	55	0.8	This study
CBSR	36	8.5	60	55	6.3	This study

HfMBR: Hollow fiber membrane reactor; C_{VFA}: concentration of VFA delivered in the effluent; VP: VFA volumetric productivity; [a] pH control with chemostat. [b] Pressurized reactor above 1 bar of H_2.

In conclusion, un-optimized CBSR (with feature identical to the device here used) can be already considered a low-cost device, which can be manufactured in simple way from biochar and polystyrene waste (PS foam waste), allow the production of a quite concentrated solution of VFA with acceptable V_P. Such system can be improved with some changes in geometry of the system, achieving V_P and concentration that is potentially outstanding. Such results probably come from a combination of various enhancement that owe to the presence microstructured system within biochar, like physical increase of K_La, DIET and increase of microorganisms' tolerance toward VFA.

5.3.3. SEM Photos and DNA Sequencing of CBSR Microbiota

SEM photos of biochar and manufactured biochar/PS composite shows the typical xylem-derived structure (Figure 5.8, left and middle pictures), with 10-20 μm communicating channels which can, in principle, provide a support for growth of prokaryotes and a media for Direct Interspecies Electron Transfer, abbreviated as DIET [87], [137]. Looking to SEM picture of biochar/PS monolith after the 100 days experiment (Figure 5.8, right) it is possible to notice the presence of bacillus and cocci-like shapes, and minor number of other shapes, which can be considered as microorganisms.

Beside the large heterogeneity of the samples, and lack of data about hidden surfaces, the overall density of microorganisms in the biochar cavity can be considered comparable to that observed in previous investigations about biochar attached microbiota [138], and suggests a close interaction between the microorganism and the supporting material.

In order to highlight the main microorganism involved in H_2/CO_2 fermentation within the CBSR, the microbially colonized sparger was subjected to 16S rRNA Gene Sequencing. In addition, to highlight the actual role of biochar/PS monolith in supporting biofilm growth, biomass withdrawn from the fermentation liquid of CBSR and from a standard H_2/CO_2 bubbled CSTR were subjected to the same characterization procedure.

Figure 5.9, shows the taxonomic composition of microbiota of CBSR biofilm, CBSR suspended biomass, as well as bubbled CSTR biofilm (microorganism that fouled the commercial porous stone) and CSTR suspended biomass.

Such analysis shows that, even starting from quite biodiverse inoculum (taxonomic composition in [101], the fermentation of H_2/CO_2 selects, over long time, one genus, which is probably the most competitive one in term of gas utilization and VFA tolerance.

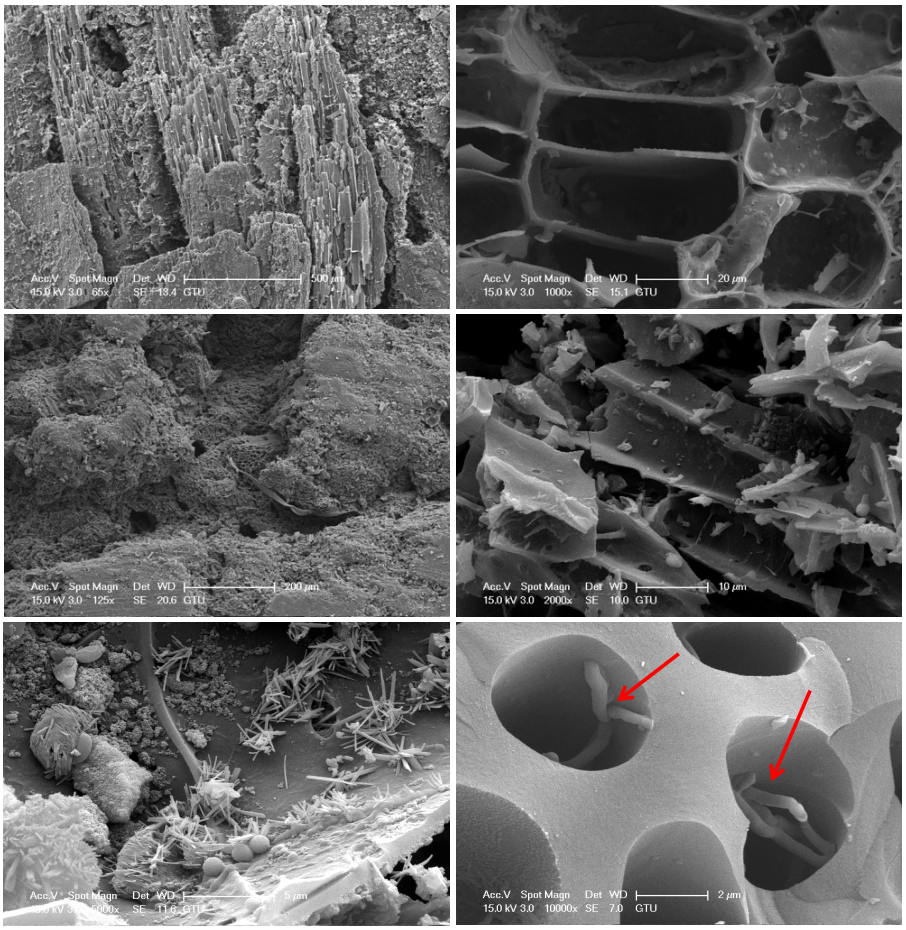

Figure 5.8: SEM photographs of; biochar as raw material (up), clean char-based sparger (middle), and microbially colonized sparger after the experiment (bottom).

CBSR become selectively enriched in a single genus, namely *Acetobacterium,* which actually include some of the most known gas fermenting strains, namely *Acetobacterium woodii* is one of the best characterized strains able to use the Wood–Ljungdahl Pathway or CO_2 Reduction [139]. Such *Acetobacterium* enrichment fits very well with the abundant fusiform like shapes detected within SEM picture, which are similar to that of *Acetobacterium woodii* previously reported [140]. A similar single-genus enrichment was also observed in H_2/CO_2 bubbled CSTR, which showed

a microbiota almost totally dominated by *Clostriudium.* Interestingly, the composition of minor amount of suspended microbiota in CBSR is comparable with that of biofilm on the sparger. In a specular way, the relative composition of microorganisms found in porous stone of CSTR is almost identical to that of CSTR suspended biomass, but with a significant enrichment of *Acetobacterium* genus. This suggests that, although *Acetobacterium* is favored in biofilm formation, the largest population share, namely suspended one for standard CSTR and biofilm one for CBSR, rules the entire reactor microbiota.

Although is difficult to find comparable conditions and study length, this selection of a single genus was previously shown by several authors, which observed an increased dominance of *Clostridium* [117], [120], [141] or *Acetobacterium* [136] upon feeding with H_2/CO_2 as sole feedstock. Nonetheless, the degree of selection observed during this study was more marked than those previously observed, with just one dominant genus, namely *Acetobacterium,* which account for more than 90% of the microbiota. Moreover, even if the inoculum and conditions (T, P, pH, time) were identical, the evolution of microbial composition of CBSR was totally different from that observed for H_2/CO_2 bubbled CSTR highlighting a clear role of biochar in selection of *Acetobacterium* over *Clostridium*.

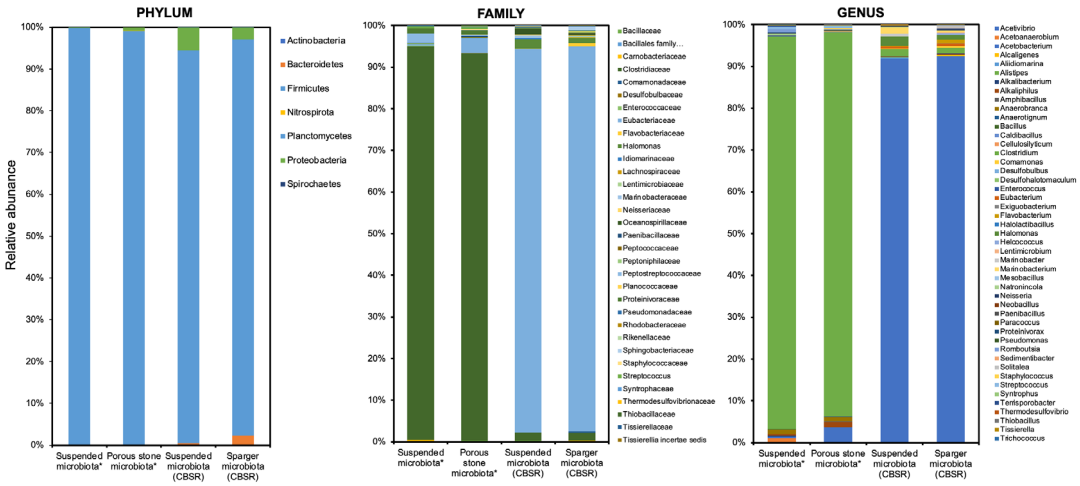

Figure 5.9: Taxonomic analysis of microbial communities found in CBSR and conventional bubbled CSTR fermenting H_2/CO_2 (only phyla with a r.a.> 0.5% in families or genus with a r.a. >0.1% in at least 1 sample were showed).

Some reason for this effect can be found in some peculiar interactions between *Acetobacterium* and biochar. For instance, *Acetobacterium woodii* is known to use

aromatic compounds as electron acceptor [142], as electron donor [143] and/or obtain electrons from conductive material (within microbial electrosynthesis cell [144]).

Such features of *Acetobacterium* could be extremely advantageous in the peculiar environment of biochar-based sparger, providing a way for indirect (through a chemical mediator) and/or direct (through polyaromatic structures) interspecies electron transfer. Such mechanisms could play a role in providing a higher V_P, as well as to cope with higher VFA concentration and related toxicity. In principle, when microbiota can perform interspecies electron transfer (namely DIET or transfer through chemical mediator) just a portion of the bacteria, which reducing CO_2 to VFA, is subjected to the adverse effect of VFA. Whereas the H_2 oxidation can be performed in a spatially different location. Being the H_2 solubilization/oxidation the limiting step within the H_2/CO_2 fermentation [145], a healthier (shielded from VFA) H_2 oxidating biofilm could increase the overall rate of homoacetogens when VFA are at high concentration. In addition, given that biochar contains free radicals which could react chemically with H_2 [146], the bacteria that can use biochar as source of reducing power could circumvent H_2 solubilization steps. Although it is out of the scope of this paper to establish exact type/extent of mechanism for biochar enhancement of H_2/CO_2 fermentation, the phenomena observed suggests several interesting aspects of microbiota-biochar interaction that could be explored in future.

5.4. Conclusion

A novel char-based biofilm reactor was proposed, designed, manufactured, and tested for H_2/CO_2 acidogenic fermentation experiment with MMC. The system was monitored during a 100-day continuous fermentation experiment, changing HRT and evaluating the effect on V_P and concentration of VFA. Using HRT higher than 5.5 days, the system demonstrated a V_P in the 0.8 – 1.3 $gCOD_{VFA}\ L^{-1}\ d^{-1}$ range, delivering a VFA concentration higher than 15 $gCOD\ L^{-1}$. Such performance, which was obtained using only a portion (1/8) of reactor volume, was actually close to that obtained with hollow fiber membrane reactor, and can be drastically improved by simple geometrical adaptations, to reach a V_P in the 6-18 $gCOD_{VFA}\ L^{-1}\ d^{-1}$ range. Besides this, an extraordinary peak VFA concentration equal to 58 $gCOD\ L^{-1}$ was achieved at 60 days residence time operation. To the best of authors knowledge, such VFA concentration was actually the highest concentration ever obtained by anaerobic microbial

communities, and the survival of biofilm in such extreme conditions could indicate the creation of a quite peculiar environment within the biochar-based sparger.

From SEM observation and 16S rRNA Gene Sequencing, it was possible to demonstrate that biochar stimulated the growth of bacteria belonging to *Acetobacterium* genus, which colonizes the xylem derived cavities. Some species in that genus are known to be able to interact with biochar structure (through DIET and other indirect electron donation/withdrawal), and this could suggest that the interaction between *Acetobacterium* and porous conductive structure of biochar could be pivotal for the overall rate of conversion within a VFA-stressed system.

According to the results obtained, CBSR can be considered as a novel reactor with improved gas fermentation performances. Given the low cost of biochar/polystyrene sparger and simple manufacturing, the CBSR reactor can be already proposed as a replicable strategy for gas fermentation approaches to obtain building block chemicals and/or commodity chemicals.

6. VFA TO PHA BIOCONVERSION

Plastic waste pollution has become a significant environmental global pollution in the last decades. Due to their physicochemical persistent characteristics and fossil-based origin, plastic waste pollution has been considered as one of the most significant environmental problems. Conventional petroleum originated plastics are recalcitrant chemicals in nature and threaten all living forms. For this reason, innovative plastic-like biodegradable polymers are quite interesting alternatives to the conventional plastics. PHA are one of the most advantageous biopolymers with a biodegradable characteristic and non-fossil based origin, as an alternative to petroleum-based plastics. In this study, a new continuous mode combined PHA enrichment and accumulation micro-plant was designed, developed, and tested for evaluating the PHA production potential of VFA rich streams, within a microaerophilic-aerobic hybrid biological pathway.

6.1. Introduction to PHA Bioaccumulation

Plastics are obtained by the polymerization of hydrocarbons obtained from fossil carbons such as petroleum, whose name originated from the "plastikos" word used to mean shapable in Greek language. By means of the unique properties of plastics (e.g. easy-to-shape structure, lightness), plastic materials are one of the most widely used commodity chemicals in a lot of different applications such as construction, electronics, automotive, healthcare, packaging, painting, coating, and etc. [147]. However, due to their fossil carbon origin and refractory characteristics, they become persistent in the nature and exposing a public health threat. Plastic pollution is one of the most significant global anthropogenic problem, which has been considered for causing irreversible natural problems. Conventional plastics also threaten many ecosystems by polluting the soil, water and air either in a direct or in-direct ways.

Biodegradable plastics (i.e. bioplastics, biopolymers) are environmentally friendly plastic-like materials, can be decomposed by living organisms in the environment. As one of the bio-based polymers, PHAs are a group of biopolymers that can be accumulated by various microorganisms as an intracellular carbon and energy reserve, under specific conditions where carbon resources are excess, and growth is restricted by means of stressing conditions (e.g. lacking nutrient, limited oxygenation)

[148] VFA are the most favored carbon source for PHA bioaccumulation by means of several different metabolic pathways. Because these fatty acids are direct metabolic precursors in the PHA biosynthesis pathway [149]. Many of the PHA accumulator strains are capable of utilizing VFAs as carbon source for their metabolic activities, including PHA accumulation. Polyhydroxy butyrate (PHB) is the most common PHA type, and they show some functional thermoplastic properties such as, melting point at 180 °C, high crystallinity (55-80%), low-moderate flexibility (2-10%), and glass transition temperature at 4 °C.

There are two main biological processes existing for the production of PHA-rich sludges. First is called as aerobic dynamic feeding process (ADF) and it was found as early as 90s. Working principle of ADF systems is depended on following the 'feast and famine' cycles which means that two operational phases, one with excess carbon (feast) and another without (famine), are applied to enrich the peculiar aerobic PHA accumulating strains [150]. On the other hand, anaerobic–aerobic (An/Ae) process that is also called as enhanced biological phosphorus removal process (EBPR), is a common phenomenon seen in advanced biological wastewater treatment plants with anoxic phosphorus removal stage. The chemical energy obtained through the hydrolysis of polyphosphates, are used to capture external carbon feedstock for intracellular accumulation of PHA under anaerobic/anoxic stage [151]. Later, accumulated PHA are degraded in aerobic section followed by an increase in polyphosphates inside the cells. In that case, mainly the PHA accumulating microbes can survive in aerobic famine phase which is enrichment principle of the An/Ae bioprocesses. *Ahmadi et al.* studied the performance difference between ADF and An/Ae (EBPR) processes for PHA accumulation potential of mixed cultures and reported that anoxic-aerobic (or in other names, microaerophilic-aerobic) integrated biological processes are extremely more advantageous over to ADF, in terms of both average PHA content of cells and energy consumption [152]. Nonetheless, more detailed metabolic discussions are available in the literature [153]–[155]

6.2. Methodology

A continuous plant suitable for conversion of 1 L/d of syngas fermentation broth was designed on the basis of microaerophilic-aerobic MMC-based process, proposed by *Satoh et al*. [155] with some modifications (Figure 6.1). The system was inoculated

with a 0.5 g of mixture of lyophilized PHA accumulating sludge obtained from operations of feast and famine SBR of B-PLAS DEMO plant [156], [157].

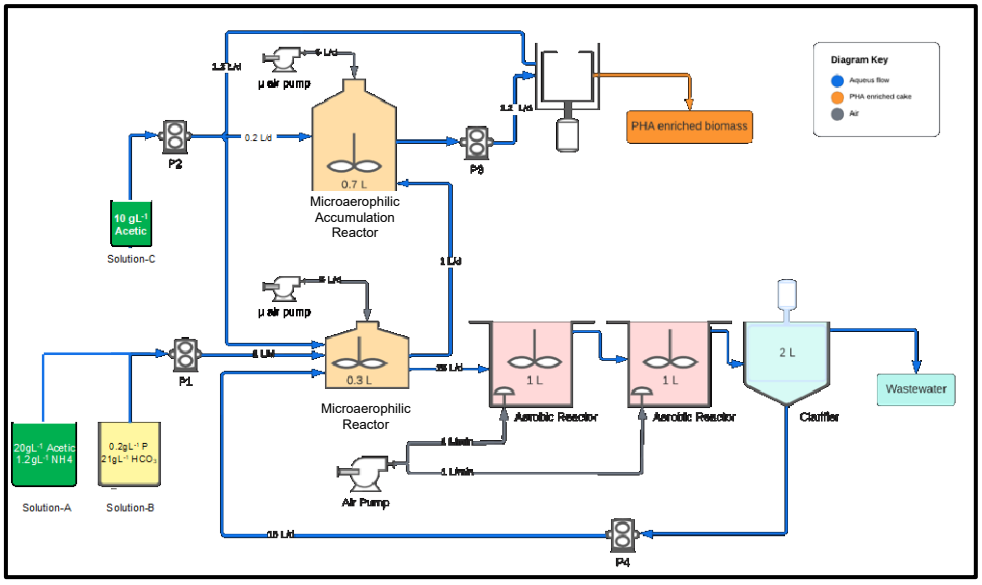

Figure 6.1: Continuous anoxic-aerobic combined biological system (micro-plant) for conversion of VFA-rich effluent into PHA enriched bacteria.

The system includes the structure with the inclusion of anoxic or microaerophilic accumulation stage within the system as proposed and tested by *Satoh et al.* [155] in batch mode. The working principle of the developed microaerophilic-aerobic hybrid micro-plant was depending on the idea of stressing conditions not through by only feast-famine conditions, yet with an additional positive selection via microaerophilic conditions at feast zone. Briefly it consists of two microaerophilic reactors, which consists in a pair of connected stirred glass bottle (1 L total) positioned at different heights in order to have one with 0.3 L (microaerophilic/anoxic reactor) and the other one with 0.7 L (microaerophilic accumulation reactor). The two bottles were mixed with 500 rpm stirrer and purged with a regulated amount of air, namely 5 L/d, through a micro-air pump managed by a timer.

The microaerophilic reactor was connected to two consecutive aerobic reactors and a subsequent 2 L clarifier. Sequential multiple aerobic reactors were designed to guarantee famine conditions in at least one reactor of the system, considering the possibility receiving minor amount of carbon from microaerophilic zone. Aerobic reactors were mixed with pulsed high-speed impellers (100 rpm for 2 seconds per minute) and aerated, through a porous stone, with 1 L/min of pre-moisturized air (to

avoid excessive evaporation in such small scale). Clarifier consisted of 2 L Imhoff cone equipped with a hydraulic overflow and 2 rpm scraper that continuously remove the settled sludge from the wall. In experience, PHA accumulating MMC was found to has a more settable characteristic.

A peristaltic pump was used to transfer 15 L d^{-1} settled sludge and recirculation flow from the bottom of the clarifier to microaerophilic reactor, whereas a 1.2 L d^{-1} pump was used to withdraw PHA enriched microbial slurry from the system, through the microaerophilic accumulation section, and pump it into a 2 cm radius solid basket centrifuge (3000 g) which separates the cake (≈15% dry-matter) and sent back the reject water free from suspended matters back to the microaerophilic reactor.

To demonstrate the VFA-to-PHA conversion, 1 L d^{-1} of synthetic syngas fermentation effluent (combination of Solution-A and Solution-B) was provided to microaerophilic reactor and 0.2 L d^{-1} of synthetic nutrient (N/P) deprived fermentation effluent (Solution-C: 10 g L^{-1} acetic acid) was provided to the microaerophilic accumulation reactor (Table 6.1). The reason behind the splitting of microaerophilic zone into two reactors was for pushing the accumulation reactor for reaching its maximal PHA accumulation potential by providing only carbon.

6.3. Results and Discussion

6.3.1. PHA accumulation capacity of syngas fermentation effluent

As mentioned above, to provide a proof-of-principle demonstration of the VFA-to-PHA concept, a synthetic solution with a chemical composition similar to that of fermentation effluents was provided to a fully continuous bench scale plant for production of PHA enriched bacteria, based on microaerophilic-aerobic MMC process. Such plant was used as a micro-demonstrator, therefore a continuous collection of PHA enriched biomass was undertaken, evaluating the stability of the process as consequence of constant biomass removal rate. Figure 6.2 shows the trend of PHA content (w/w_{dry}) during the study. The system was inoculated with frost lyophilized MMC (already adapted for PHA production) and operated without accumulation and biomass recovery for about 1 week. Interestingly, such procedure, induced a relatively fast start in the accumulation capacity of the bacteria, as revealed by increase of volatile suspended solids (VSS) and by the PHA content. VSS increased

from almost zero to 1 g L^{-1} in one week and PHA content reached to 30% w/w. Meanwhile soluble COD in last aerobic reactor were always close to the value predicted by the ammonia's COD content, suggesting the presence of a famine conditions. According to that observation, the system was switched to standard operation, with accumulation stage and biomass recovery. Even with biomass recovery, the amount of VSS doubled in the subsequent week, with PHA content that reacted 50% in the collected biomass.

Table 6.1: Synthetic fermentation effluents used for micro-plant.

	Chemical Compounds	Concentration (mg/L)
Solution-A	CH_3COOH	20,790
	NH_4OH (30%)	1,212
	$CaCl_2$-$2H_2O$	94
	$MgSO_4$-$7H_2O$	189
	KCl	66
	$FeCL_3$	3.76
	Titriplex III (EDTA)	5.68
	$ZnSO_4$-$7H_2O$	0.19
	$MnCl_2$-$4H_2O$	0.06
	H_3BO_3	0.57
	$CoCl_2$-$6H_2O$	0.38
	$NiCl_2$-$6H_2O$	0.04
	$CuCl_2$-$2H_2O$	0.02
	$NaMoO_4$-$2H_2O$	0.07
Solution-B	Na_2HPO_4-$12H_2O$	2,640
	$NaHCO_3$	19,800

Such parallel increase of PHA content and biomass concentration provided a final PHA yield ($gCOD_{PHA}/gCOD_{VFA}$) that was in line with the literature about conversion of VFA to PHA by means of MMC [51], namely 30-45% yield observed between 10 and 14 days of operations (Figure 6.3). After biomass production peaking, the system suffered some operational problems which impacted on the amount of suspended biomass in all reactors, which drops to low level. As a result, the system was inoculated with lyophilized biomass obtained (as back-up) at day 14 and operated without accumulation for two weeks. After 28 days, standard operational method

restarted. PHA content and VSS stayed lower than previous period. Yet, it showed a constant improvement over time by means of VSS and PHA content, which increased gradually, and finally stabilized to 2-4 g-L^{-1} and 40-50% PHA content. As a whole the trend suggests a significant variability of the system, especially as consequence of external shocks, nonetheless it provided a general indication of stability of the conversion of effluent obtained from syngas fermentation into PHA.

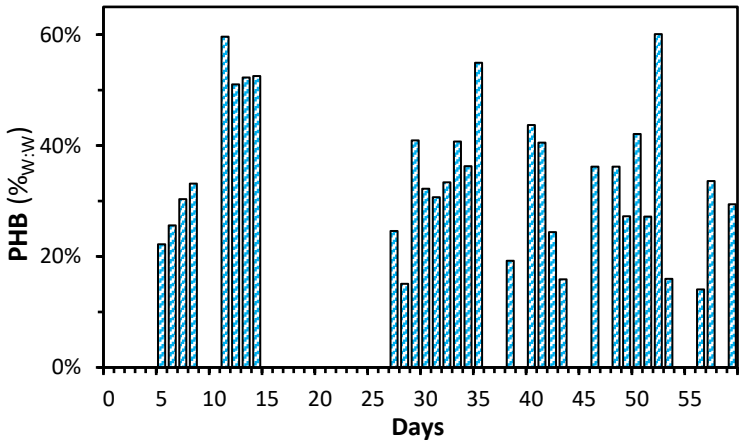

Figure 6.2: PHA level of enriched biomass obtained by VFA-to-PHA microplant.

Considering the performance of VFA-to-PHA yield, even in very high PHA content were obtained, the overall yield (for the entire experiment) of micro-plant test was 0.16 $gCOD_{PHA}/gCOD_{VFA}$, such data is less than half that previously demonstrated in SBR [51] reactor based on feast-famine cycle, revealing some under performances in total biomass produced. Such phenomena were mainly due to operational problems between day 15 and 27 and especially to variable/low biomass yield in the late part of the experiment. The latter phenomenon was related to the fact that a relatively long (up to 10 days) sludge age was used, which calculated as total biomass in the system (VSS plus biomass which fouls the surfaces) dived by the biomass that was recovered per day. In terms of bacterial energetics, higher sludge age means more bacteria maintenance and lower sludge yield [158]. Since the final PHA content is high, we can assume that the level of adaptation of MMC, even in the final part of the experiment, was quite good [154]. Therefore sludge age could be decreased to obtain higher microbial biomass yield. Such effect was actually clear in the beginning of the study when, in spite of low biomass concentration, the system was operated with lower sludge residence time (SRT), providing PHA yield as high as 45%.

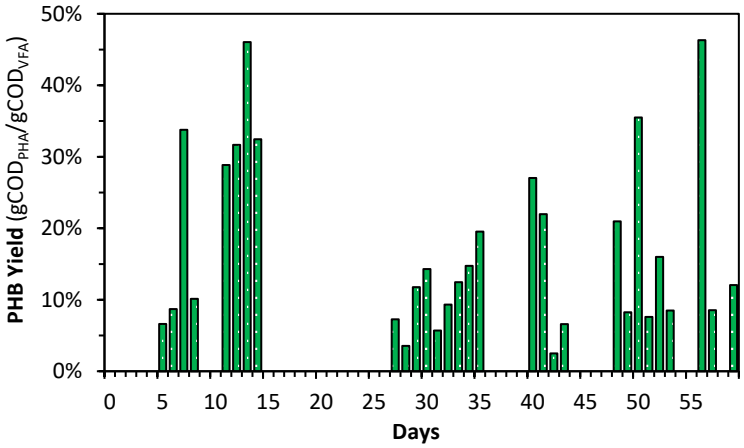

Figure 6.3: PHA yields during continuous operation of VFA-to-PHA microplant.

6.4. Conclusion

The new fully continuous microaerophilic-aerobic biological micro-plant was operated for two months for evaluating the PHA accumulation potential of the VFA rich effluents obtained by the anaerobic fermentation process as the secondary stage of the developed biorefinery. In summary, the new micro-plant, was found successful for enriching PHA accumulating peculiar MMC, since PHB content of the produced sludges were reached up to 60% levels in dry matter basis. On the other hand, VFA-to-PHB yields were also promising by means of maximal values obtained around 45%$_{COD}$ yet an equilibrium condition could not be sustained. However, yields might be increased by means of lowering the SRT followed by a longer adaptation.

Figure 6.4: Example of an extracted PHA polymer obtained from this study.

7. OVERALL CONCLUSION

At the first process of developed biorefinery, namely thermochemical conversion, biomass was subjected to pyrolysis under different temperatures followed by biochar gasification process, to obtain high yields of fermentable (i.e. bioavailable) materials such as syngas and WS. As a result, pyrolysis of wooden biomass at either 450 °C or 550 °C coupled with the gasification of biochars obtained through the biomass pyrolysis, was found to be useful to obtain bioavailable products which conditions provided up to 66% COD yield for bioavailable products {Chapter 2}. However, due to the slightly higher yields (>0.5% $_{COD}$) of bioavailable compounds at low temperature (450 °C) pyrolysis followed by biochar gasification, was appeared to be revealing the most suitable scenario for the proposed HTB system.

Later, the water-soluble fraction of pyrolysis liquids was subjected to acidogenic anaerobic fermentation within a special biochar-packed reactor [25] for upgrading the VFA content of such anhydrous-sugar (e.g. levoglucosan) rich materials. This was the first acidogenic bioconversion test of pyrolysis liquids in the literature, to the best of our knowledge. Although some difficulties were faced during the initial fermentation tests of WS materials, external glucose aided bioaugmentation approach was found a promising strategy for enriching peculiar microbial consortia which are capable of degrading pyrolysis products (named as *pyrotrophs*) with the help of positive selectivity of biochar material as one of the main products of thermochemical conversion. At the end, around 600 mg$_{COD}$/L-day volumetric productivity was recorded by the developed anaerobic system for producing VFA-rich effluents [101].

In later sections where gas fermentation strategies are involved in, a novel CBSR was developed for taking advantage of biochars' physicochemical characteristics which were previously found as a quite promising method for, increasing product yields; stabilization of bioconversion; immigration of inhibition phenomena; positive selectivity of microbial communities. At either with biomass derived syngas or renewable power originated H_2 and CO_2, it was found that the CBSR is a quite promising biological tool with a volumetric productivity up to 18 g$_{COD}$/L-day. The maximum tenable VFA concentration levels were detected around 9 g$_{COD}$/L and 58 g$_{COD}$/L for syngas and H_2/CO_2 fermentation, respectively. Such extreme difference in the maximum VFA levels for different gas substrates, can be speculated with a possible

different microbial consortium formed on CBSR depending on the gas substrate. For instance, for H_2/CO_2 fermentation experiment with an extremely high VFA tolerance level, the only abundant gene was Acetobacterium, which is known to be quite intolerant to CO as the main gas of syngas. According to this we can assume that CBSR system can serve as a quite productive biological gas fixation tool for either C1 or H_2 gasses, yet with a different VFA concentrations at output. At this point, it can be noted that CBSR integrated power-to-x approach can serve as a direct way to produce green chemicals (namely, acetic acid), thanks to the very high aqueous product concentration which allows traditional extraction methods. In the case of hybrid thermochemical-biological approach where CO-rich syngas is used as substrate, CBSR can serve as an intermediate process for the subsequent unit that can utilize VFA-rich aqueous effluents such as PHA accumulation systems, as it was proposed by this study.

Lastly, a fully continuous innovative micro-plant for biological upgrade of obtained VFA-rich streams into biopolymers (namely PHA) were developed, which was developed on the basis of microaerophilic-aerobic selection of peculiar PHA accumulation consortia. This biological microplant was provided promising yields of PHB rich cakes (up to 55%$_{COD}$) converted from acetate feeding which was representing the VFA-rich effluents of previous anaerobic fermentation processes within this new biorefinery schema.

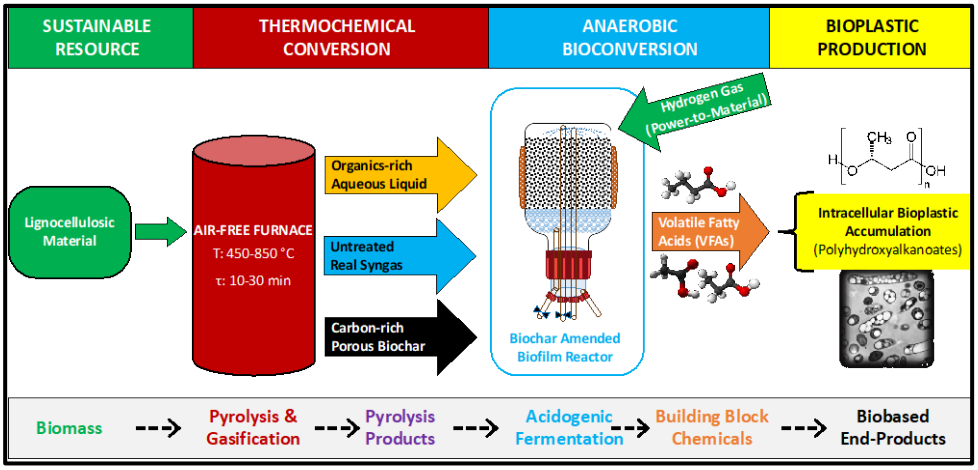

Figure 7.1: Simplified flow-diagram of the proposed new biorefinery.

According to the optimized conditions of each sub-process, "Sankey" flow-diagrams on COD basis, were made for each biorefinery scenario; namely, HTB and power-to-x. In conclusion, hybrid thermochemical-biological schema optimized for

the revalorization of lignocellulosic biomass, was corresponded a 24% net yield of intracellular polyhydroxyalkanoates (Figure 7.2). In comparison, power-to-x approach where water electrolysis derived H_2 together with CO_2 were used as the feedstock, was revealed a better performance for plastic-like sustainable PHA production with 24% of net COD yield (Figure 7.3). Being the fact of techno-economic analysis and life cycle assessment of the proposed biorefinery schemas were beyond the scope of this work, it is not realistic to choose one scenario to another for scaling-up. Future efforts are required to reveal the commercial potential of the developed biorefinery approach.

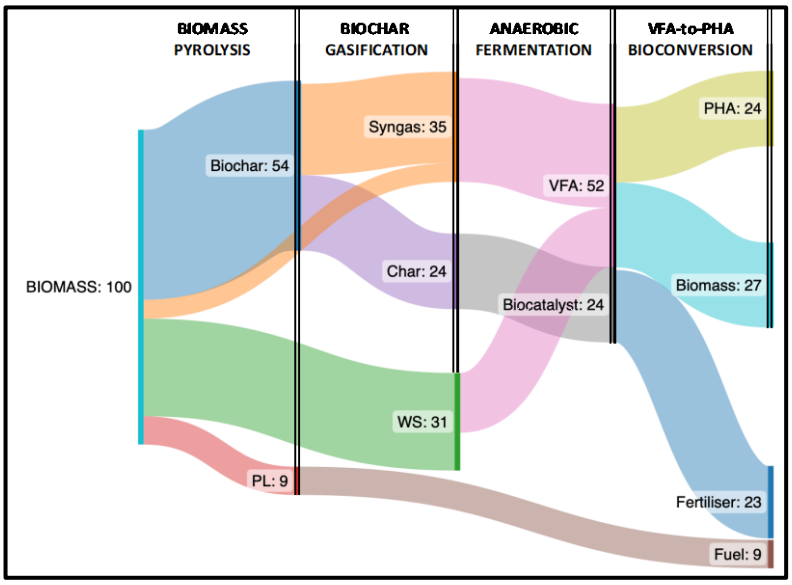

Figure 7.2: Product yields for the HTB schema of the developed biorefinery.

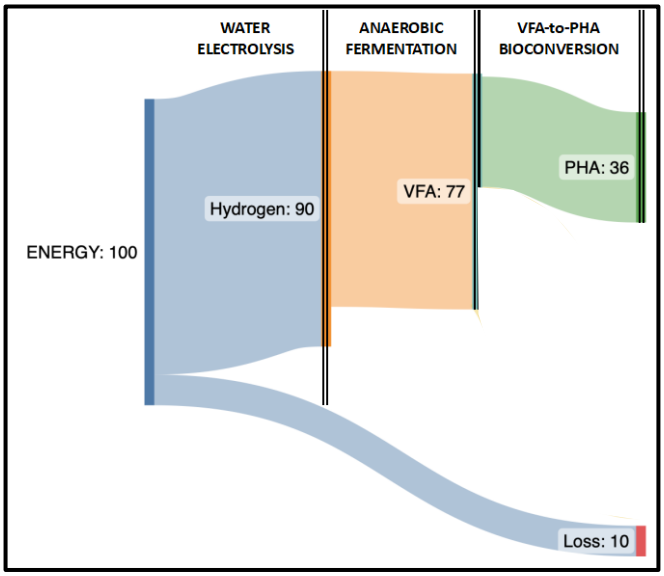

Figure 7.3: Product yields for the power-to-x schema of the developed biorefinery.

REFERENCES

[1] Brown R. C., (2007), "Hybrid thermochemical/biological processing: Putting the cart before the horse?", Applied Biochemistry and Biotechnology, 137–140 (1–12), 947–956.

[2] Valentino F., Morgan-Sagastume F., Campanari S., Villano M., Werker A., Majone M., (2017), "Carbon recovery from wastewater through bioconversion into biodegradable polymers", New Biotechnology, 37, 9–23.

[3] Torri C., Favaro L., Facchin A., Küçükağa Y., Rombolà A. G., Fabbri D., (2022), "Could pyrolysis substitute hydrolysis in 2nd generation biomass valorization strategies? A chemical oxygen demand (COD) approach", Journal of Analytical and Applied Pyrolysis, 163, 105467.

[4] Arnold W., (1976), "Path of electrons in photosynthesis", Proceedings of the National Academy of Sciences of the United States of America, 73 (12), 4502–4505.

[5] Kleerebezem R., Joosse B., Rozendal R., Van Loosdrecht M. C. M., (2015), "Anaerobic digestion without biogas?", Reviews in Environmental Science and Biotechnology, 14 (4), 787–801.

[6] Channiwala S. A., Parikh P. P., (2002), "A unified correlation for estimating HHV of solid, liquid and gaseous fuels", Fuel, 81 (8), 1051–1063.

[7] Torri C., Rombolà A. G., Kiwan A., Fabbri D., (2021), "Biomass Processing via Thermochemical-Biological Hybrid Processes", In: Davide Ravelli,, Chiara Samori, Editors, "Biomass Valorization: Sustainable Methods for the Production of Chemicals", John Wiley & Sons, Ltd.

[8] Kleerebezem R., van Loosdrecht M. C., (2007), "Mixed culture biotechnology for bioenergy production", Current Opinion in Biotechnology, 18 (3), 207–212.

[9] Wen Z., Jarboe L. R., (2019), "Hybrid Processing", In: "Thermochemical Processing of Biomass", Wiley Online Library.

[10] Islam Z. U., Zhisheng Y., Hassan E. B., Dongdong C., Hongxun Z., (2015), "Microbial conversion of pyrolytic products to biofuels: a novel and sustainable approach toward second-generation biofuels", Journal of Industrial Microbiology and Biotechnology, 42 (12), 1557–1579.

[11] Shen Y., Jarboe L., Brown R., Wen Z., (2015), "A thermochemical-biochemical hybrid processing of lignocellulosic biomass for producing fuels and chemicals", Biotechnology Advances, 33 (8), 1799–1813.

[12] Jiang L. Q., Fang Z., Zhao Z. L., Zheng A. Q., Wang X. B., Li H. Bin, (2019), "Levoglucosan and its hydrolysates via fast pyrolysis of lignocellulose for microbial biofuels: A state-of-the-art review", Renewable and Sustainable Energy Reviews, 105 (January), 215–229.

[13] Basaglia M., Favaro L., Torri C., Casella S., (2021), "Is pyrolysis bio-oil prone to microbial conversion into added-value products?", Renewable Energy, 163, 783–791.

[14] Wright M. M., Brown R. C., (2011), "Costs of Thermochemical Conversion of Biomass to Power and Liquid Fuels", Thermochemical Processing of Biomass: Conversion into Fuels, Chemicals and Power, 307–322.

[15] Schwartz T. J., Shanks B. H., Dumesic J. A., (2016), "Coupling chemical and biological catalysis: A flexible paradigm for producing biobased chemicals", Current Opinion in Biotechnology, 38, 54–62.

[16] Linger J. G., Vardon D. R., Guarnieri M. T., Karp E. M., Hunsinger G. B., Franden M. A., Johnson C. W., Chupka G., Strathmann T. J., Pienkos P. T., Beckham G. T., (2014), "Lignin valorization through integrated biological funneling and chemical catalysis", Proceedings of the National Academy of Sciences of the United States of America, 111 (33), 12013–12018.

[17] So K. S., Brown R. C., (1999), "Economic Analysis of Selected Lignocellulose-to-Ethanol Conversion Technologies BT - Twentieth Symposium on Biotechnology for Fuels and Chemicals: Presented as Volumes 77–79 of Applied Biochemistry and Biotechnology Proceedings of the Twentieth Symposium", In: Brian H. Davison,, Mark Finkelstein, Editors, Humana Press.

[18] Piccolo C., Bezzo F., (2009), "A techno-economic comparison between two technologies for bioethanol production from lignocellulose", Biomass and Bioenergy, 33 (3), 478–491.

[19] Teixeira L. V., Moutinho L. F., Romão-Dumaresq A. S., (2018), "Gas fermentation of C1 feedstocks: commercialization status and future prospects", Biofuels, Bioproducts and Biorefining, 12 (6), 1103–1117.

[20] Karlson B., Bellavitis C., France N., (2018), "Commercializing LanzaTech, from waste to fuel: An effectuation case", Journal of Management & Organization, 1–22.

[21] Daniell J., Köpke M., Simpson S. D., (2012), "Commercial biomass syngas fermentation", Energies, 5 (12), 5372–5417.

[22] Stoll I. K., Boukis N., Sauer J., (2020), "Syngas Fermentation to Alcohols: Reactor Technology and Application Perspective", Chemie-Ingenieur-Technik, 92 (1–2), 125–136.

[23] Arnold S., Moss K., Henkel M., Hausmann R., (2017), "Biotechnological Perspectives of Pyrolysis Oil for a Bio-Based Economy", Trends in Biotechnology, 35 (10), 925–936.

[24] Ragsdale S. W., Pierce E., (2008), "Acetogenesis and the Wood-Ljungdahl pathway of CO2 fixation", Biochimica et Biophysica Acta - Proteins and Proteomics, 1784 (12), 1873–1898.

[25] Küçükağa Y., Facchin A., Torri C., Kara S., (2022), "An original Arduino-controlled anaerobic bioreactor packed with biochar as a porous filter media", MethodsX, 9 (2022), 10615.

[26] Sadhwani N., Adhikari S., Eden M. R., (2016), "Biomass Gasification Using Carbon Dioxide: Effect of Temperature, CO2/C Ratio, and the Study of Reactions Influencing the Process", Industrial and Engineering Chemistry Research, 55 (10), 2883–2891.

[27] Ghidotti M., Fabbri D., Torri C., Piccinini S., (2018), "Determination of volatile fatty acids in digestate by solvent extraction with dimethyl carbonate and gas chromatography-mass spectrometry", Analytica Chimica Acta, 1034, 92–101.

[28] Hübner T., Mumme J., (2015), "Integration of pyrolysis and anaerobic digestion - Use of aqueous liquor from digestate pyrolysis for biogas production", Bioresource Technology, 183, 86–92.

[29] Itabaiana Junior I., Avelar Do Nascimento M., de Souza R. O. M. A., Dufour A., Wojcieszak R., (2020), "Levoglucosan: A promising platform molecule?", Green Chemistry, 22 (18), 5859–5880.

[30] Lian J., Garcia-Perez M., Chen S., (2013), "Fermentation of levoglucosan with oleaginous yeasts for lipid production", Bioresource Technology, 133, 183–189.

[31] Chang D., Islam Z. U., Yang Z., Thompson I. P., Yu Z., (2021), "Conversion efficiency of bioethanol from levoglucosan was improved by the newly engineered Escherichia coli", Environmental Progress and Sustainable Energy, 40 (6), 13687.

[32] Wright M. M., Brown T., (2019), "Costs of thermochemical conversion of biomass to power and liquid fuels", Thermochemical Processing of Biomass: Conversion into Fuels, Chemicals and Power, 337–353.

[33] Linger J. G., Vardon D. R., Guarnieri M. T., Karp E. M., Hunsinger G. B., Franden M. A., Johnson C. W., Chupka G., Strathmann T. J., Pienkos P. T., Beckham G. T., (2014), "Lignin valorization through integrated biological funneling and chemical catalysis", Proceedings of the National Academy of Sciences of the United States of America, 111 (33), 12013–12018.

[34] Xu D., Tree D. R., Lewis R. S., (2011), "The effects of syngas impurities on syngas fermentation to liquid fuels", Biomass and Bioenergy, 35 (7), 2690–2696.

[35] Tian F. J., Yu J. L., Mckenzie L. J., Hayashi J. I., Chiba T., Li C. Z., (2005), "Formation of NOx precursors during the pyrolysis of coal and biomass. Part VII. Pyrolysis and gasification of cane trash with steam", Fuel, 84 (4), 371–376.

[36] Kanaujia P. K., Sharma Y. K., Agrawal U. C., Garg M. O., (2013), "Analytical approaches to characterizing pyrolysis oil from biomass", TrAC - Trends in Analytical Chemistry, 42, 125–136.

[37] Mettler M. S., Vlachos D. G., Dauenhauer P. J., (2012), "Top ten fundamental challenges of biomass pyrolysis for biofuels", Energy & Environmental Science, 5 (7), 7797–7809.

[38] Pinheiro Pires A. P., Arauzo J., Fonts I., Domine M. E., Fernández Arroyo A., Garcia-Perez M. E., Montoya J., Chejne F., Pfromm P., Garcia-Perez M., (2019), "Challenges and opportunities for bio-oil refining: A review", Energy and Fuels, 33 (6), 4683–4720.

[39] Blin J., Volle G., Girard P., Bridgwater T., Meier D., (2007), "Biodegradability of biomass pyrolysis oils: Comparison to conventional petroleum fuels and alternatives fuels in current use", Fuel, 86 (17–18), 2679–2686.

[40] Campisi T., Samorì C., Torri C., Barbera G., Foschini A., Kiwan A., Galletti P., Tagliavini E., Pasteris A., (2016), "Chemical and ecotoxicological properties of three bio-oils from pyrolysis of biomasses", Ecotoxicology and Environmental Safety, 132, 87–93.

[41] Buendia-Kandia F., Greenhalf C., Barbiero C., Guedon E., Briens C., Berruti F., Dufour A., (2020), "Fermentation of cellulose pyrolysis oil by a Clostridial bacterium", Biomass and Bioenergy, 143 (November), 105884.

[42] Luque L., Oudenhoven S., Westerhof R., Van Rossum G., Berruti F., Kersten S., Rehmann L., (2016), "Comparison of ethanol production from corn cobs and switchgrass following a pyrolysis-based biorefinery approach", Biotechnology for Biofuels, 9 (1), 1–14.

[43] Luque L., Westerhof R., Van Rossum G., Oudenhoven S., Kersten S., Berruti F., Rehmann L., (2014), "Pyrolysis based bio-refinery for the production of bioethanol from demineralized ligno-cellulosic biomass", Bioresource Technology, 161, 20–28.

[44] Torri C., Fabbri D., (2014), "Biochar enables anaerobic digestion of aqueous phase from intermediate pyrolysis of biomass", Bioresource Technology, 172, 335–341.

[45] Yang Y., Heaven S., Venetsaneas N., Banks C. J., Bridgwater A. V., (2018), "Slow pyrolysis of organic fraction of municipal solid waste (OFMSW): Characterisation of products and screening of the aqueous liquid product for anaerobic digestion", Applied Energy, 213, 158–168.

[46] Doddapaneni T. R. K. C., Praveenkumar R., Tolvanen H., Palmroth M. R. T., Konttinen J., Rintala J., (2017), "Anaerobic batch conversion of pine wood torrefaction condensate", Bioresource Technology, 225, 299–307.

[47] Wen C., Moreira C. M., Rehmann L., Berruti F., (2020), "Feasibility of anaerobic digestion as a treatment for the aqueous pyrolysis condensate (APC) of birch bark", Bioresource Technology, 307.

[48] Torri C., Pambieri G., Gualandi C., Piraccini M., Rombolà A. G., Fabbri D., (2020), "Evaluation of the potential performance of hyphenated pyrolysis-anaerobic digestion (Py-AD) process for carbon negative fuels from woody biomass", Renewable Energy, 148, 1190–1199.

[49] Shen Lee W., Seak May Chua A., Koon Yeoh H., Cheng Ngoh G., (2013), "A review of the production and applications of waste-derived volatile fatty acids", 235 (2014), 83-99.

[50] Moita Fidalgo R., Ortigueira J., Freches A., Pelica J., Gonçalves M., Mendes B., Lemos P. C., (2014), "Bio-oil upgrading strategies to improve PHA production from selected aerobic mixed cultures", New Biotechnology, 31 (4), 297–307.

[51] Villano M., Valentino F., Barbetta A., Martino L., Scandola M., Majone M., (2014), "Polyhydroxyalkanoates production with mixed microbial cultures: From culture selection to polymer recovery in a high-rate continuous process", New Biotechnology, 31 (4), 289–296.

[52] Hübner T., Mumme J., (2015), "Integration of pyrolysis and anaerobic digestion - Use of aqueous liquor from digestate pyrolysis for biogas production", Bioresource Technology, 183, 86–92.

[53] Facchin A., (2021), New path for thermochemical-biological conversion with a power-to-material approach, Master's, Alma Mater Studiorum - Università di Bologna, 2021.

[54] Stankovikj F., McDonald A. G., Helms G. L., Olarte M. V., Garcia-Perez M., (2017), "Characterization of the Water-Soluble Fraction of Woody Biomass Pyrolysis Oils", Energy and Fuels, 31 (2), 1650–1664.

[55] Torri C., Kiwan A., Cavallo M., Pascalicchio P., Fabbri D., Vassura I., Rombolà A. G., Chiaberge S., Carbone R., Paglino R., Miglio R., (2021), "Biological treatment of Hydrothermal Liquefaction (HTL) wastewater: Analytical evaluation of continuous process streams", Journal of Water Process Engineering, 40 (2021), 101798.

[56] Qureshi N., Annous B. A., Ezeji T. C., Karcher P., Maddox I. S., (2005), "Biofilm reactors for industrial bioconversion process: Employing potential of enhanced reaction rates", Microbial Cell Factories, 4, 1–21.

[57] Karadag D., Köroğlu O. E., Ozkaya B., Cakmakci M., (2015), "A review on anaerobic biofilm reactors for the treatment of dairy industry wastewater", Process Biochemistry, 50 (2), 262–271.

[58] di Biase A., Kowalski M. S., Devlin T. R., Oleszkiewicz J. A., (2019), "Moving bed biofilm reactor technology in municipal wastewater treatment: A review", Journal of Environmental Management, 247 (June), 849–866.

[59] Cooney M. J., Lewis K., Harris K., Zhang Q., Yan T., (2016), "Start up performance of biochar packed bed anaerobic digesters", Journal of Water Process Engineering, 9, e7–e13.

[60] Li W., Loyola-Licea C., Crowley D. E., Ahmad Z., (2016), "Performance of a two-phase biotrickling filter packed with biochar chips for treatment of wastewater containing high nitrogen and phosphorus concentrations", Process Safety and Environmental Protection, 102, 150–158.

[61] Kizito S., Jjagwe J., Mdondo S. W., Nagawa C. B., Bah H., Tumutegyereize P., (2022), "Synergetic effects of biochar addition on mesophilic and high total solids anaerobic digestion of chicken manure", Journal of Environmental Management, 315, 115192.

[62] Dalahmeh S., Ahrens L., Gros M., Wiberg K., Pell M., (2018), "Potential of biochar filters for onsite sewage treatment: Adsorption and biological degradation of pharmaceuticals in laboratory filters with active, inactive and no biofilm", Science of the Total Environment, 612, 192–201.

[63] Kaetzl K., Lübken M., Uzun G., Gehring T., Nettmann E., Stenchly K., Wichern M., (2019), "On-farm wastewater treatment using biochar from local agroresidues reduces pathogens from irrigation water for safer food production in developing countries", Science of the Total Environment, 682, 601–610.

[64] Zhao W., Yang H., He S., Zhao Q., Wei L., (2021), "A review of biochar in anaerobic digestion to improve biogas production: Performances, mechanisms and economic assessments", Bioresource Technology, 341 (June), 125797.

[65] Tang S., Wang Z., Liu Z., Zhang Y., Si B., (2020), "The role of biochar to enhance anaerobic digestion: A review", Journal of Renewable Materials, 8 (9), 1033–1052.

[66] Wang D., Ai J., Shen F., Yang G., Zhang Y., Deng S., Zhang J., Zeng Y., Song C., (2017), "Improving anaerobic digestion of easy-acidification substrates by promoting buffering capacity using biochar derived from vermicompost", Bioresource Technology, 227, 286–296.

[67] Mumme J., Srocke F., Heeg K., Werner M., (2014), "Use of biochars in anaerobic digestion", Bioresource Technology, 164, 189–197.

[68] Kaur G., Johnravindar D., Wong J. W. C., (2020), "Enhanced volatile fatty acid degradation and methane production efficiency by biochar addition in food waste-sludge co-digestion: A step towards increased organic loading efficiency in co-digestion", Bioresource Technology, 308 (March), 123250.

[69] Wang C., Liu Y., Gao X., Chen H., Xu X., Zhu L., (2018), "Role of biochar in the granulation of anaerobic sludge and improvement of electron transfer characteristics", Bioresource Technology, 268 (866), 28–35.

[70] Pundir A. S., Singh K., (2019), "Temperature control of real-time identified fixed bed reactor by adaptive sliding mode control equipped with Arduino in Matlab", Asia-Pacific Journal of Chemical Engineering, 14 (2), 1–15.

[71] Barreto J. A., Lemos V. A., de Oliveira D. M., Cerqueira U. M. F. M., Meira L. A., Bezerra M. A., (2020), "Use of Arduino in the development of a new and fast automated online preconcentration system based on double-knotted reactor for the Mn determination determination in tea samples by flame atomic absorption spectrometry", Journal of the Brazilian Chemical Society, 31 (1), 15–24.

[72] Rombolà A. G., Fabbri D., Baronti S., Vaccari F. P., Genesio L., Miglietta F., (2019), "Changes in the pattern of polycyclic aromatic hydrocarbons in soil treated with biochar from a multiyear field experiment", Chemosphere, 219, 662–670.

[73] Temudo M. F., Kleerebezem R., van Loosdrecht M., (2007), "Influence of the pH on (Open) mixed culture fermentation of glucose: A chemostat study", Biotechnology and Bioengineering, 98 (1), 69–79.

[74] Klindworth A., Pruesse E., Schweer T., Peplies J., Quast C., Horn M., Glöckner F. O., (2013), "Evaluation of general 16S ribosomal RNA gene PCR primers for classical and next-generation sequencing-based diversity studies", Nucleic Acids Research, 41 (1), e1–e1.

[75] Masella A. P., Bartram A. K., Truszkowski J. M., Brown D. G., Neufeld J. D., (2012), "PANDAseq: paired-end assembler for illumina sequences", BMC Bioinformatics, 13 (1), 1–7.

[76] Bolyen E., Rideout J. R., Dillon M. R., Bokulich N. A., Abnet C. C., Al-Ghalith G. A., Alexander H., Alm E. J., Arumugam M., Asnicar F., (2019), "Reproducible, interactive, scalable and extensible microbiome data science using QIIME 2", Nature Biotechnology, 37 (8), 852–857.

[77] Callahan B. J., McMurdie P. J., Rosen M. J., Han A. W., Johnson A. J. A., Holmes S. P., (2016), "DADA2: High-resolution sample inference from Illumina amplicon data", Nature Methods, 13 (7), 581–583.

[78] Rognes T., Flouri T., Nichols B., Quince C., Mahé F., (2016), "VSEARCH: a versatile open source tool for metagenomics", PeerJ, 4, e2584.

[79] Quast C., Pruesse E., Yilmaz P., Gerken J., Schweer T., Yarza P., Peplies J., Glöckner F. O., (2012), "The SILVA ribosomal RNA gene database project: improved data processing and web-based tools", Nucleic Acids Research, 41 (D1), D590–D596.

[80] Grady Jr C. P. L., Lim H. C., (1999), "Biological Wastewater Treatment. Mercel Dekker", Inc. New York,.

[81] Haris Nalakath Abubackar, María C. Veiga C. K., (2011), "Biological conversion of carbon monoxide: rich syngas or waste gases to bioethanol", Biofuels, Bioproducts and Biorefining, 5 (1), 93–114.

[82] Jayakody L. N., Horie K., Hayashi N., Kitagaki H., (2013), "Engineering redox cofactor utilization for detoxification of glycolaldehyde, a key inhibitor of bioethanol production, in yeast Saccharomyces cerevisiae", Applied Microbiology and Biotechnology, 97 (14), 6589–6600.

[83] Pinheiro Pires A. P., Arauzo J., Fonts I., Domine M. E., Fernández Arroyo A., Garcia-Perez M. E., Montoya J., Chejne F., Pfromm P., Garcia-Perez M., (2019), "Challenges and opportunities for bio-oil refining: A review", Energy and Fuels, 33 (6), 4683–4720.

[84] Alou M. T., Ndongo S., Frégère L., Labas N., Andrieu C., Richez M., Couderc C., Baudoin J. P., Abrahão J., Brah S., Diallo A., Sokhna C., Cassir N., La Scola B., Cadoret F., Raoult D., (2018), "Taxonogenomic description of four new Clostridium species isolated from human gut: 'Clostridium amazonitimonense', 'Clostridium merdae', 'Clostridium massilidielmoense' and 'Clostridium nigeriense'", New Microbes and New Infections, 21 128–139.

[85] Lü F., Luo C., Shao L., He P., (2016), "Biochar alleviates combined stress of ammonium and acids by firstly enriching Methanosaeta and then Methanosarcina", Water Research, 90 34–43.

[86] Lokesh S., Kim J., Zhou Y., Wu D., Pan B., Wang X., Behrens S., Huang C. H., Yang Y., (2020), "Anaerobic Dehalogenation by Reduced Aqueous Biochars", Environmental Science and Technology, 54 (23), 15142–15150.

[87] Pytlak A., Kasprzycka A., Szafranek-Nakonieczna A., Grządziel J., Kubaczyński A., Proc K., Onopiuk P., Walkiewicz A., Polakowski C., Gałązka A., Lalak-Kańczugowska J., Stępniewska Z., Bieganowski A., (2020), "Biochar addition reinforces microbial interspecies cooperation in methanation of sugar beet waste (pulp)", Science of the Total Environment, 730.

[88] Liu H., Wang J., Wang A., Chen J., (2011), "Chemical inhibitors of methanogenesis and putative applications", Applied Microbiology and Biotechnology, 89 (5), 1333–1340.

[89] Jahangiri H., Bennett J., Mahjoubi P., Wilson K., Gu S., (2014), "A review of advanced catalyst development for Fischer-Tropsch synthesis of hydrocarbons from biomass derived syn-gas", Catalysis Science and Technology, 4 (8), 2210–2229.

[90] Vega J. L., Clausen E. C., Gaddy J. L., (1990), "Design of Bioreactors for Coal Synthesis Gas Fermentations", .

[91] Infantes A., Kugel M., Neumann A., (2020), "Evaluation of media components and process parameters in a sensitive and robust fed-batch syngas fermentation system with clostridium ljungdahlii", Fermentation, 6 (2).

[92] Gunes B., (2021), "A critical review on biofilm-based reactor systems for enhanced syngas fermentation processes", Renewable and Sustainable Energy Reviews, 143 (March), 110950.

[93] Andreides D., Fliegerova K. O., Pokorna D., Zabranska J., (2022), "Biological conversion of carbon monoxide and hydrogen by anaerobic culture: Prospect of anaerobic digestion and thermochemical processes combination", Biotechnology Advances, 58.

[94] Bae J., Song Y., Lee H., Shin J., Jin S., Kang S., Cho B. K., (2022), "Valorization of C1 gases to value-added chemicals using acetogenic biocatalysts", Chemical Engineering Journal, 428.

[95] He Y., Kennes C., Lens P. N. L., (2022), "Enhanced solventogenesis in syngas bioconversion: Role of process parameters and thermodynamics", Chemosphere, 299.

[96] Pei R., Loosdrecht M. C. M. van, Kleerebezem R., Werker A., (2021), "Bioresource Technology Scaling-up microbial community-based polyhydroxyalkanoate production : status and challenges", Bioresource Technology, 327 (February).

[97] Obruca S., Sedlacek P., Slaninova E., Fritz I., Daffert C., Meixner K., Sedrlova Z., Koller M., (2020), "Novel unexpected functions of PHA granules", Applied Microbiology and Biotechnology, 104 (11), 4795–4810.

[98] Mongili B., Fino D., (2021), "Carbon monoxide fermentation to bioplastic: the effect of substrate adaptation on Rhodospirillum rubrum", Biomass Conversion and Biorefinery, 11 (2), 705–714.

[99] Brandl H., Knee E. J., Fuller R. C., Gross R. A., Lenz R. W., (1989), "Ability of the phototrophic bacterium Rhodospirillum rubrum to produce various poly (fl-hydroxyalkanoates): potential sources for biodegradable polyesters", .

[100] Liew F. M., Martin M. E., Tappel R. C., Heijstra B. D., Mihalcea C., Köpke M., (2016), "Gas Fermentation-A flexible platform for commercial scale production of low-carbon-fuels and chemicals from waste and renewable feedstocks", Frontiers in Microbiology, 7 (MAY).

[101] Küçükağa Y., Facchin A., Kara S., Nayır T. Y., Scicchitano D., Rampelli S., Candela M., Torri C., (2022), "Conversion of Pyrolysis Products into Volatile Fatty Acids with a Biochar-Packed Anaerobic Bioreactor", Industrial & Engineering Chemistry Research, 61 (45), 16624–16634.

[102] Infantes A., Kugel M., Raffelt K., Neumann A., (2020), "Side-by-side comparison of clean and biomass-derived, impurity-containing syngas as substrate for acetogenic fermentation with clostridium ljungdahlii", Fermentation, 6 (3).

[103] American public health association, Rice E. W., Baird R. B., Eaton A. D., Clesceri L. S., (2012), "Standard Methods for the Examination of Water and Wastewater", American public health association Washington, DC.

[104] Monir M. U., Aziz A. A., Khatun F., Yousuf A., (2020), "Bioethanol production through syngas fermentation in a tar free bioreactor using Clostridium butyricum", Renewable Energy, 157, 1116–1123.

[105] Ahmed A., Cateni B. G., Huhnke R. L., Lewis R. S., (2006), "Effects of biomass-generated producer gas constituents on cell growth, product distribution and hydrogenase activity of Clostridium carboxidivorans P7T", Biomass and Bioenergy, 30 (7), 665–672.

[106] Kundiyana D. K., Huhnke R. L., Wilkins M. R., (2010), "Syngas fermentation in a 100-L pilot scale fermentor: Design and process considerations", Journal of Bioscience and Bioengineering, 109 (5), 492–498.

[107] Ramachandriya K. D., Wilkins M. R., Patil K. N., (2013), "Influence of switchgrass generated producer gas pre-adaptation on growth and product distribution of Clostridium ragsdalei", Biotechnology and Bioprocess Engineering, 18 (6), 1201–1209.

[108] Liakakou E. T., Infantes A., Neumann A., Vreugdenhil B. J., (2021), "Connecting gasification with syngas fermentation: Comparison of the performance of lignin and beech wood", Fuel, 290, 120054.

[109] Datar R. P., Shenkman R. M., Cateni B. G., Huhnke R. L., Lewis R. S., (2004), "Fermentation of biomass-generated producer gas to ethanol", Biotechnology and Bioengineering, 86 (5), 587–594.

[110] Gong J., English N. J., Pant D., Patzke G. R., Protti S., Zhang T., (2021), "Power-to-X: Lighting the Path to a Net-Zero-Emission Future", ACS Sustainable Chemistry and Engineering, 9 (21), 7179–7181.

[111] Diekert G., Wohlfarth G., (1994), "Metabolism of Homoacetogens", Antonie Van Leeuwenhoek, 66 (1), 209-221.

[112] Drake H. L., Gößner A. S., Daniel S. L., (2008), "Old acetogens, new light", In: "Ann N Y Acad Sci", Blackwell Publishing Inc.

[113] Geinitz B., Hüser A., Mann M., Büchs J., (2020), "Gas Fermentation Expands the Scope of a Process Network for Material Conversion", Chemie-Ingenieur-Technik, 92 (11), 1665–1679.

[114] Yasin M., Jeong Y., Park S., Jeong J., Lee E. Y., Lovitt R. W., Kim B. H., Lee J., Chang I. S., (2015), "Microbial synthesis gas utilization and ways to resolve kinetic and mass-transfer limitations", Bioresource Technology, 177, 361–374.

[115] Illi L., Lecker B., Lemmer A., Müller J., Oechsner H., (2021), "Biological methanation of injected hydrogen in a two-stage anaerobic digestion process", Bioresource Technology, 333.

[116] Omar B., Abou-Shanab R., El-Gammal M., Fotidis I. A., Kougias P. G., Zhang Y., Angelidaki I., (2018), "Simultaneous biogas upgrading and biochemicals production using anaerobic bacterial mixed cultures", Water Research, 142, 86–95.

[117] He Y., Cassarini C., Marciano F., Lens P. N. L., (2021), "Homoacetogenesis and solventogenesis from H2/CO2 by granular sludge at 25, 37 and 55 °C", Chemosphere, 265, 128649.

[118] Modestra A. J., Katakojwala R., Venkata Mohan S., (2020), "CO2 fermentation to short chain fatty acids using selectively enriched chemolithoautotrophic acetogenic bacteria", Chemical Engineering Journal, 394.

[119] Katakojwala R., Tharak A., Sarkar O., Venkata Mohan S., (2022), "Design and evaluation of gas fermentation systems for CO2 reduction to C2 and C4 fatty acids: Non-genetic metabolic regulation with pressure, pH and reaction time", Bioresource Technology, 351.

[120] Wang Y. Q., Zhang F., Zhang W., Dai K., Wang H. J., Li X., Zeng R. J., (2018), "Hydrogen and carbon dioxide mixed culture fermentation in a hollow-fiber membrane biofilm reactor at 25 °C", Bioresource Technology, 249 (October 2017), 659–665.

[121] Wang Y. Q., Yu S. J., Zhang F., Xia X. Y., Zeng R. J., (2017), "Enhancement of acetate productivity in a thermophilic (55 °C) hollow-fiber membrane biofilm reactor with mixed culture syngas (H2/CO2) fermentation", Applied Microbiology and Biotechnology, 101 (6), 2619–2627.

[122] Zhang F., Ding J., Shen N., Zhang Y., Ding Z., Dai K., Zeng R. J., (2013), "In situ hydrogen utilization for high fraction acetate production in mixed culture hollow-fiber membrane biofilm reactor", Applied Microbiology and Biotechnology, 97 (23), 10233–10240.

[123] Zhang F., Ding J., Zhang Y., Chen M., Ding Z. W., van Loosdrecht M. C. M., Zeng R. J., (2013), "Fatty acids production from hydrogen and carbon dioxide by mixed culture in the membrane biofilm reactor", Water Research, 47 (16), 6122–6129.

[124] Kreutzer M. T., Kapteijn F., Moulijn J. A., Ebrahimi S., Kleerebezem R., van Loosdrecht M. C. M., (2005), "Monoliths as biocatalytic reactors: Smart gas-liquid contacting for process intensification", In: "Ind Eng Chem Res", 44 (25), 9646-9652.

[125] Qiu L., Deng Y. F., Wang F., Davaritouchaee M., Yao Y. Q., (2019), "A review on biochar-mediated anaerobic digestion with enhanced methane recovery", Renewable and Sustainable Energy Reviews, 115.

[126] Lokesh S., Kim J., Zhou Y., Wu D., Pan B., Wang X., Behrens S., Huang C. H., Yang Y., (2020), "Anaerobic Dehalogenation by Reduced Aqueous Biochars", Environmental Science and Technology, 54 (23), 15142–15150.

[127] Sun X., Thunuguntla R., Zhang H., Atiyeh H., (2022), "Biochar amended microbial conversion of C1 gases to ethanol and butanol: Effects of biochar feedstock type and processing temperature", Bioresource Technology, 360.

[128] Torri C., Pambieri G., Gualandi C., Piraccini M., Rombolà A. G., Fabbri D., (2020), "Evaluation of the potential performance of hyphenated pyrolysis-anaerobic digestion (Py-AD) process for carbon negative fuels from woody biomass", Renewable Energy, 148, 1190–1199.

[129] Santos A., van Aerle R., Barrientos L., Martinez-Urtaza J., (2020), "Computational methods for 16S metabarcoding studies using Nanopore sequencing data", Computational and Structural Biotechnology Journal, 18, 296–305.

[130] Clarke K. R., Gorley R. N., (2015), "Getting Started with PRIMER v7 Plymouth Routines In Multivariate Ecological Research", Revista Mexicana de Biodiversidad, 89 (3), 898–909.

[131] Simonetti S., Saptoro A., Martín C. F., Dionisi D., (2020), "Product concentration, yield and productivity in anaerobic digestion to produce short chain organic acids: A critical analysis of literature data", Processes, 8 (12), 1–17.

[132] Andrés-Barrao C., Saad M. M., Cabello Ferrete E., Bravo D., Chappuis M. L., Ortega Pérez R., Junier P., Perret X., Barja F., (2016), "Metaproteomics and ultrastructure characterization of Komagataeibacter spp. involved in high-acid spirit vinegar production", Food Microbiology, 55, 112–122.

[133] Yan Y., Yan M., Ravenni G., Angelidaki I., Fu D., Fotidis I. A., (2022), "Novel bioaugmentation strategy boosted with biochar to alleviate ammonia toxicity in continuous biomethanation", Bioresource Technology, 343.

[134] Mohd Azhar S. H., Abdulla R., Jambo S. A., Marbawi H., Gansau J. A., Mohd Faik A. A., Rodrigues K. F., (2017), "Yeasts in sustainable bioethanol production: A review", Biochemistry and Biophysics Reports, 10 (March), 52–61.

[135] Zhang F., Ding J., Shen N., Zhang Y., Ding Z., Dai K., Zeng R. J., (2013), "In situ hydrogen utilization for high fraction acetate production in mixed culture hollow-fiber membrane biofilm reactor", Applied Microbiology and Biotechnology, 97 (23), 10233–10240.

[136] Calvo D. C., Ontiveros-Valencia A., Krajmalnik-Brown R., Torres C. I., Rittmann B. E., (2021), "Carboxylates and alcohols production in an autotrophic hydrogen-based membrane biofilm reactor", Biotechnology and Bioengineering, 118 (6), 2338–2347.

[137] Chen S., Rotaru A. E., Shrestha P. M., Malvankar N. S., Liu F., Fan W., Nevin K. P., Lovley D. R., (2014), "Promoting interspecies electron transfer with biochar", Scientific Reports, 4.

[138] Salehiyoun A. R., Zilouei H., Safari M., di Maria F., Samadi S. H., Norouzi O., (2022), "An investigation for improving dry anaerobic digestion of municipal solid wastes by adding biochar derived from gasification of wood pellets", Renewable Energy, 186, 1–9.

[139] Müller V., (2019), "New Horizons in Acetogenic Conversion of One-Carbon Substrates and Biological Hydrogen Storage", Trends in Biotechnology, 37 (12), 1344–1354.

[140] Bengelsdorf F. R., Beck M. H., Erz C., Hoffmeister S., Karl M. M., Riegler P., Wirth S., Poehlein A., Weuster-Botz D., Dürre P., (2018), "Chapter Four - Bacterial Anaerobic Synthesis Gas (Syngas) and CO2+H2 Fermentation", In: Sima Sariaslani,, Geoffrey Michael Gadd, Editors, "Adv Appl Microbiol", Academic Press.

[141] Wang H. J., Dai K., Wang Y. Q., Wang H. F., Zhang F., Zeng R. J., (2018), "Mixed culture fermentation of synthesis gas in the microfiltration and ultrafiltration hollow-fiber membrane biofilm reactors", Bioresource Technology, 267, 650–656.

[142] Imkamp F., Biegel E., Jayamani E., Buckel W., Müller V., (2007), "Dissection of the caffeate respiratory chain in the acetogen Acetobacterium woodii: Identification of an Rnf-type NADH dehydrogenase as a potential coupling site", Journal of Bacteriology, 189 (22), 8145–8153.

[143] Bache R., Pfennig N., (1981), "Selective isolation of acewbacterium woodii on methoxylated aromatic acids and determination of growth yields", 130 (3), 255-261.

[144] Roy M., Yadav R., Chiranjeevi P., Patil S. A., (2021), "Direct utilization of industrial carbon dioxide with low impurities for acetate production via microbial electrosynthesis", Bioresource Technology, 320.

[145] Elisiário M. P., de Wever H., van Hecke W., Noorman H., Straathof A. J. J., (2022), "Membrane bioreactors for syngas permeation and fermentation", Critical Reviews in Biotechnology, 42 (6), 856–872.

[146] Yuan J., Wen Y., Dionysiou D. D., Sharma V. K., Ma X., (2022), "Biochar as a novel carbon-negative electron source and mediator: electron exchange capacity (EEC) and environmentally persistent free radicals (EPFRs): a review", Chemical Engineering Journal, 429.

[147] Gibb B. C., (2019), "Plastics are forever", Nature Chemistry, 11 (5), 394–395.

[148] Keenan T. M., Nakas J. P., Tanenbaum S. W., (2006), "Polyhydroxyalkanoate copolymers from forest biomass", In: "J Ind Microbiol Biotechnol", .

[149] Szacherska K., Oleskowicz-Popiel P., Ciesielski S., Mozejko-Ciesielska J., (2021), "Volatile fatty acids as carbon sources for polyhydroxyalkanoates production", Polymers, 13 (3), 1–21.

[150] Serafim L. S., Lemos P. C., Albuquerque M. G. E., Reis M. A. M., (2008), "Strategies for PHA production by mixed cultures and renewable waste materials", Applied Microbiology and Biotechnology, 81 (4), 615–628.

[151] Xiao Y., Fang Q., Xie Y., Zhang K., Ping Q., Wang Z., (2022), "Feeding in Oxygen-Limiting Phase: An Optimized Anaerobic–Aaerobic Process for Polyhydroxyalkanoates Accumlation and a Selective Pressure for Bacterial Communities' Direct Succession", Waste and Biomass Valorization, 1-11.

[152] Ahmadi F., Zinatizadeh A. A., Asadi A., (2020), "The effect of different operational strategies on polyhydroxyalkanoates (PHAs) production at short-term biomass enrichment", Journal of Environmental Chemical Engineering, 8 (3).

[153] Mino T., van Loosdrecht M. C. M., Heijnen J. J., (n.d.), "microbiology and biochemistry of the enhanced biological phosphate removal process", Water Research 32 (11), 3193-3207.

[154] Pei R., Estévez-Alonso Á., Ortiz-Seco L., van Loosdrecht M. C. M., Kleerebezem R., Werker A., (2022), "Exploring the Limits of Polyhydroxyalkanoate Production by Municipal Activated Sludge", Environmental Science & Technology, 56 (16), 11729–11738.

[155] Satoh H., Iwamoto Y., Mino T., Matsuo T., (1998), "Activated sludge as a possible source of biodegradable plastic", Water Science and Technology, 38 (2), 103–109.

[156] (2021), "B-PLAS DEMO: Creating Bioplastics from Industrial Organic Waste".

[157] Guerrini Luca, (2021), Process optimization for polyhydroxyalkanoate production by mixed microbial cultures within the B-PLAS project, Master Thesis (2nd Cycle), Alma Mater Studiorum –University of Bologna, 2021.

[158] Sherrard J. H., Schroeder E. D., (1973), "Cell yield and growth rate in activated sludge", Journal (Water Pollution Control Federation), 1889-1897.

[159] El-Gammal M., Abou-Shanab R., Angelidaki I., Omar B., Sveding P. V., Karakashev D. B., Zhang Y., (2017), "High efficient ethanol and VFA production from gas fermentation: Effect of acetate, gas and inoculum microbial composition", Biomass and Bioenergy, 105, 32–40.

[160] Liu C., Luo G., Wang W., He Y., Zhang R., Liu G., (2018), "The effects of pH and temperature on the acetate production and microbial community compositions by syngas fermentation", Fuel, 224 537–544.

[161] Miller T. L., Wolin M. J., (2001), "Inhibition of growth of methane-producing bacteria of the ruminant forestomach by hydroxymethylglutaryl~SCoA reductase inhibitors", Journal of Dairy Science, 84 (6), 1445–1448.

[162] Faseleh Jahromi M., Liang J. B., Ho Y. W., Mohamad R., Goh Y. M., Shokryazdan P., Chin J., (2013), "Lovastatin in Aspergillus terreus: Fermented rice straw extracts interferes with methane production and gene expression in Methanobrevibacter smithii", BioMed Research International, 2013.

[163] Fernández-Naveira Á., Veiga M. C., Kennes C., (2017), "Effect of pH control on the anaerobic H-B-E fermentation of syngas in bioreactors", Journal of Chemical Technology and Biotechnology, 92 (6), 1178–1185.

[164] Abubackar H. N., Veiga M. C., Kennes C., (2018), "Production of acids and alcohols from syngas in a two-stage continuous fermentation process", Bioresource Technology, 253, 227–234.

[165] Chakraborty S., Rene E. R., Lens P. N. L., Veiga M. C., Kennes C., (2019), "Enrichment of a solventogenic anaerobic sludge converting carbon monoxide and syngas into acids and alcohols", Bioresource Technology, 272, 130–136.

[166] Liu K., Atiyeh H. K., Stevenson B. S., Tanner R. S., Wilkins M. R., Huhnke R. L., (2014), "Continuous syngas fermentation for the production of ethanol, n-propanol and n-butanol", Bioresource Technology, 151, 69–77.

[167] Liu K., Atiyeh H. K., Stevenson B. S., Tanner R. S., Wilkins M. R., Huhnke R. L., (2014), "Mixed culture syngas fermentation and conversion of carboxylic acids into alcohols", Bioresource Technology, 152, 337–346.

[168] Liu K., Atiyeh H. K., Tanner R. S., Wilkins M. R., Huhnke R. L., (2012), "Fermentative production of ethanol from syngas using novel moderately alkaliphilic strains of Alkalibaculum bacchi", Bioresource Technology, 104, 336–341.

[169] Association A. P. H., (1920), "Standard Methods for the Examination of Water and Wastewater", American public health association.

[170] Ma H., Hu Y., Wu J., Kobayashi T., Xu K.-Q., Kuramochi H., (2022), "Enhanced anaerobic digestion of tar solution from rice husk thermal gasification with hybrid upflow anaerobic sludge-biochar bed reactor", Bioresource Technology, 347 (January), 126688.

[171] Qiu L., Deng Y. F., Wang F., Davaritouchaee M., Yao Y. Q., (2019), "A review on biochar-mediated anaerobic digestion with enhanced methane recovery", Renewable and Sustainable Energy Reviews, 115 (August), 109373.

BIOGRAPHY

Yusuf Küçükağa was born in Istanbul, Turkey in 1991. He received his bachelor's degree (BSc) in Environmental Engineering from Sakarya University in 2014 with a high honor certificate. During his undergraduate education, he studied one year at Umea University, Sweden within the scope of Erasmus Exchange program (2011-2012). In 2014, he started Master of Science (MSc) degree at in Environmental Engineering program of Gebze Technical University (GTU). He successfully graduated from MSc with a thesis titled as "Effect of Geotextile Layer on Leachate Quality in Recirculated Landfill Bioreactor" in 2016. He has been working as a research assistant at Engineering Faculty of GTU since 2015. For his doctoral education, he has conducted an internationally collaborated thesis study within a specific "co-tutelle" (co-tutorship) agreement between Alma Mater Studiorum - Universita di Bologna (UniBo) and GTU for awarding a double doctoral degree. According to the co-tutelle agreement, he is expected to receive the titles of 'PhD in Chemistry' from UniBo and 'PhD in Environmental Engineering' from GTU. The joint research study under his PhD scope, was related to integration of hybrid thermo-chemical biological refinery system and innovative "power-to-x" approach for obtaining bioplastics (namely; polyhydroxyalkanoates, PHA). He is the author of 7 indexed scientific papers and has more than 15 international conference proceedings.

APPENDICES

Appendix A: Publications

Scientific Papers:

Torri C., Favaro L., Facchin A., Küçükağa Y., Rombolà A. G., Fabbri D., (2022), "Could pyrolysis substitute hydrolysis in 2nd generation biomass valorization strategies? A chemical oxygen demand (COD) approach", Journal of Analytical and Applied Pyrolysis, 163 105467 (Review Paper). doi/10.1016/j.jaap.2022.105467

Küçükağa Y., Facchin A., Torri C., Kara S., (2022), "An original Arduino-controlled anaerobic bioreactor packed with biochar as a porous filter media", MethodsX, 9. doi.org/10.1016/j.mex.2021.101615

Küçükağa Y., Facchin A., Kara S., Nayır T. Y., Scicchitano D., Rampelli S., Candela M., Torri C., (2022), "Conversion of Pyrolysis Products into Volatile Fatty Acids with a Biochar-Packed Anaerobic Bioreactor", Industrial & Engineering Chemistry Research, 61 (45), 16624–16634. doi.org/10.1021/acs.iecr.2c02810

[1] Chapter 3 was modified and reprinted with permission from the mentioned research articles.

Conference Proceedings:

Küçükağa Y., Facchin A., Kara S., Fabbri D., Torri C., (2021), "Revalorization of Biomass Through a Hybrid Thermochemical-Biological Biorefinery Concept: Pyrolysis Liquid and Syngas as Feedstock for Building Block Chemicals Fermentation", In: "3rd International Conference for Bioresource Technology for Bioenergy, Bioproducts & Environmental Sustainability", Bioresource Technology.

Küçükağa Y., Facchin A., Torri C., Kara S., (2022), "Microbial Funneling of Pyrolysis Product for the Production of Green Chemicals: Preliminary Investigations with Microbial Mixed Cultures", In: "18th International Conference on Renewable Resources & Biorefineries (RRB)".

Facchin A., Küçükağa Y., Alfonsi A., Torri C., Kara S., (2022), "Improvement of power to PHA pathway: Mixed culture fermentation of hydrogen within biochar based materials", In: "18th International Conference on Renewable Resources & Biorefineries (RRB)".

Küçükağa Y., Facchin A., Torri C., Kara S., (2022), "Inorganic Gasses into Organic Acids for Polyhydroxyalkanoates Production: An Integrated Lab-Scale System for the Syngas Fermentation Coupled PHA Production", In: "9th International Conference on Sustainable Solid Waste Management (CORFU2022)".

Facchin A., Küçükağa Y., Torri C., Kara S., Fabbri D., (2021), "Thermochemical-Biological Systems : Pyrolysis Products as a source of green chemicals", In: "5th EuChemS Conference on Green and Sustainable Chemistry (5th EuGSC)", European Chemical Society (EuChemS).

Appendix B: Supplementary Experiments (CD)

- Initial Pyrolysis Experiments
- Preliminary WS Fermentation Tests
- Synthetic Syngas Fermentation Test
- Preliminary CBSR Tests

Appendix B: Supplementary Experiments (CD)

Initial Pyrolysis Experiments

Syngas fermentation studies have been attracted in recent years with its remarkable potential to convert inorganic gaseous substrates into variety of different chemical products, namely VFA and ethanol. Most of the studies have investigated some different operational conditions with different setups using synthetic gaseous mixtures. In contrast, there are only very few studies about fermentation of potentially fermentable pyrolytic liquid and gaseous pyrolysis products together. Although water-soluble fraction of pyrolysis products is more easily bioavailable, biodegradation complexity and toxicity of PyP have some challenging aspects. To address issue related to PyP valorization, WS and syngas might be used as substrate for MMC evaluating the chemical fate of main PyP constituents.

Prior to the fermentation experiments, a series of batch pyrolysis experiments were conducted to determine the operational conditions of pyrolysis to maximize the potentially fermentable products from raw biomass material.

Results and Discussion

It is known that the distribution and characterization of syngas, pyrolytic liquid and biochar contents change depending on the pyrolytic conditions. In this reason, it was concluded that the pyrolytic conditions should be studied before the fermentation of pyrolysis products experiments.

Sawdust as a typical organic biomass, were used in the optimization of pyrolysis conditions experiments, to obtain consistent results to examine the yield of organic matter (in terms of COD) from unit biomass under various pyrolytic conditions (Figure A.1). Except for the first two pyrolysis experiments (Pyro-1 & Pyro-2), all experiments were conducted duplicate or triplicate.

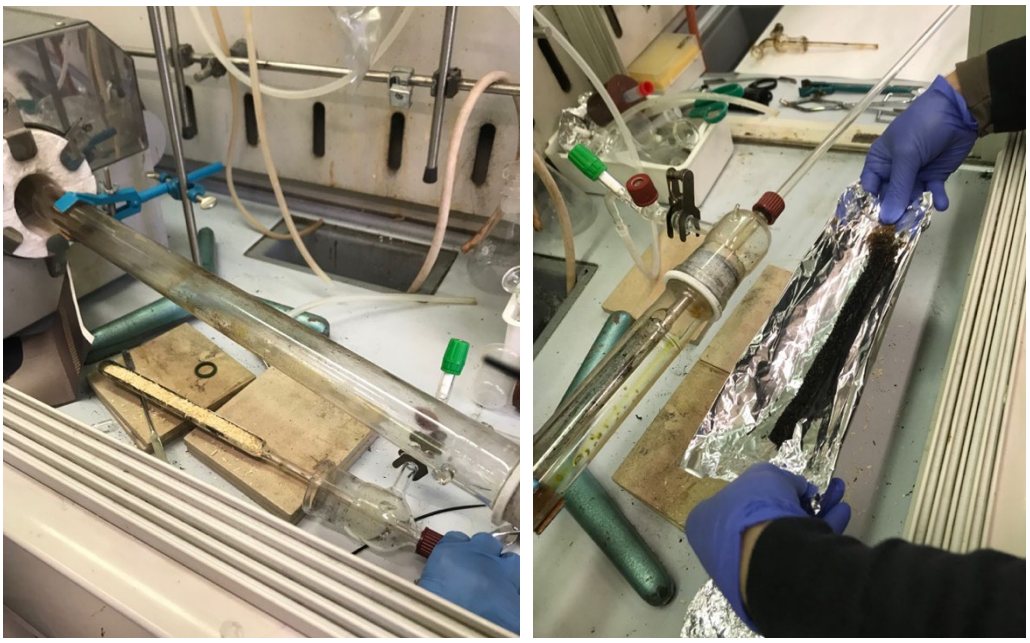

Figure A.1: Sawdust as a representative biomass sample for pyrolysis experiments: raw biomass as sawdust (left), pyrolyzed biomass as biochar (right).

Two-step pyrolysis experiments

There are two different furnaces available in the analytical pyrolysis laboratory; one is a horizontal type with a slightly larger diameter round mouth and the other is a more compact vertical type tube furnace. Pyrolysis experiments were started in a horizontal tube furnace in order to keep the amount of biomass relatively high (Figure A.2). Batch fixed-bed pyrolysis experiments were carried out with using a biomass transfer apparatus with a sawdust capacity of approximately 3 grams (Figure A.1). Nitrogen gas (N_2) was used as carrier gas in all two-step pyrolysis experiments. In this way, the effect of temperature and duration time on the formation rate, amount, and content of syngas production, was investigated to obtain the highest possible thermochemical conversion of biomass into most suitable products for the latter fermentation process. It is known that fermentative microorganisms are capable of transforming a wide range of water-soluble organic and inorganic carbon sources (e.g., CO gas) into various products such as short chain fatty acids (i.e.VFAs). Various experimental conditions and different configurations have been investigated for maximizing the ratio of WS and fermentable inorganic gas molecules such as carbon monoxide (CO) and hydrogen (H_2) (Table A.1).

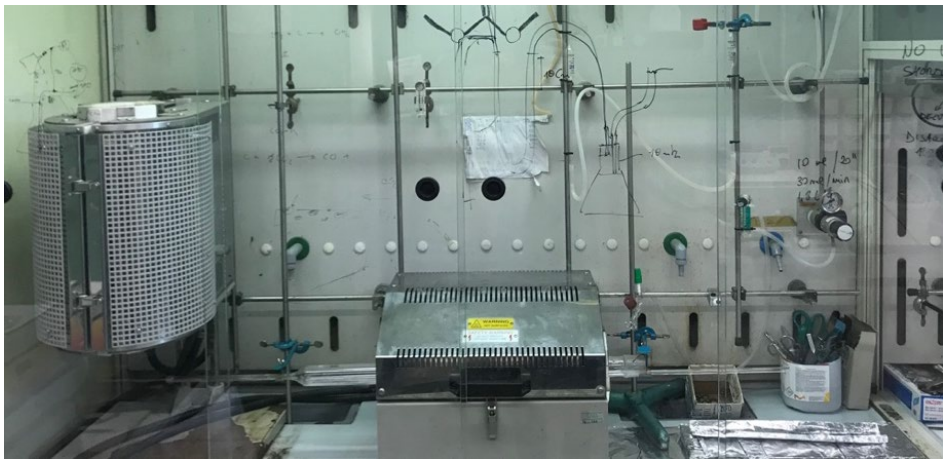

Figure A.2: Available pyrolysis furnaces in the lab: vertical tube furnace (left), horizontal larger tube furnace (right)

Table A.1: Experimental conditions and COD yields of the two-step pyrolysis

Parameters	**Pyro-1**		**Pyro-2**		**Pyro-3**	
Pyrolysis Reactor	Fixed Bed Batch Type		Fixed Bed Batch Type		Fixed Bed Batch Type	
Pyrolysis Type	Fast Pyrolysis Horizontal		Fast Pyrolysis Horizontal		Fast Pyrolysis Vertical	
Feeding Type	Gas Recirculation		Gas Recirculation		Gas Recirculation	
Carrier Gas	Nitrogen (N2)		Carbon dioxide (CO2)		Nitrogen (N2)	
Gas Feed Rate	0.10 L/min		0.10 L/min		0.10 L/min	
1st Temperature	200 to 550°C in 27min		350°C for 60min		350°C for 60min	
2nd Temperature	550°C for 13min		550°C for 60min		550°C for 60min	
Biomass Type	Sawdust		Sawdust		Sawdust	
Biomass Amount	3.63 g-COD	3.00 g	3.63 g-COD	3.00 g	3.64 g-COD	3.01 g
COD Yields	***g-COD***	***%***	***g-COD***	***%***	***g-COD***	***%***
Syngas	0.23	6%	0.11	3%	0.46	13%
WS Liquid	0.42	12%	0.89	24%	1.02	28%
WI Liquid	0.06	2%	0.22	6%	0.38	10%
Biochar	1.58	44%	1.58	44%	1.61	44%
Fermentable*	0.57	16%	0.90	25%	1.31	36%
Overall Yield	2.29	63%	2.80	77%	3.47	95%

Initially (Pyro-1), a configuration was established to achieve a concentrated syngas by providing the carrier gas (N2) with the lowest feed rate that can be manageable (Figure A.3). In this initial setup, two impingers with containing 50mL of pure water in each, were placed in series as water traps at the exit of the pyrolysis reactor. A cotton trap is placed after the water traps to absorb the residual non-gaseous

products. Two plastic chemical containers filled with water and equipped with custom caps and gas tubing with a total volume of 5.8 liters, were connected at the end of the process. By this simple and effective gasometer system that is based on the principle of water-displacement, were used to track the amount of pyrolysis gas flowrate and produced total syngas amount at the end. In this first experiment where nitrogen gas was used as carrier gas with a constant rate of 40 mL/min, two-step pyrolysis has been made as follow: initial temperature was 200°C followed by a temperature ramp of 13°C/min in average up to the 550°C, then a constant temperature was applied in the second step (550°C for 13 min).

Figure A.3: Experimental setup of the Pyro-1: overall view of the system (top), product capture & collecting apparatus (left), inlet part with N_2 feed (right).

First result of this preliminary experiment; a very low negligible amount of COD content was observed in the 2nd water trap and all the rest COD was found in the 1st water trap that is formed by water soluble pyrolytic liquids. As a result of the Pyro-1 experiment, 63% COD yield was obtained, and it was observed that total portion of syngas constituted only 6% (Table A.1). Thus, different experimental conditions

maybe with higher carrier gas feed rate needed to be studied for obtaining a better overall COD yield and for syngas yield in particular.

In the second pyrolysis experiment (Pyro-2), it was aimed to convert biomass into more stable intermediate products with a higher conversion efficiency in terms of COD. For this purpose, carrier gas (N_2) feed rate, which was thought to be the main reason for relatively low COD conversion obtained in the first experiment, was increased to 100 mL/min. In addition, total duration time was increased to 2 hours consisting of two-steps with identical 1-hour durations with a constant temperature of 350°C and 550°C respectively. Eventually, a much larger gasometer was needed. For this purpose, a 30-liter plastic container was placed horizontally and transformed into a large gasometer (Figure A.4).

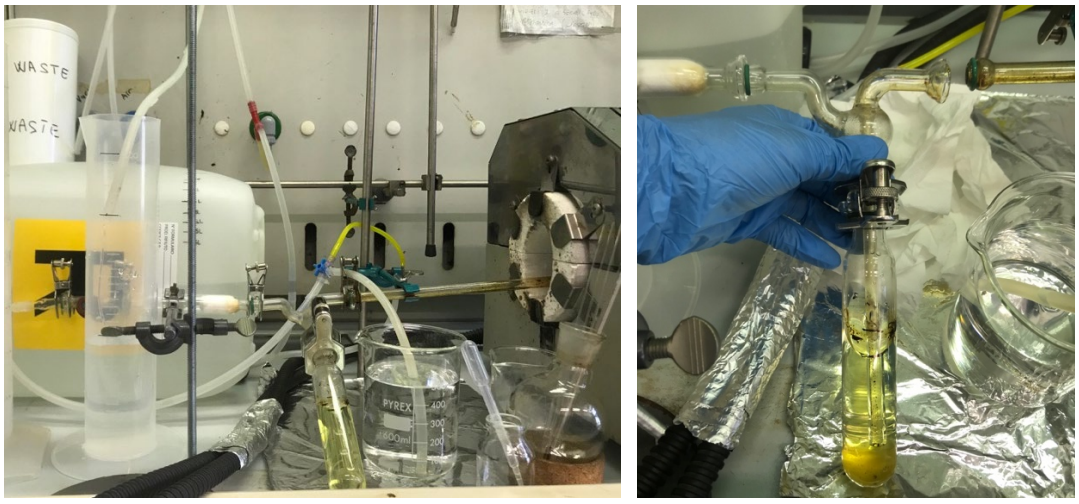

Figure A.4: Experimental setup of Pyro-2: Big gas tank as gasometer at the back (left), the view of water trap after the pyrolysis experiment (right).

During the total 2-hour duration experiment, the amount of gas released from the system was monitored instantaneously in order to examine the effect of temperature and duration. According to the data obtained, pyrolysis gas production was fluctuating and low in the first half hour, and almost no gas production was observed in the second half hour. In contrast at the beginning of 2nd step, a sudden increase in the amount of gas was observed as the temperature increased between 60-70 minutes. Then until the 90th minutes of operation, a decreasing trend was observed in terms of gas production. Later on, there was no significant gas production until the end (Figure A.5).

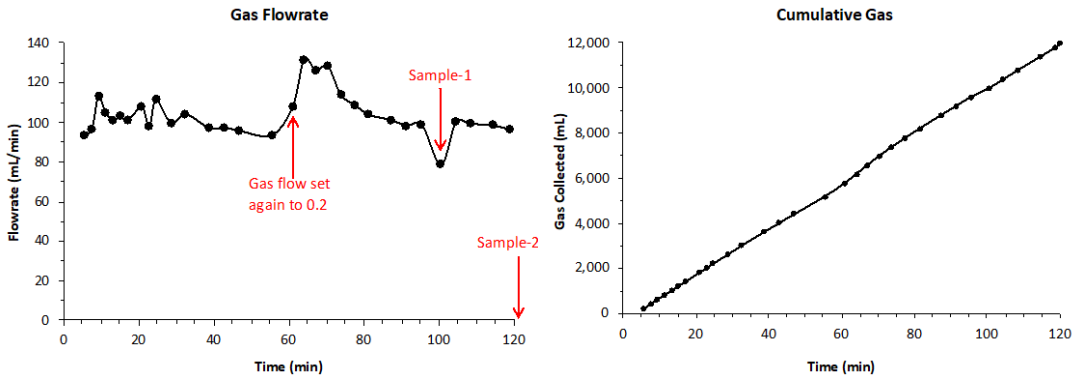

Figure A.5: Experimental setup of Pyro-2: Big gas tank as gasometer at the back (left), the view of water trap after the pyrolysis experiment (right).

Under these experimental conditions at the 2nd pyrolysis experiment, it was detected as only 71% (COD-eq) of raw biomass was converted into pyrolysis products (Table A.1). No difference was detected in the biochar rate yield (44%) as compared the first experiment, and it was observed that the most serious difference was in the WS with a COD yield of 22.5%. In this respect, increasing the carrier gas feed rate from 40 mL/min to 100 mL/min has also encouraged the thermochemical conversion efficiency of biomass. In contrast to this, a decrease in COD of produced gas was detected with a total 3% COD yield. It is also needed to be noted that, a high feeding rate of carrier gas encourages the efficient conversion of biomass, however this approach dilutes the produced gas concentration in a serious rate. Therefore, a new alternative has been sought for dealing with carrier gas during the pyrolysis.

In order to achieve a more concentrated syngas, a peristaltic pump was connected into the pyrolysis system to the purpose of recirculation of inert carrier gas inside the system at 3rd pyrolysis experiment (Pyro-3). In this way, it was aimed to keep the total N_2 amount constant, at the same time sustain an efficient rate of gas feeding that has been found as an important parameter in terms good thermochemical conversion. For this new experiment, experimental apparatus of the pyrolysis system was updated again with a better gasometer system in terms of gas leaking. The newer gasometer was built for the determination of syngas amount and the storage of synthesis gases. A plastic chemical container used as a gasometer which was replaced upside-down at this time, equipped with a water-tight cap that allows a safer way to transfer gas and water (Figure A.6, left). In this way, it was aimed to prevent any possible leaks of syngas components from the bottle cap which was now submerged to the water. So that, the collected gas had no way to escape from the system. Additionally, a graduated

cylinder was replaced at the water exit of the gasometer to monitor the produced syngas amount instantly during the pyrolysis experiments.

Three grams of raw sawdust was used again as biomass input in this new experiment, pyrolysis time was again 2 hours in total consisting of two steps in equal duration. Pyrolysis temperature program was also same as previous one which was 350°C constant temperature at 1st step, then a rapid ramp up to 550°C and stayed in this higher temperature until the end. A loop system was built for this updated pyrolysis experimental setup with an addition of peristaltic pump. Prior to the pyrolysis, the pyrolysis reactor and all the tubing were flushed and filled with nitrogen. Then a gas flow was maintained inside the loop system with a rate of 100 mL/min. Triplicate experiments were made in these conditions and all were showing a similar high total COD yield of biomass with an average of 95%. More importantly, a significant increase was observed for the syngas yield (13% COD-eq) in addition to higher COD yields of gas products, 4% increase of COD yield was observed for WS liquids (Figure A.6, middle). Biochar content has remained same level (44%), but a slight increase in COD yield of WI fraction was detected, that corresponds the 10% of the total COD yield (Figure A.6, right). Last but not least, fermentable fraction of pyrolysis products has been increased to 36%, which expresses the sum of the COD equivalents of produced WS liquid, CO and H_2 gases.

Figure A.6: Experimental setup of the Pyro-3: New gasometer and gas recirculating system equipped with peristaltic pump (left), water soluble fraction of pyrolysis products (middle), acetone washed in-soluble products (bottom-right), residual in-soluble products (top-right).

During this Pyro-3 experiments, the cumulative gas production and concentration of syngas components were monitored over time and temperature (Figure A.7). It can be concluded that syngas released from the thermochemical conversion of biomass took place only at the beginnings of each step (0-5 min and 60-75 min). It was also observed that other gas molecules except carbon monoxide (CO) remained almost constant during the experiment. On the other hand, it has been noted that CO reached its maximum level (28%) just after the temperature increase happened between 60 – 80 minutes and remained almost constant until the end of experiment. According to the results obtained from this experiment, it has been determined that the recirculation of a certain amount of nitrogen gas at constant speed is a very promising way of thermochemical conversion of biomass. However, it can also be concluded as a result of the fact that release of gas products was dominantly occurred in 2nd step with a higher temperature (550°C), it may not be very necessary to conduct the pyrolysis experiments in two different steps. By this current question mark, one-step pyrolysis experiments were become a necessity to examine prior to the fermentation experiments.

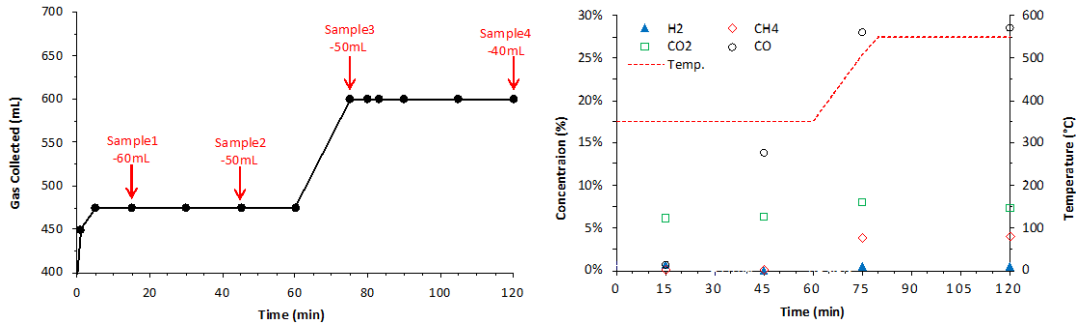

Figure A.7: Gas production amount (left) and variation of gas components (right) during the Pyro-3.

One-step pyrolysis experiments

Same pyrolysis setup of the Pyro-3 experiment (Figure A.6) was used for single step pyrolysis experiments. All single step experiments were carried out in same constant temperature at 550 °C for 1 hour duration.

The results of Pyro-4 single-step pyrolysis experiment is available at Table A.2. By this forth experiment a very high COD yield with 98% was obtained. At the same time, the COD yield of the fermentable fractions has also encouraged by this new experiment, with a COD yield of 43%.

In the Pyro-5 experiment, the effect of using carbon dioxide (CO_2) instead of N_2 as carrier gas was investigated in the same loop pyrolysis system. Compared to the Pyro-4 results, where all pyrolytic conditions were remained same except the carrier gas, it has been observed that there is no change in the overall COD yield. However, a slight increase of 2% was observed for the COD yield of total fermentable fraction (Figure A.6).

After the significant overall COD yields obtained in Pyro-4 and Pyro-5 experiments, it was examined whether it would be possible to work with lower biomass quantities in the more portable vertical pyrolysis furnace (Figure A.2, left). In this new experiment (Pyro-6), in which almost half less sawdust biomass was used, N_2 gas was recirculated at a constant rate of 100mL/min again as carrier gas. By this last experiment, the highest COD yield with 99% was achieved, without observing a serious decrease in the fermentable products' COD yield (Figure A.6). Lastly, in all last three one-step pyrolysis experiments release of syngas during the pyrolysis has been monitored only in the first 15 minutes of the process.

Table A.2: Experimental conditions and COD yields of the one-step pyrolysis

Parameters	Pyro-4		Pyro-5		Pyro-6	
Reactor	Fixed Bed Batch Type		Fixed Bed Batch Type		Fixed Bed Batch	
Pyrolysis Type	Fast & Horizontal		Fast & Horizontal		Fast & Vertical	
Feeding Type	Gas Recirculation		Gas Recirculation		Gas Recirculation	
Carrier Gas	Nitrogen (N2)		Carbon dioxide (CO2)		Nitrogen (N2)	
Gas Flow Rate	0.10 L/min		0.10 L/min		0.10 L/min	
Temperature	550°C for 60min		550°C for 60min		550°C for 60min	
Biomass Type	Sawdust		Sawdust		Sawdust	
Biomass Amount	3.01 g	3.65 g-COD	3.00 g	3.63 g-COD	1.45 g	1.75 g-COD
COD Yields	g-COD	%	g-COD	%	g-COD	%
Syngas	0.49	13%	0.54	15%	0.17	10%
WS Liquid	1.26	34%	1.24	34%	0.62	36%
WI Liquid	0.52	14%	0.51	14%	0.21	12%
Biochar	1.29	35%	1.27	35%	0.71	41%
Fermentable*	1.57	43%	1.63	45%	0.75	43%
Overall Yield	3.56	98%	3.56	98%	1.72	99%

** Fermentable fraction is considered as sum of WS Liquid, CO and H_2 gasses.*

Final Discussion

Results of the pyrolysis experiments showed that single-step pyrolysis process, with a constant temperature of 550°C using the N_2 at constant recirculation rate (0.10L/min) as carrier gas, regardless the amount of biomass and position of pyrolysis furnace (vertical or horizontal) can provide a very efficient thermochemical conversion of biomass (Table A.1 and Table A.2). It is also concluded that 1 hour residence time was highly enough for the pyrolysis process and even a shorter duration might result a similar productivity in terms of COD yield. The results of syngas amount and composition variation during the pyrolysis experiments encourages to shorten the residence time down to half an hour.

According to the results of pyrolysis experiments prior to the fermentation research, biomass can be thermochemically converted into biochar, pyrolytic liquids and syngas with a total COD yield of 98% with the optimized pyrolytic conditions. More importantly, total potentially fermentable fraction was corresponding as much as 43% of the total COD yield (Table A.1). It has also observed that the use of CO_2 as a carrier gas instead of N_2, was not resulted in a significant difference in terms of COD yields. For this reason, it was concluded that it is more appropriate to continue with nitrogen gas, which seems to be more suitable techno-economically.

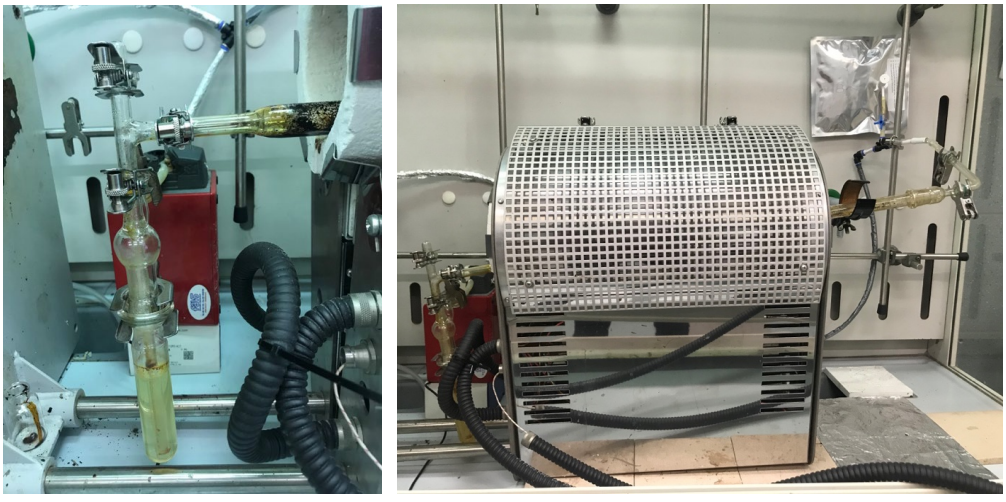

Figure A.8: Gas recirculated compact pyrolysis system equipped with; water trap for WS products (left) and leakproof foil gas-bag for syngas storing (top-right-corner).

Preliminary WS Fermentation Tests

It was necessary to design and develop a bioreactor system that can deal with both very tiny syngas molecules and WS liquid as another potentially fermentable fraction of intermediate pyrolysis products. For this purpose, a trickling bed anaerobic system was designed and constructed very carefully to be able to succeed in a continuous mode of fermentative operation at specific temperature conditions. This methodological duty was a tricky and very important one for the further biological conversion part of the thesis research. Eventually, a unique bench-scale bioreactor system was manufactured and tested {Chapter 3.2.2} in several ways prior to the start-up of fermentation. Five different experiments were conducted in previously constructed tetrapod bioreactors. All performed preliminary WS fermentation experiments will be explained, together with a results and discussion.

Methodology

Inoculum, Medium and Substrate

A mixed culture anaerobic sludge was used as inoculum. The sludge suspension was originated from an anaerobic digester of a wine industry plant located in Faenza, Italy (Caviro Extra S.p.A), where different type organic wastes including sewage sludge, agricultural wastes are treated. Prior to the inoculation of the bioreactor, the MMC with a neutral pH, was thermally pre-treated in an oven at 85°C for 1 hour to eliminate the methane-producers, which are known to be not capable of forming spores under extreme conditions such as high temperature. By this commonly used method for acidogenic fermentation studies, it was aimed to concentrate the spore-forming acidogenic microorganisms [117], [159], [160]. A modified cultivation medium was prepared based on Temudo et al.'s (2007) study. However, all compounds were prepared ten times more concentrated, and glucose did not include (Table 3.3).

Feeding materials for the fermentation experiments with pyrolysis products were obtained by the intermediate pyrolysis of sawdust biomass, which its conditions presented in the previous section {Appendix A: Initial Pyrolysis Experiments}. All materials obtained by the periodically conducted pyrolysis were stored under desired conditions until the day of use for the fermentation bioreactors.

Experimental Set-up

In the previous sections {Chapter 3.2.2}, most of the details of the 'tetrapod's which are the special-made bioreactor systems assembled by the research team for fermentation studies, were already shared. In this reason, only a brief methodological information will be presented in this chapter for the bioreactor operation. Besides, operational procedures of each set of fermentation experiment will be presented together with its results in following sections.

The common operational and set-up parameters of all tetrapod experiments (so far) are presented in Table B.1. Tetrapods were designed and operated as anaerobic biotrickle bed bioreactors which are very useful and easy-to-operate systems for the bio-conversion of many types of liquid and gas components. While the microbial community is fixed to a certain type of filter media (e.g., sand, glass, polymerics), biotrickle reactors provide a homogenous and clear (low suspended concentrations) outputs. Continuous and pulse modes for feeding or recirculation of fluids are commonly used. In this study, pulse mode of liquid recirculation was applied in all experiments except Tetrapod-3 (T-3), to avoid overflowing of bio-liquids above the filter media. The pulse mode liquid recirculation was conducted with using an Arduino based script that allows the submerged-type mini pump with a flow capacity of 220 L/hr to work for only 10 seconds in each minute. However, recirculation pump was continuously working during the T-3 experiment, since there was no overflowing in case of inert bed (only glass-balls) trickle media. The total free bio-liquid volume was 200 mL and temperature condition of the bioreactor was maintained at around 36.0 °C in all experiments. Hydraulic retention time of the liquid compounds were 10 days in each experiment by applying daily 20mL of feeding/discharging cycles (except the batch period of T-4).

Table B.1: Methodologic details of the preliminary WS fermentation experiments.

Reactor Type	Anaerobic Trickling Bed
Operation Type	Daily Fed Continuous Operation
Recirculation Pump Capacity	220 L/hr
Total Bio-liquid Volume	200 mL
Set Temperature	36.0 °C
Hydraulic Retention Time (HRT)	10 days

Two types of tetrapods were used for the experiments of this period of study. One is constructed with a conventional inert filling material with 7.8mm grain diameter glass-balls. The second type of tetrapod's filter media were consisted of; coarse biochar granules, big glass-balls (Ø7.8mm) and smaller glass-balls (Ø4.0mm) which is presented in (Figure B.1).

Figure B.1: Coarse biochar granules as filter media a), tetrapod with biochar amended filter media b), submerged biochar part of the trickle bed

Results and Discussion

Glucose fermentation experiments

This first experiments of the tetrapod fermentation series were conducted with glucose feeding, which can be considered as control experiments either. The purpose of this first two experiments was to investigate the suitability and efficiency of the constructed tetrapods for the purpose of anaerobic bioconversion of substrates into short-chain (e.g., acetic, butyric, valeric) and some medium-chain (e.g., caproic, enanthic, caprylic) fatty acids. Glucose was chosen as substrate to sustain a homogenous and easy-to-degrade environment inside the bioreactors.

In Table B.2 all important operational and set-up parameters were presented for the glucose fermentation experiments. The only and main difference between these two experiments was the filter medias. T-1 was conducted in inert filter bed, while T-2 was conducted with biochar amended filter bed. In both experiments, known amount of lovastatin as a methanogenesis inhibitor [161], [162] was provided in certain days together with aqueous feeding to control the methane production by MMC. Both

experiments were conducted at same load with 20 g-COD/L with same 0.4 g-COD/L-day OLR. The feeding materials were dominantly consisted of glucose with 98.5% of the total input COD.

Table B.2: Operational and set-up parameters of T-1 and T-2.

Parameters	Tetrapod-1 (T-1)	Tetrapod-2 (T-2)
Experiment	Glucose Fermentation	Glucose Fermentation
Filling/Filter Material	**Glassball** *	**Biochar** + **Glassball** **
Feeding Material	**Glucose**	**Glucose**
Operational Interferences	Daily pH Adjustment Lovastatin Addition (CH_4 Inhibitor)	Daily pH Adjustment Lovastatin Addition (CH_4 Inhibitor)
Input Concentration	20.0 g-COD.L^{-1}	20.0 g-COD.L^{-1}
Organic Loading Rate	0.4 g-COD.L^{-1}.day^{-1}	0.4 g-COD.L^{-1}.day^{-1}
Input Load Ratios	98.5% : 1.5% [a]	98.5% : 1.5% [a]

[a]Glucose:Medium in COD basis ; *Glassball inert material with Ø7.8mm ; **Coarse biochar, glasballs with Ø7.8mm and Ø4.0mm were used at the volume to volume ratios of 36/24/40 respectively.

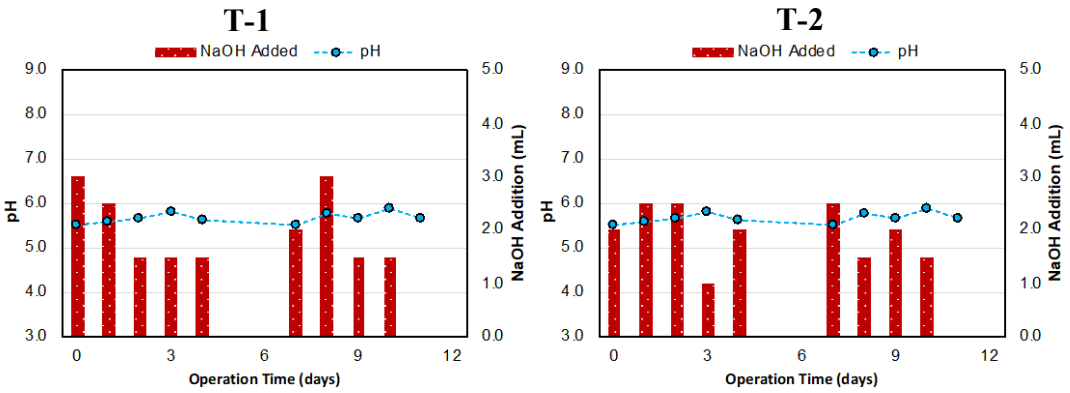

Figure B.2: pH trend of the glucose fermentation experiments

During the operation of eleven consequential days, pH trend was quite similar for both experiments (Figure B.2). Average pH values of the experiments were calculated as 5.66 (±0.12) and 5.70 (±0.13) for T-1 and T-2 respectively, showing that the pH values were quite similar throughout the study. Also, total added 1M of NaOH amounts were very close to each other, showing that acidity of the systems was quite similar during the experiments.

Figure B.3 presents the gas variations of the system during the experiments that allows to track any uptake or release of gas components. Carbon dioxide (CO_2) as a

natural end-product of many biological pathways, were found in considerable positive amounts throughout the experiments, indicating that microbial consortium was active for both cases. The peak CO_2 amounts found in Day-7 was a result of accumulation of the gas components during the two-days weekend period. The only hydrogen (H_2) uptake was occurred in Day-1 was originated from the residual gaseous kept inside the headspace of the tetrapods from previous experiment (not presented). So that, it can be considered as an exceptional behavior. Methane production was observed from the beginning of T-2 experiment, while in T-1 it was started later (Day 7). For this reason, lovastatin was applied from the beginning of T-2, while it was applied only Day 7 and Day 8 in T-1. However, this well-known inhibitor for methanogenic microbes, was not well efficient in our experiments, even at much higher concentrations than reported concentrations. Especially in the presence of biochar in T-2, 10 milli-molar of lovastatin was provided in total which is 100 times higher than reported by Miller and Wolin, 2001 and 8 times higher than reported by Faseleh Jahromi et al., 2013. This phenomenon can be correlated with very low water solubility of the inhibitor compound, and also might be linked with a very wide range of different strains available in MMC systems. As can be seen from the below graph, lovastatin has showed a weak inhibition effect on methane production in both tetrapod experiments with glucose fermentation.

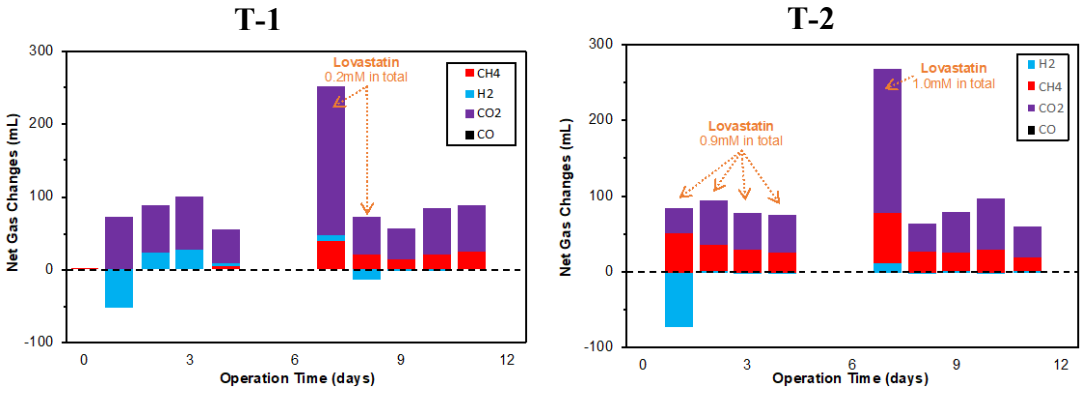

Figure B.3: Variation of produced or consumed gas amounts for T-1 and T-2.

Figure B.4 presents the total and soluble COD concentrations detected in bio-liquid samples discharged as daily output material. Throughout the experiments, soluble COD concentrations were nearly stabilized around 15-16 g/L in both experiments. The average soluble COD values were found as 15.9 (±0.8) and 15.1 (±0.9) for T-1 and T-2 respectively. However, 5-10% of higher total COD values over

soluble COD for T-1 experiment were detected in most of the operational days, whereas in T-2 with biochar amended trickle media there was no such constant behavior. This difference in the characteristics of the bio-liquid samples from the experiments suggesting that biochar amended trickle bed provides less particulated liquids with more homogenous and clear characterization. It may also be linked with a possible better biofilm accumulation either on the surfaces or inside the porous interior of the biochar granules.

It can also be tracked total VFA concentration as equivalent COD basis and VFA yield trend in Figure B.4. VFA yield values correspond the percentage of total VFA content over the total COD, which shows a slightly more stabilized trend in biochar amended tetrapod experiment (T-2) than T-1. Total VFA concentrations of both experiments were also found nearly stabile throughout the study resulting average VFA concentrations of 12.1 (±0.5) and 11.3 (±0.7) g-COD/L for R-1 and R-2 respectively. A slightly lower average COD and VFA values obtained in T-2 may be linked with a possible adsorption of fermentation products into biochar granules, since the VFA yields were quite good and similar (72% and 75%).

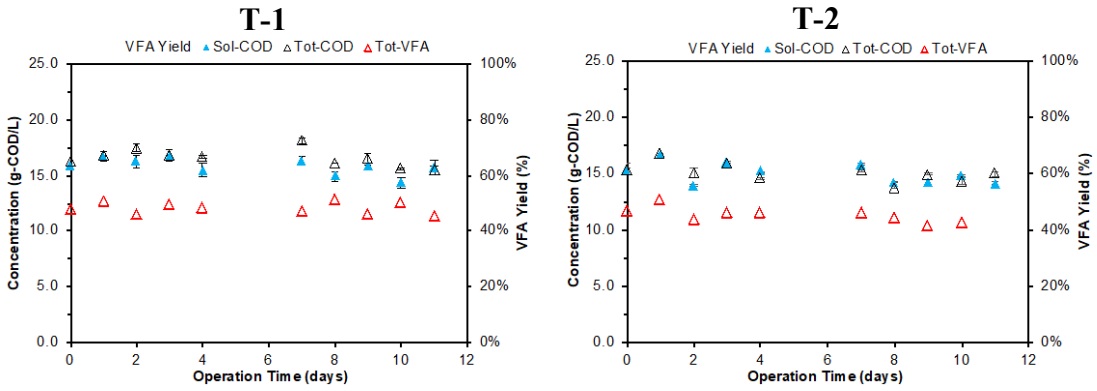

Figure B.4: Total COD, soluble COD, total VFA concentration and VFA percentage trends for T-1 and T-2 experiments.

Figure B.5 presents the concentration trends of each VFA component available in bio-liquid samples of the experiments. As it can be seen from the below graphs, the distribution of VFA components quite similar to each other. An obvious difference for the available VFAs only detected for; the one with highest number of carbons (Caprylic acid; $C_8H_{16}O_2$) and the one with lowest number of carbons (Acetic acid; $C_2H_4O_2$). At the end of study for T-2, all caprylic acid was already consumed, however a higher concentration of acetic acid was detected as compared to T-1.

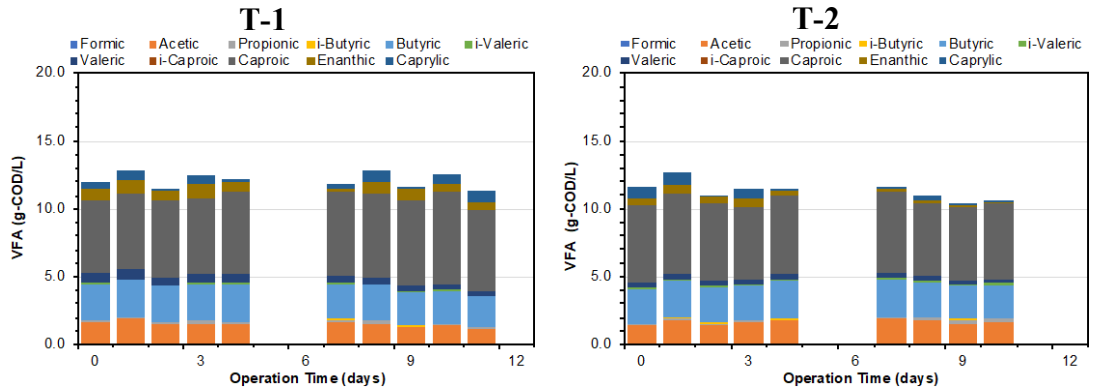

Figure B.5: Concentration trends of each VFA component for T-1 and T-2.

More importantly, variation of daily produced and consumed fermentation products is presented as column graphs in Figure B.6. Especially in this kind of biological systems, a continuous production of bio-products is very desirable. Below figure shows us in which days the tetrapods produced or consumed which type of VFA components.

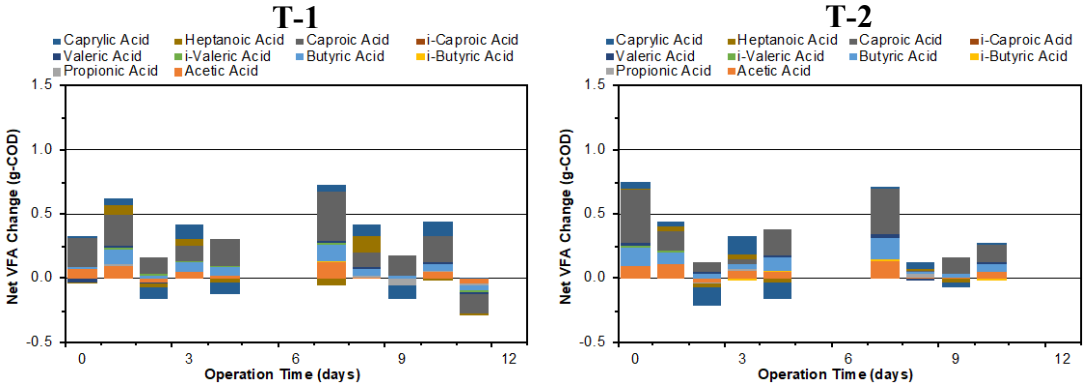

Figure B.6: Daily variation of produced or consumed VFAs for T-1 and T-2.

The overall mass balance calculations for the glucose experiments based on the available data obtained by the measurements were summarized in Table B.3. The selected Day-0 to Day-10 period for the mass balance corresponds one HRT cycle of operation and 4.0 grams of COD equivalent feeding was provided in this period to both reactors. As a result, 3.5 (87% recovery) and 3.8 (95% recovery) grams of COD was obtained for T-1 and T-2 in their output materials as VFA enriched liquid (bio-liquid) and carbon dioxide enriched gas (biogas). It means that a very promising COD balance can be obtained from the constructed tetrapod bioreactors. The low gap between input and output total CODs can be correlated with a possible biofilm growth during the operation. In contrast to the similar and high COD recovery ratios, the

calculated net produced VFA amounts and accordingly overall VFA yields were different and lower in T-2 where the biochar was available inside the system. This phenomenon can be correlated with two possible reasons. One is that a higher unstoppable continuous methane production occurred in T-2 may lower the VFA yield. Secondly, this result may also suggest that biochar has a good VFA adsorption capacity. However, this possible adsorption capacity issue will need to be discussed and investigated further.

Table B.3: Operational and set-up parameters of T-1 and T-2.

Parameters	**Unit**	**Tetrapod-1 (T-1)**	**Tetrapod-2 (T-2)**
COD Balance Period	days	10.0	10.0
Total Input Material	g-COD	4.0	4.0
Total Output Material	g-COD	3.5	3.8
Recovered COD Ratio	-	87%	95%
Produced Net VFA	g-COD	2.8	2.1
Overall VFA Yield	-	80%	55%

Pyrolysis products fermentation experiments

Pyrolysis products fermentation experiments as the core target of this study has started with these experiments to investigate the bio-conversion potential of bio-available products of intermediate pyrolysis, namely water-soluble fraction of bio-oil and pyrolytic gaseous substances (i.e., syngas). The first two pyrolysis products fermentation experiments were conducted in very similar operational conditions at same input concentration (20g-COD/L) with previous glucose fermentation experiments.

Table B.4 summarizes the operational and set-up details of this set of experiments. The main goal of this first two fermentation experiments with pyrolysis products was to investigate the acidogenic bioconversion capacity of pyrolytic aqueous liquid (i.e., WS liquid, Pyro-WS, aqueous bio-oil) at 20g-COD/L input level with 0.4 g-COD/L-day organic loading rate and 10 days of hydraulic retention time.

Tetrapod-3 (T-3) was conducted in conventional inert filter, while in Tetrapod-4 (T-4) biochar amended biotrickling bed was used. Biochar as a potential detoxifier material for the redoubted intermediate pyrolysis products, was used for providing a better environment for the MMC. Both reactors were initially operated with glucose feeding during the enrichment period (5-6 days of operation) where a healthy anaerobic microbial biofilm formation was targeted through the trickle beds. Then a transition phase was applied to prevent any possible shocking effect by new challenging substrates, with a mixed feeding input that consist of both glucose and PyP in a gradually increased amount of PyP. Furthermore, bromoethane sulfonate (BES) was used as chemical inhibitor for methanogenic activity instead of lovastatin that was previously found as not very effective tool for the tetrapods in glucose fermentation experiments. BES was not used in T-3 experiment since it was not necessary throughout the PyP fermentation phase of the experiment.

Table B.4: Operational and set-up parameters of T-3 and T-4.

Parameters	Tetrapod-3 (T-3)	Tetrapod-4 (T-4)
Experiment	Glucose Fermentation	Glucose Fermentation
Filling/Filter Material	Glassball *	Biochar + Glassball **
Feeding Material	Pyro-WS + Syngas	Pyro-WS + Syngas
Operational Interferences	Semi Controlled pH	Daily pH Adjustment
	No Chemical Inhibitor	BES Addition (CH_4 Inhibitor)
Input Concentration	20.0 g-COD.L^{-1}	20.0 g-COD.L^{-1}
Organic Loading Rate (OLR)	0.4 g-COD.L^{-1}.day^{-1}	0.4 g-COD.L^{-1}.day^{-1}
Input Load Ratios	88.5% : 10.0% : 1.5% [a]	88.5% : 10.0% : 1.5% [a]

[a]WS:Syngas:Medium in COD basis ; *Glassball inert material with Ø7.8mm ; **Coarse biochar, glasballs with Ø7.8mm and Ø4.0mm were used at the volume to volume ratios of 36/24/40 respectively.

During the first attempt of PyP fermentation studies conducted in tetrapods, pH profile and added base amounts are presented in . As a result of no intervention to pH values during the first couple of days of operation in T-3, very low pH values are observed in subsequential days of 3 and 4. In contrast, at T-4 with biochar amended filter it was never obtained that much low pH values even some pH fluctuations were observed at initial days of operations. This phenomenon can be correlated with a possible better buffer capacity occurring by the presence of organic biochar filter bed.

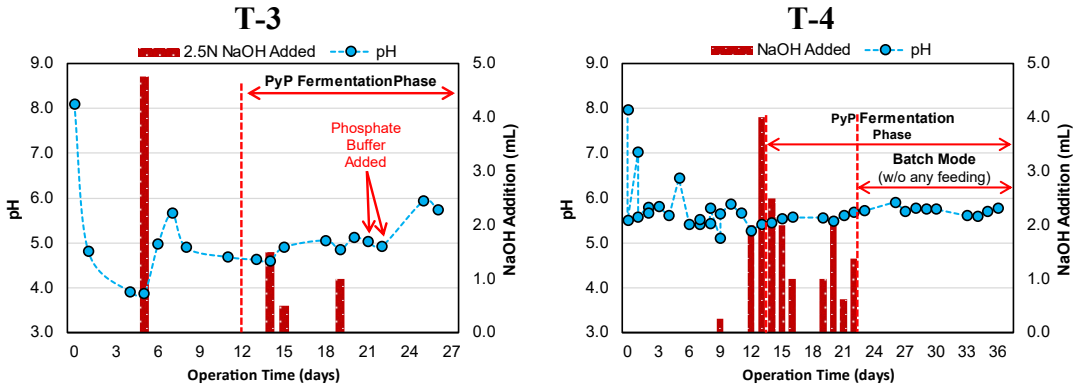

Figure B.7: pH trend of T-3 and T-4 experiments

Figure B.8 presents the variations of the gas compounds during the experiments. First days of operation a serious amounts of biogas production can normally occur as a result of inoculation of bioreactors with fresh methanogenesis dominant MMC. In this reason, that extraordinary biogas productions were considered as exceptional and not fully included into the graphs to sustain a better visualization for PyP fermentation phases with much lower volumes of gas variations. Methane production was observed only in the days of 8 and 11 during the transition phase of T-3, just after the pH was manually increased to above 5.5 value and then stopped suddenly when the system started to be fed only with PyP. However, in T-4 experiment a limited amount of continuous methane production was monitored until the spikes of BES was applied at 2.50 mM overall concentration. This disagreement in CH_4 formations may be linked with lower pH profile of T-3. Very low pH values obtained in the initial days of T-3 operation might have inactivated methanogenic strains. More importantly, a possible detoxifying effect of biochar granules available in T-4 can be another reason behind the continuous formation of methane even after the bioreactor started to be fed only with PyP materials.

Another important difference is the much higher uptake amounts of carbon monoxide (CO) in T-4 as compared to T-3. A continuous uptake of CO was observed during the PyP fermentation phase where syngas was inserted corresponding 10% of total daily input COD. This different behavior in CO uptake can also be correlated with biochar filter media which is inserted and positioned at the top of the trickle bed where the filter media get contact with headspace gas molecules (Figure B.8). Apparently coarse biochar granules provide a better environment for the bio-conversion of gas molecules might be related with the unique porous structure of bio-char grains which may serve as a trap for the CO molecules.

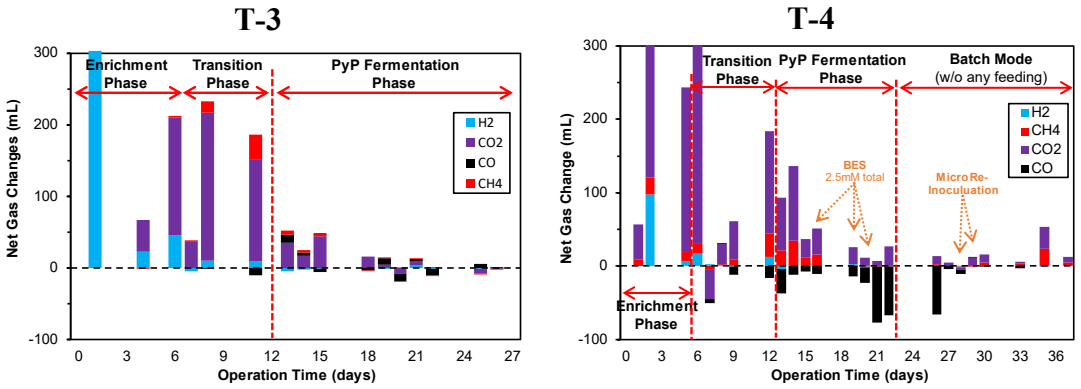

Figure B.8: Daily produced or consumed gas amounts for T-3 and T-4 experiments

Then change in total COD, soluble COD and COD equivalent total VFA concentrations of bio-liquid samples can be tracked in Figure B.9. COD values of T-3 was more stable throughout the experiment as compared to T-4. However, after PyP fermentation phase started, a relatively stable COD trends were also observed in T-4. Fluctuations in COD especially occurred in transition phase was resulting from some experimental and operational difficulties occurred during that specific dates of operation. While these strange exceptional errors were before the PyP fermentation phase, it should not effect dramatically the results obtained during the fermentation phase. Transition phase with gradually increased amount of PyP feeding had been started when total VFA concentrations were reached around 70% of total COD in both experiments. However, after 2-3 days later when PyP was started to be used as only feeding material, a similar decreasing trend was observed for total VFA in both cases, suggesting a possible toxification by WS liquid. After two weeks operation only with PyP feeding, total VFA concentration was gradually decreased down to the level of 4.8 from the maximum level of 14.9 g-COD/L obtained just before the PyP

fermentation phase started. Similarly in T-4 experiment, VFA percentage was decreased to the 30% from over 85% levels (again observed just before PyP fermentation phase). Then, continuous daily feeding and discharging of T-4 was stopped and it started to be operated in batch mode to investigate if the toxification was irreversible. Eventually, just after 5 days of batch operation, a sudden increase in VFA amount was detected, that is showing the possible toxification of MMC by WS liquid was reversible. Furthermore, around 50% to 70% of VFA yield was monitored at the last days of operation, which was similar values obtained when the PyP fermentation was initiated.

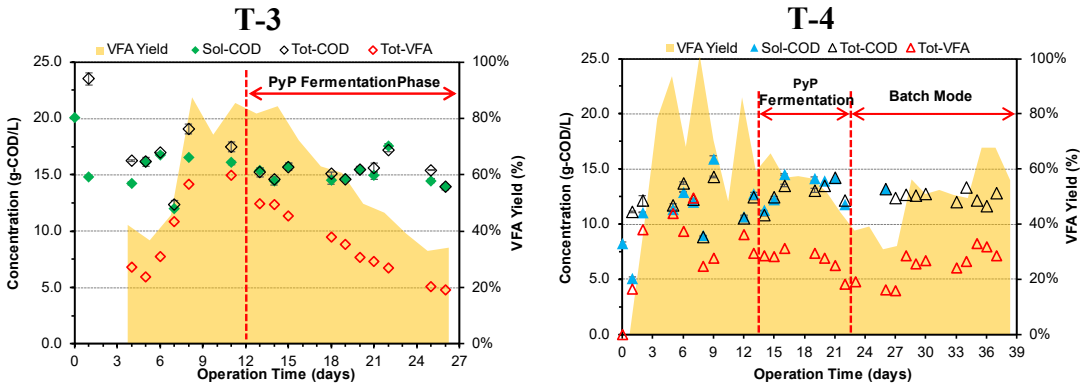

Figure B.9: Total COD, soluble COD, total VFA concentration and VFA percentage trends for T-3 and T-4 experiments

Figure B.10 presents the concentration trends of each measured VFA component for T-3 and T-4 experiments. The main difference in the distribution of VFA components were found for Acetic, Butyric, and Valeric acids. Acetic acid was corresponding the highest concentrations for T-4, while Butyric acid and Valeric acid was found to be biggest portions in VFA analysis of the bio-liquid samples of T-3 experiment.

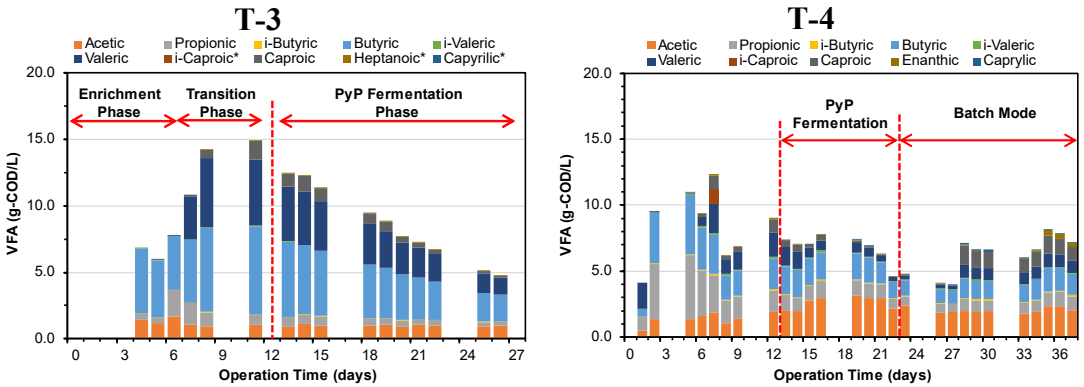

Figure B.10: VFA composition trends for T-3 and T-4 experiments

Figure B.11 presents the net VFA changes during the operation of the first set of PyP fermentation experiments. In contrast to the previous VFA concentration graphs, more importantly in this one, a promising continuous VFA formation was seems to be achieved, even at the days of sharp decreasing trend of VFA concentrations were occurred. The results obtained at batch period of T-4 may provide some extra information as well since sharp daily production of various VFA components occurred couple of times following with non-productive days. This phenomenon needs to be further discussed by investigating the fate of pyrolytic molecules, which may suggest that some specific robust molecules can be degraded by MMC in hunger regime.

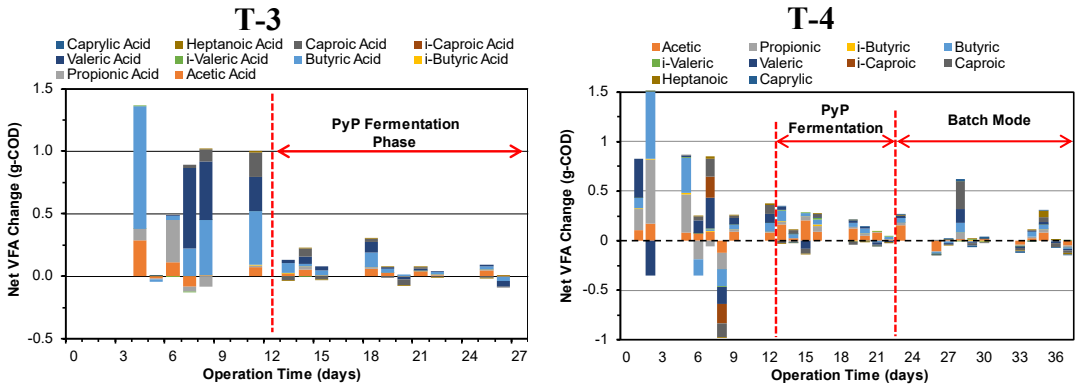

Figure B.11: Daily produced or consumed VFA components for T-3 and T-4.

Table B.5: Mass balance summary of the PyP experiments.

Parameters	Unit	Tetrapod-3 (T-3)	Tetrapod-4 (T-4)
COD Balance Period	days	12.0	10.0
Total Input Material	g-COD	4.8	4.4
Total Output Material	g-COD	3.8	3.8
Recovered COD Ratio	-	79%	86%
Produced Net VFA	g-COD	0.7	1.1
Overall VFA Yield	-	18%	28%

The overall mass balance calculations for the first set of PyP fermentation experiments with 20 g-COD/L input material are presented in Table B.5. The mass balance calculations were restricted only for approximately one HRT cycle period

during the continuous PyP fermentation phases of the experiments. The mass balance was conducted for the days between 13th and 25th for T-3, and 13th to 23rd days of operation for T-4. As a result, a better COD recovery was again obtained in case of biochar available experiment (T-4) with reaching up to 86% of total input COD for the period of time. However, for T-3 with inert bed filter media COD recovery was stayed below 80%. Even thought, much lower net VFA yields are obtained in PyP fermentation experiments compared to the preliminary control experiments with glucose feeding, a relatively higher net VFA yield in biochar amended reactor (T-4) than the traditional one (T-3) was found as a promising* outcome. Since it was previously concluded that the biochar has a good capability of absorbing VFA compounds, a higher net VFA yield is a quite interesting result.

Pyro-WS fermentation at low OLR

The last fermentation experiment conducted in this section was a continuation of T-4 experiment but with half input material and half OLR. For this purpose, all available bio-liquid and biogas found at the end of T-4 was removed, then an input liquid mixture with 10.0 g-COD/L concentration which dominantly occurred by WS liquid was inserted into the same bioreactor with already available possible MMC biofilm formed in previous experiment (T-4). The main purpose of this experiment was to increase the net VFA yield formed by bio-degradation of WS liquid. Besides, it was also aimed to understand that if Pyro-WS as a mono substrate can be bio-converted into VFAs. In this reason, any syngas material was not injected into the bioreactor during this experiment (Table B.6). Another different approach applied in this experiment was no addition of chemical inhibitors, while it was seen in previous experiments that all methane production was already stopped after the continuous feeding with PyP. This single experiment with only WS liquid feeding at half OLR of input was conducted only in the bioreactor with biochar amended trickle bed, because of previously conducted experiments suggested that biochar added biological trickle systems have several advantageous over the traditional inert filter bed bioreactors.

The initial pH of the start-up mixture for the Tetrapod-5 (T-5) experiment was already set to 6.10 to provide a better environmental condition for the acidogenic biofilm. For this purpose, a considerable amount of 1M of NaOH solution was provided initially (Figure B.12a). Then a daily 0.5 mL of 1M of NaOH solution was inserted together with feeding material to sustain a stable condition around pH 6.0.

This fixed amount of NaOH provision was found quite effective resulting with an average pH value of 5.9 (±0.1) during the 17 days of continuous operation.

In Figure B.12b, it is presented the daily change of biogas molecules throughout the operation and no methane production was observed as expected. However, relatively lower production of CO_2 might be correlated with a possible shock toxification. This situation was found as engrossing and can be related with direct application of 200mL of completely new feeding material dominantly comprised by Pyro-WS that potentially consist of different of several toxic compounds even at high concentrations. Nevertheless, very small but positive CO_2 values were suggesting that the MMC biofilm was not completely inactivated. Eventually, daily re-inoculation procedure was started after the 1st week of operation in very small amounts (1 mL/day = 1% of input COD), to increase the possibility of a better microbial bio-degradation.

Table B.6: Operational and set-up parameters of T-5 experiment.

Parameters	Tetrapod-5 (T-5)
Experiment	Pyro-WS Fermentation
Filling/Filter Material	Biochar + Glassball **
Feeding Material	Pyro-WS
Operational Interferences	Daily pH Adjustment No Chemical Inhibitor
Input Concentration	10.0 g-COD.L^{-1}
Organic Loading Rate (OLR)	0.2 g-COD.L^{-1}.day^{-1}
Input Load Ratios	98.5% : 0.0% : 1.5% [b]

[a]WS:Syngas:Medium in COD basis ; *Glassball inert material with Ø7.8mm ; **Coarse biochar, glasballs with Ø7.8mm and Ø4.0mm were used at the volume to volume ratios of 36/24/40 respectively.

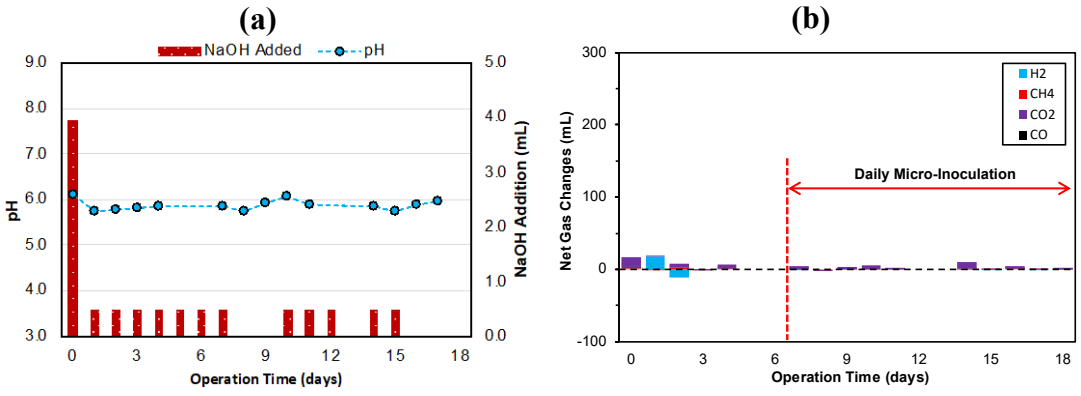

Figure B.12: pH trend a) and variation of gas molecules b) during T-5 experiment

A relatively stable COD values were monitored for T-5 experiment (Figure B.13). The maximum VFA content was achieved at 2nd day with equal to 4.5 g-COD/L concentration. However, a continuous decreasing trend in VFA yield was observed after that peak concentration. Figure B.13b presents the change in concentration of VFA components distribution. From the graph, it can be concluded that the MMC prefer to eat first bigger molecules such as caproic acid and valeric acid in case of toxification.

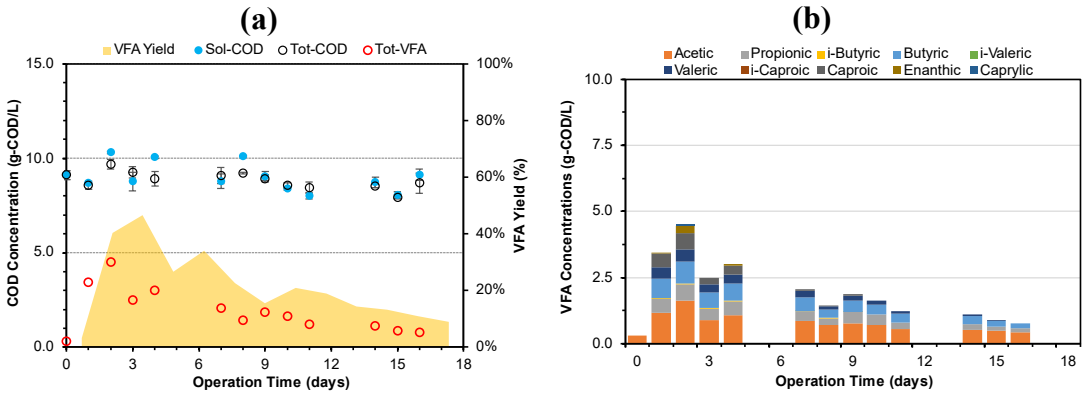

Figure B.13: COD and VFA variation a) and VFA profile b) during T-5 experiment

Figure B.14 shows a better understanding of what is occurring in terms of net VFA productions. There was not any relevant trend available which can be discussed easily from the data of VFA variations. However, a continuous VFA production was not maintained during the 17 days of continuous operation. This issue again might be about the shocking toxic effect of direct WS feeding without any initial enrichment and/or transition phases which were applied in previous experiments.

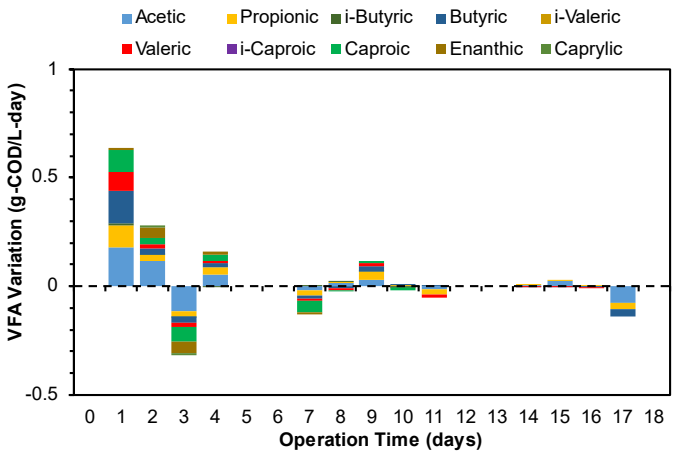

Figure B.14: Daily variation of produced or consumed VFA components for T-5.

The mass balance estimations of the first 10 days of operation were provided the results shared in Table B.7. In contrast to the not very promising trends observed in above mentioned graphs, overall mass balance with 92% of COD recovery, and 34% of net VFA yield value makes this T-5 experiment as the best attempt so far for the bio-conversion of WS liquid containing feeding materials. In conclusion, less concentrated WS liquid has resulted a better VFA yield.

Table B.7: Mass balance summary of the T-5 experiment.

Parameters	Unit	Tetrapod-5 (T-5)
COD Balance Period	days	10.0
Total Input Material	g-COD	2.0
Total Output Material	g-COD	1.8
Recovered COD Ratio	-	92%
Produced Net VFA	g-COD	0.6
Overall VFA Yield	-	34%

Final Discussion

The first preliminary glucose fermentation experiments conducted in tetrapod bioreactors were provided some basis information for the latter pyrolysis products fermentations. Fermentation of PyP experiments were conducted in both inert filter bed and also biochar amended trickle bed bioreactors. Lastly, another fermentation experiment was conducted with half OLR to investigate the solo fermentation of WS liquid as a challenging substrate. Main conclusions obtained by the experiments of this research period are listed below:

- Biochar as a trickle bed media provides cleaner bio-liquid output with less suspended materials
- Lovastatin was not very effective tool for methanogenic activity, while BES as highly soluble chemical inhibitor was highly efficient even at 2.5 mM concentration.

- Biochar should have detoxifying feature and buffering effect on anaerobic MMC.
- Remarkably better uptake of carbon monoxide was obtained in biochar amended tetrapod system.
- Toxification by WS liquid was not irreversible, just requires longer time period for the MMC to be re-activated in the presence of PyP.
- Subsequential enrichment, transition and fermentation phases might be compulsory for a continuous bio-conversion.
- Lower OLR with 0.2 g-COD/L-day enhances the acidogenic bio-conversion rates of Pyro-WS.
- Even lower input concentrations with lower OLR of Pyro-WS feeding should be considered for further research.
- Batch tests with different conditions may provide a comprehensive information about the optimal continuous operation of tetrapods.
- Obtaining different type of Pyro-WS derived from either different biomass materials (probably non-wooden) or different pyrolysis conditions might be crucial way to enhance the continuous bio-conversion of PyP.
- Biochar can be considered as an efficient tool for the recovery of VFA components with its possible high adsorption capacity for the fermentation products.

Synthetic Syngas Fermentation Test

The first syngas fermentation experiment under this PhD study will be presented under this chapter. The aim of this first set of experiments was, enrichment of the mixed anaerobic culture and producing short chain fatty acids (i.e. VFAs) in a bubble column bioreactor. The experimental methodology and results of the 18-days long first experiment will be shared.

Methodology

Inoculum and medium

The anaerobic inoculum that is used in the fermentation experiment was taken from a yeast industry plant (Pak Gıda Co. - Izmit Plant). The sludge suspension was obtained from an anaerobic wastewater treatment tank of the plant. The anaerobic tank with a relatively higher VFAs content and lower methanization efficiency, it is assumed that fermentative and acetogenic microorganisms are predominated. The basic characterization of the seed inoculum is shown in Table C.1.

Table C.1: Basic characterization of anaerobic inoculum.

Parameter	Value
pH	8.4
Oxidation reduction potential (ORP, mV)	- 343.0
Total solids (TS, mg/L)	6,632
Total suspended solids (TSS, mg/L)	2,750
Optical density (OD600, abs)	6.14 ± 0.00
Chemical oxygen demand (COD, mg/L)	2,678 ± 258
Total nitrogen (TN, mg/L)	161
Volatile fatty acids (T-VFAs, mg/L)	1,554

A modified basal medium had the following composition in per liter: 1.0 g yeast extract, 100 mL mineral solution, 10 mL trace metal solution, 2 mL resazurin, 0.5 g cysteine-HCl [163]. Vitamin solution was not included the medium, since the mixed seed culture suspension is expected to have enough vitamin content. Also, some studies has shown that CO fermenting cultures are able to grown with no additional vitamin addition [164], [165]. Mineral stock solution and trace metal stock solution compositions are presented in Table C.2 and some basic chemical characteristics of the medium are shown in Table C.3.

Table C.2: Fermentation medium basic chemical characterization.

Parameter	**Value**
pH	6.2
Optical density (OD600, abs)	0.25 ± 0.01
Chemical oxygen demand (COD, mg/L)	1,394 ± 30

Table C.3: Enrichment medium composition.

	Chemical Name	**Chemical Formula**	**Unit**	**Concentration**
Mineral Solution	Ammonium chloride	NH4-Cl	g/L	25.00
	Sodium chloride	NaCl	g/L	20.00
	Magnesium sulfate heptahydrate	MgSO4-7H2O	g/L	5.00
	Potassium chloride	KCl	g/L	2.50
	Potassium dihydrogen phosphate	KH2PO4	g/L	2.50
	Calcium chloride dihydrate	CaCl2-2H2O	g/L	1.32
Trace Metal Solution	Nitrilotriacetic acid	N(CH2COOH)3	g/L	2.00
	Manganese sulfate monohydrate	MnSO4-H2O	g/L	1.00
	Ammonium iron(II) sulfate hexahydrate	Fe(NH4)2(SO4)2-6H2O	g/L	0.80
	Cobalt (II) chloride hexahydrate	CoCl2.6H20	g/L	0.20
	Zinc chloride	ZnCl2	g/L	0.09
	Copper (II) chloride dihydrate	CuCl2.2H20	g/L	0.02
	Nickel (II) chloride hexahydrate	NiCl2 .6H2O	g/L	0.02
	Sodium molybdate dihydrate	Na2MoO4-2H2O	g/L	0.02
	Sodium selenate	Na2SeO4	g/L	0.02
	Sodium tungstate	Na2WO4	g/L	0.02
Others	Yeast extract	-	g/L	1.00
	Resazurin (0,1%)	C12H7NO4	mL/L	2.00
	Cysteine-HCl	HSCH2CH(NH2)COOH-HCl	g/L	0.50

Experimental set-up and operation

A bench-scale continuous gas-fed stirred tank bioreactor was designed and constructed for the syngas fermentation experiment. A 500 mL glass bottle was used as a bioreactor. A silicone stopper with 5 openings was used to maintain gas-tight environment. In this system, gas feed was maintained to the liquid medium by using a nano type atomizer (i.e. CO_2 diffuser) to increase the dissolution of the poorly soluble syngas components via gas injection port. One pipe was immobilized to the silicone, which is located at top of the headspace for gas outlet (i.e. gas sampling port). Another pipe with 2 mm internal diameter was immersed to the liquid and equipped with watertight pneumatic valve at the outside part. This liquid port was used for liquid sampling and liquid injection (if necessary). One another opening was also equipped with an immersed pipe as a backup port.

Temperature control and stirring was maintained by using a hotplate magnetic stirrer equipped with a stainless-steel thermocouple that was submersed to the liquid through the last opening of the silicone head (Figure C.1). Synthetic syngas mixture with following composition: 5.4% CO_2, 17.2% H_2, 55.7% N_2, 17.9% CO was fed to the bioreactor at a relatively constant flowrate with using double stage gas regulator (Kasweld 7008-L1) following with a gas flowmeter (Dwyer Instruments RMA-151-SSV). Gas outlet piping was connected to a silica-gel column to remove the moisture content of the gas samples.

Figure C.1: Images of the experimental set-up prior to the fermentation.

After mixing 100 mL mineral stock solution and 10 mL trace metal stock solution in 1-Liter volumetric flask, 2 mL of 0.10% resazurin (ORP indicator) and 1.0 gram of yeast extract was added to the fermentation medium and filled up to 1 liter. The initial pH of the basal medium was set to 6.2 with 1M of NaOH and citrate buffer solution. Citrate buffer stock solution was prepared as follows: 7.2 mL of 0.1M citric acid solution and 42.8 mL of 0.1M sodium citrate dihydrate solution is mixed and adjusted the final volume to 100 mL with deionized water.

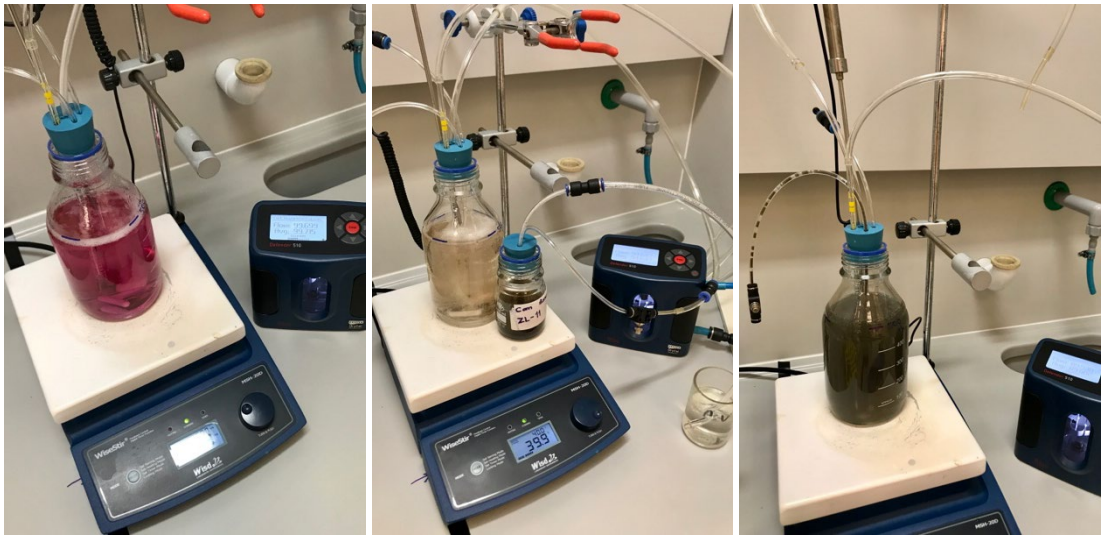

Figure C.2: Color change of the bioreactor during start-up: a) after autoclaving the media, b) after cysteine-HCl addition, c) after inoculation

It is important point that biomethanation of CO-rich gases is easier than acid forming fermentation process. So, the inhibition of methanogenic microorganisms, is a crucial step for syngas fermentation processes with MMC. A 450 mL portion of the medium was transferred to the bioreactor bottle (500 mL glass bottle) and autoclaved. In the meantime, anaerobic inoculum was also autoclaved at 90°C for 15 minutes to inhibit the methanogenic bacteria and archaea groups that are not capable of forming spores under extreme conditions such as high temperature, strongly acidic or basic conditions and so on [159], [160]. In this way, acetogenic microorganisms were expected to grow more easily and produce the target organic acids. Both the medium and the inoculum was cooled down to 38°C by purging with nitrogen gas (N_2) for 1 hour at 100 mL/min flow. Cysteine-HCL oxygen reducer chemical was added to the bioreactor for consuming residual dissolved oxygen in the medium. After the medium became almost colorless which represents the anaerobic environment inside the

bioreactor, 50 mL oxygen free inoculum was injected to the bioreactor through the liquid port. In this way, 10% of inoculum (v/v) was achieved in the bioreactor, as same as many other previous studies [159], [165]–[168]. The bioreactor was continuously purged with N_2 through the gas injection port ending with an atomizer for further 6 hours with a 50 mL/min flowrate to sustain a strict anaerobic environment (Figure C.2).

Fermentation experiment was carried out at 38 °C (±1.0) with 5.20 mL/min (±0.50) continues syngas feed. Medium suspension is stirred at 500 rpm speed during the fermentation experiment for total 18 days of operation.

Sampling and analytical methods

Frequent liquid samplings were carried out periodically on almost every day or on alternate days. Prior to the sampling, agitation speed was increased to 1000 rpm to sustain a better homogenization in the liquid suspension. Approximately 2.5 to 3.0 mL liquid samples were withdrawn with plastic syringes by using the liquid port of the bioreactor. Oxidation reduction potential (ORP) and pH measurements were done just after the sampling.

The liquid samples pH values were measured with using a multiparameter device (Mettler Toledo, SevenExcellence) equipped with a pH electrode (Mettler Toledo, InLab® Expert Go-ISM). ORP was obtained by a redox electrode (Mettler Toledo, InLab® Redox) via a portable pH meter (Mettler Toledo, SevenGo Duo). An UV–visible spectrophotometer (Thermo Scientific, Genesys 10S UV-VIS) was used to measure the optical density (OD600) of the 4 times diluted raw liquid samples. Total solids of the liquid samples were determined by drying in a 2 mL Eppendorf tubes at 105 °C for 2 hours. Other chemical analysis was carried out from the biomass free supernatant of the 15 minutes centrifuged (at 4 °C and 15,000 rpm speed) liquid samples. Samples for VFA analysis were initially acidified with hydrochloric acid (HCl) and stored below -20°C until analyzed. COD measurement was carried out by following the closed reflux titrimetric method of the standard methods [169].

VFA were detected by a gas chromatography (GC) system (Agilent, 6890N) equipped with a flame ionization detector (FID) and a capillary DB-Wax column (30 m length x 0.530 mm internal diameter x 0.50 μm thickness). Helium was used as the carrier gas with a 5.4 mL/min flow. The temperature of the oven was initially set at 50°C for 3 min and then it was gradually increased to 100°C by 5°C/min followed by

an increase of 8°C/min up to 120°C, and final temperature was set to 200°C with a 10°C/min heating speed. Total run time was 24.50 minutes. Temperature of the inlet and the detector was 250 °C and 260 °C respectively. Spitless injection was used for the analysis.

Gas samples were also frequently taken by using a 20 mL gas-tight glass syringe equipped with a 3-way valving system to avoid any air contamination during sampling and injection. An approximate 15mL of gas samples were taken every sampling in duplicate. 10 mL portion of the gas samples were injected to GC with a thermal conductivity detector (Agilent, 6890N) to determine the change in syngas composition. Two capillary column were connected in series. HP-Plot/Q (30m x 0.53 mm x 40µm) was used to detect CO_2 content and the HP-Molesieve column (30m x 0.53 mm x 50µm) was used for other syngas components (e.g. H_2, CO, CH_4). Argon (Ar) was used as carrier gas with a 30.0 mL/min a total flow and the inlet temperature was 150°C. Split ratio was 0.5:1 and the split flow was 9.0 mL/min. The oven temperature was set as 35°C for the first 7 min of the analysis. Then, increased to 115°C with a 40°C/min ramp and the holding time was 6 min. The TCD detector temperature was 230°C.

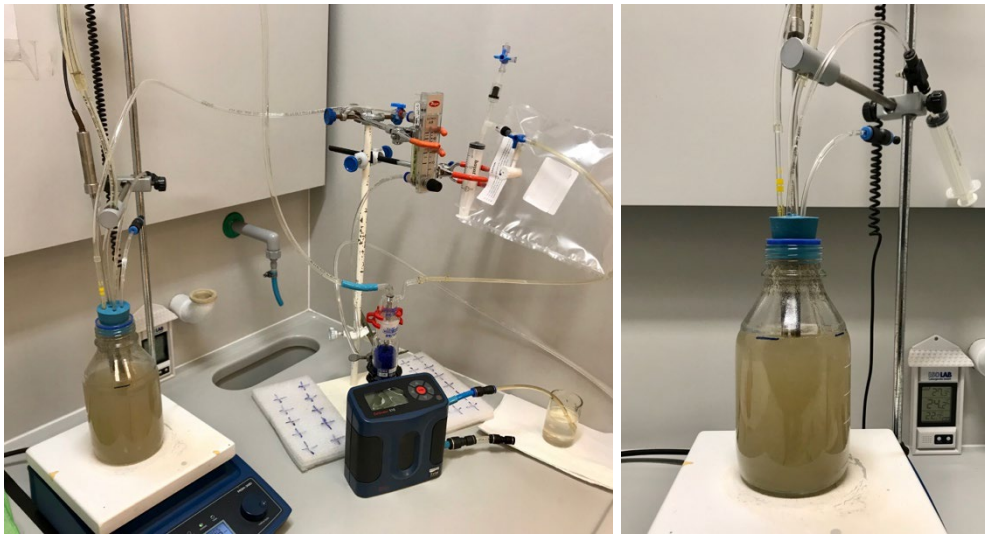

Figure C.3: Bioreactor system during the 18-days experimental research: a) Overview of the bioreactor set-up, b) Close-up image of the bioreactor

Results and Discussion

Results of the first syngas fermentation set will be shared in this section. From the data obtained from the experimental analysis suggests that lag phase of the

fermentation experiment ended at 4th day. Enrichment phase took about 5 days long and the bioreactor reached the steady-state at 9th day. About a week of stationary phase period, system started to slow down, and bacterial demolition was started after 15th day of operation.

ORP and pH change

During the 18 days of fermentation experiments, pH and ORP values were detected using reference electrodes immediately after the sampling. Medium and the anaerobic inoculum pH values were 6.2 (Table C.2) and 8.4 (Table C.1). However, the initial pH of the suspension was found in a very neutral value (pH: 7.1). During the lag phase where mixed culture is expected to start acclimation, there was a slight decrease detected in pH values. Whenever, the mixed culture has started to enrich its concentration, pH values quickly dropped down to 5.0 (at 8th day). The main reason of this dramatic decline in pH values were most likely to related with production of short chain fatty acids. After this decline, an increasing trend of pH values were observed during the stationary phase. As a result of bacterial demolition, buffer capacity of the suspension was probably decrease and pH values were again decreased to below 5.5 at the end.

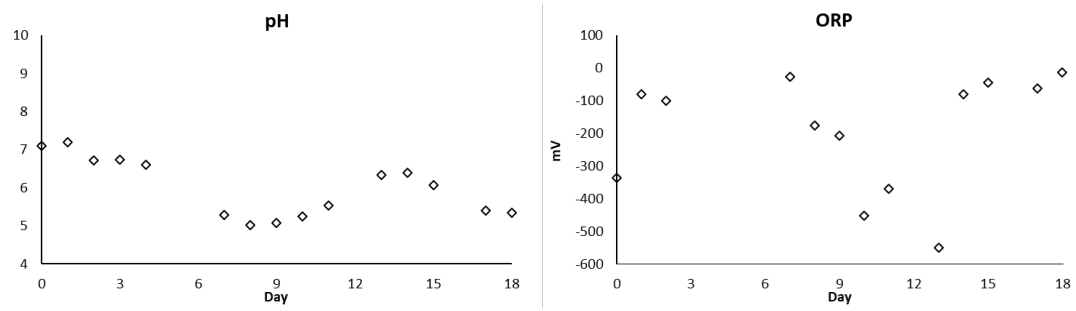

Figure C.4: a) pH change b) ORP change

Redox potential (i.e. ORP) is an easy to use and effective method to monitor the anaerobic environments such as fermenters. Strict anaerobes like methanogens and acetogens are needed and aqueous environment with a minus ORP values. The lower the ORP value, the better for anaerobic consortiums. In this case, the lowest redox potentials were recorded during the stationary phase with a minimum value of -550mV at 13th day.

Microbial cell mass concentration

A relative monitoring of microbial cell mass concentrations was carried out by measuring of OD_{600} and TS parameters in the liquid suspension. Figure C.5 shows how the biomass concentration decreasing at the first couple of days of the operation where the lag phase appears. At the beginning of the second week of fermentation, OD_{600} and TS values has started their increasing trend (enrichment phase). After about a week of stationary phase with OD_{600} values between 1.11 - 1.19, microbial concentration was started its decreasing trend. Whenever the OD_{600} value was almost equal to the lowest value of the operation at 4^{th} day (0.73 ±0.00), fermentation experiment was stopped at 18^{th} day. TS values are showing a similar trend with OD values. However, the necessity of taking a very low amount of liquid sample volumes (≈1.5-2.0mL) reduced the analytical quality of TS data. So, the microbial growth phases were detected mainly using the OD_{600} values.

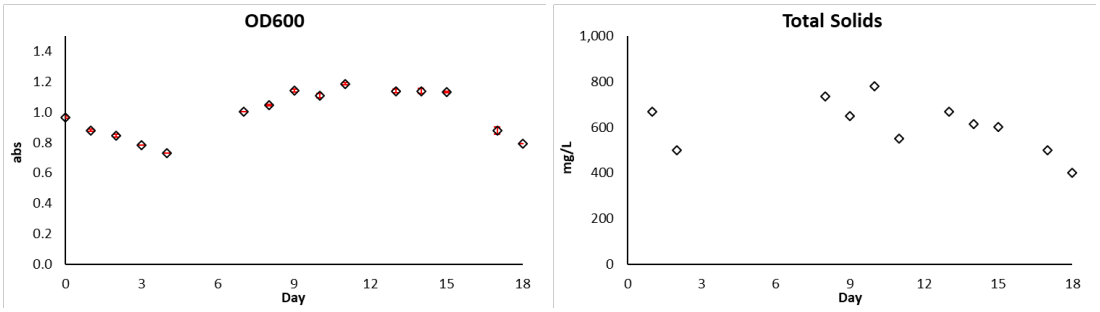

Figure C.5: a) Optical density at 600nm wavelength b) Total solids

Chemical oxygen demand (COD)

COD is a widely used relative measurement of dissolved organic chemicals in aqueous samples. In this study, biomass free liquid samples were measured for COD to monitor fermentation products such as organic acids and alcohols prior to their instrumental quantification. As it shown in the Figure C.6, immediately after the lag phase, mixed culture has started to produce some organic chemicals. An exponential increase trend was observed during the enrichment phase (i.e. log phase) between the 4th and 10th days of operation. During the stationery and death phases, COD values were not change significantly. The maximum COD value was recorded at 14th day as 7720 ± 270 mg/L.

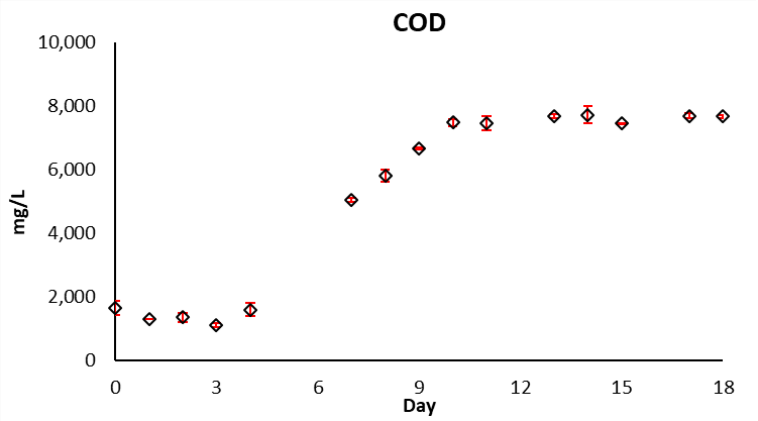

Figure C.6: Chemical oxygen demand

Product profiles

As it was concluded from the high soluble COD contents of the fermentation liquid, VFAs were most likely to present in the bioreactor. As a result of a series of qualitative analysis of the 10 times diluted and acidified liquid samples by GC-FID system, Figure C.7 was obtained. As it shown in the figure, mixed culture was firstly converted gaseous substrates to mainly acetic acid during the enrichment phase. Then, butyric acid and mainly caproic acid were become dominant species in the fermentation liquid. Highest peaks of both acids were detected in 11th day with a greater area, when the bioreactor was in the middle of stationary phase. It is also clear from the figure represented below, almost all types of commonly known short chain fatty acids including acetic, propionic, butyric, valeric, caproic and enanthic acids were somewhat found in the samples.

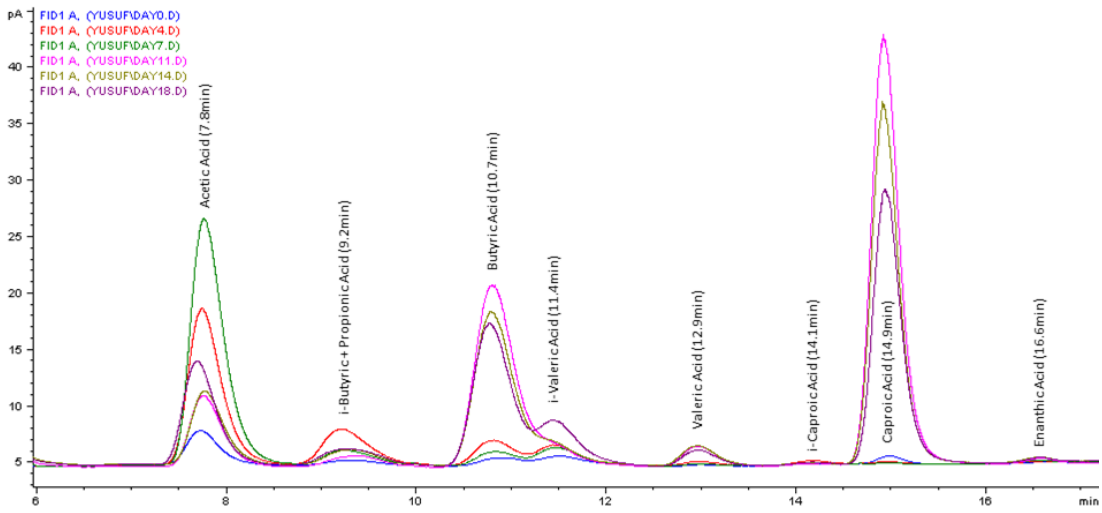

Figure C.7: VFA species of the samples as fermentation products

Off-gas Composition Profile

In Figure C.8, it is shown that how the syngas components were changed during the fermentation experiment. Some types of acetogens are known to be able to utilize some slightly soluble gas components such as CO, H_2 and CH_4 and also CO_2 gas. In this study, it was aimed that some amount of CO would be consumed by the anaerobic consortium to produce building-block intermediate chemicals. A very dramatic decrease in CO_2 value on 2nd day was most likely to related with its relatively higher water solubility, and dissolution of CO_2 was continued till 7th day where the pH was decreased to below 6 at the first time. It seems as H_2 was not remarkably used during the fermentation. Methane (CH_4) peak was only one time detected in chromatograms and was almost equal to 0%. So that it can be concluded as; preheating of the inoculum suspension was seemed to be enough to inhibit methanogenic microorganisms in the mixed culture. The maximum CO removal was detected as 0.46 at 7th day of operation (CO: 9.6 ± 0.4%) during the enrichment phase of the fermentation process. Then it showed an increasing trend up to almost its initial concentration at the end. To continue the high CO consumption, bioreactor should be kept in logarithmic growth phase.

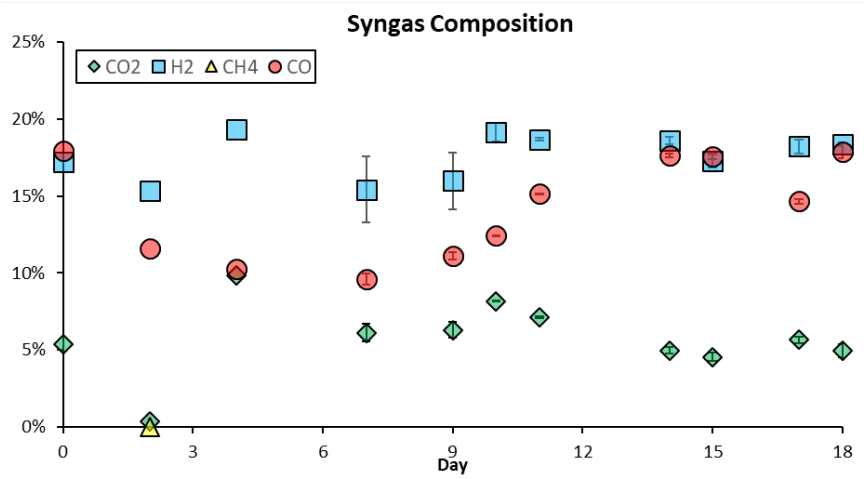

Figure C.8: Concentration profile of output gasses

Final Discussion

- The first test with bottled and clean syngas input with a continuous gas feeding via a fine bubbler (diffuser) was conducted under no liquid recycling-discharging (batch operational)
- The bioreactor was initially inoculated with a thermally-pretreated (90°C, 15 min) anaerobic digestate from a commercial Yeast Factory (Pakmaya).
- Continuous gas feeding rate was 5.20 mL/min (±0.50): 5.4% CO_2, 17.2% H_2, 55.7% N_2, 17.9% CO [0.23gCOD/L].
- At the end, bio-liquid suspension was 8 g-COD/L, which corresponds ≈1.0 g-COD/L-day V_P.
- Solventogenic production was more active than acidogenesis, which ended with 75% COD yield to Alcohols (Hexanol, Butanol, Ethanol). The rest 25% was originated from VFAs (Butyric, Acetic, etc.).

Preliminary CBSR Tests

Methodology

Char-based sparger developing

Charcoal like biochar is a solid but highly porous and conductive material that has been proved to be as a promising microbial environment for different kind of anaerobic process [44], [64], [170], [171]. In addition, amendment of microbial stimulator porous biochar was previously found as a critical approach in the anaerobic biological conversion of WS {Appendix B: Preliminary WS Fermentation Tests}. For this reason, existence of biochar would be a highly desired and unique approach also for gas fermentation experiments. However, as in the case of fermentation of WS liquid, it was sufficient to insert some raw biochar grains as a packing media like a filter-bed, since already solubilized substrate materials was expected to be directly in-contact with biochar-attached microbial communities which were sunk to the liquid medium. In contrast at gas fermentation approach, a more eligible method was required to increase the interaction possibility between gaseous substrates and porous biochar where the biofilm grows. For this purpose, a new method was developed to process and shape biochar material to manufacture a gas sparger. A biochar-based porous sparger (i.e., diffuser, bubbler, aerator) submerged into liquid medium, where the substrate gas will be fed. In this way, gas feeding rate can be regulated by an external regulator or a pump, and the gaseous substrates will be forced to perforate through the pores of biochar-sparger where the attached grown microorganisms expected to be grown.

Manufacturing of biochar sparger were visualized in Figure 4.2 and consists of several steps: grinding of pyrolysis derived biochar grains (1), screening by a coarse sieve (≈1.0 mm) to obtain powdered biochar with an approximate homogenous size distribution (2), adding acetone-melted polystyrene into the powder (3), kneading the mixture of biochar and polystyrene with subsequent additions of acetone to be able to obtain a dough-like material (4), rolling out the bio-char dough and wrapping around a cylindrical consistent pipe to have an internal hole for gas transferring (5), placing into a pattern material (e.g. syringe, soxhlet cartridge, sampling tube etc.) to give an external shape (6), drying in an oven around 60-80 °C for 1-2 hours (7), extracting the

shaped biochar-sparger from the external pattern and internal pipe (8), and lastly attaching a plastic hose by gluing with polystyrene to the internal hose of the sparger.

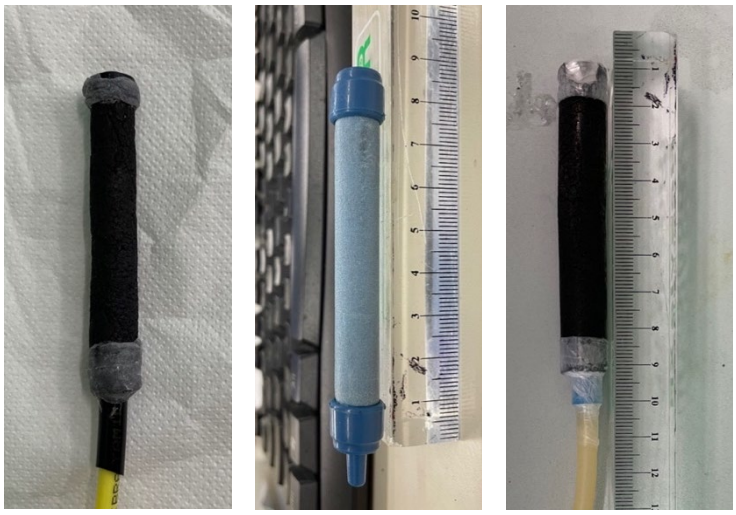

Figure D.1: Clean images of the diffusers used in this study: Biochar-sparger of R-1 (left), Commercial-diffuser of R-2 (middle), and Biochar-sparger of R-3 (right)

Three different diffusers were used in this part of gas-fermentation study. One stone-based commercial diffuser was used for the control reactor. On the other hand, two identical *biochar-spargers* were manufactured. One was made to use in syngas fermentation experiment, and the other was for power-to-material experiments (H_2/CO_2 fermentation). The geometrical details and physicochemical characteristics of the diffusers are presented in Table D.1.

Table D.1: Characteristics of the diffusers used in gas fermentation experiments

Parameters		**Biochar-Diffuser A** (used for Syngas Exp.)	**Commercial Diffuser** (used for H_2+CO_2 Exp.)	**Biochar-Diffuser A** (used for H_2+CO_2 Exp.)
Material(s)	-	Biochar, Polysterene	Non-carbonic Stone	Biochar, Polysterene
C:H:N:O Ratio[1]	*%*	76.8 : 3.7 : 0.7 : 18.9	n/a	81.0 : 4.2 : 0.6 : 14.3
Biochar : PS[2] Ratio	*M:M*	2.0	n/a	2.0
Active Length[3]	*mm*	65.0	65.0	65.0
Outer Diameter	*mm*	13.5 ± 0.75	11.0	14.0 ± 1.50
Inner Diameter	*mm*	8.5 ± 0.50	8.0	8.5 ± 0.50
Volume	*mL*	≈ 6.0	≈ 3.0	≈ 6.0
Bulk Density	*g/cm^3*	1.3	0.5	1.3

[1] Carbon, Hydrogen, Nitrogen, and Oxygen contents, [2] Polystrene, [3] Length of the non-covered active part of the diffuser

Biofilm sparger reactors

A new bioreactor system was designed to conduct gas fermentation experiments. The full set-up was consisted by three identical bench-scale gas fermenters (Table D.4). Two of them were equipped with biochar-sparger which are called as CBSR, while one of them was with a commercial inert diffuser.

In this fermentation set-up, gas substrates are filled into a special two-valved foil-gasbag and pumped through the submerged diffuser inside the bioreactor bottle. Bioreactor bottle was a standard 500 mL Pyrex bottle equipped with a special 4-ported screw-cap and placed upside-down. The four ports were used for; gas injection (1), liquid sampling (2), gas discharging (3), and the last one was used as a liquid connection port from the condenser bottle (4). A secondary smaller Pyrex bottle (100 mL) was positioned just next to the bioreactor and connected each other with a one gas and one liquid hoses. This secondary bottle was used as a gas condenser to minimize the amount of liquid loss due to both evaporation and liquid droplets jumped to the gas discharging hose due to the bubbling. Working principle of the condenser bottle was quite simple but very efficient to prevent liquid loss in long-term continues operation of bioreactor set-up. Temperature difference between the two bottles was always around 15-20 °C, since an external heating system was only covering to the bioreactor bottle (36±2 °C) and the condenser was exposed to the laboratory temperature conditions (20±5 °C). This difference in the temperature conditions between two bottles was enough to sustain an adequate re-condensation of liquid medium. The condenser was replaced in upside-down position but in a slightly higher elevation level than the bioreactor bottle to sustain condenser-to-bioreactor way of hydraulic flow. In this way, condensed liquids were forced to flow-back to the bioreactor. The condenser bottle was also combined with a multi-ported screw-cap and the ports were used as; gas inlet from bioreactor bottle (1), condensed liquid back-drainage to the bioreactor bottle (2), gas outlet to the gas-bag (3), and a reserved liquid port for final discharging (4).

A special concern was given to the gas-tightness of the overall system, since very permeable small gas molecules are the substrates. The reason behind the positioning the reactor bottles up-side down was also for providing safer environment in terms of leaking. In this way all the connection points and ports stay submerged in liquid which significantly decrease the chance of any undissolved gas leakages.

Additionally, all external plastic (PA12) hoses were again laminated by silicone and aluminum with a multi-layer approach. All valves and sample ports were chosen as gas-tight materials. Besides, the mini-vacuum type gas-pumps were specifically chosen and have been subjected to numerous tests for gas-tightness after isolating by external silicone application into the connection points. Prior to the operational start, the complete bioreactor set-up was tested several times by gas leaking tests using Helium and Hydrogen as most permeable gases. The digital controlling and electrical system of the gas-fermentation bioreactor set-up was conducted by an Arduino-based electronic controlling system. The mini gas pumps were energized and controlled by this Arduino system which allows to define the gas feeding frequency and gas flow (feed) rate.

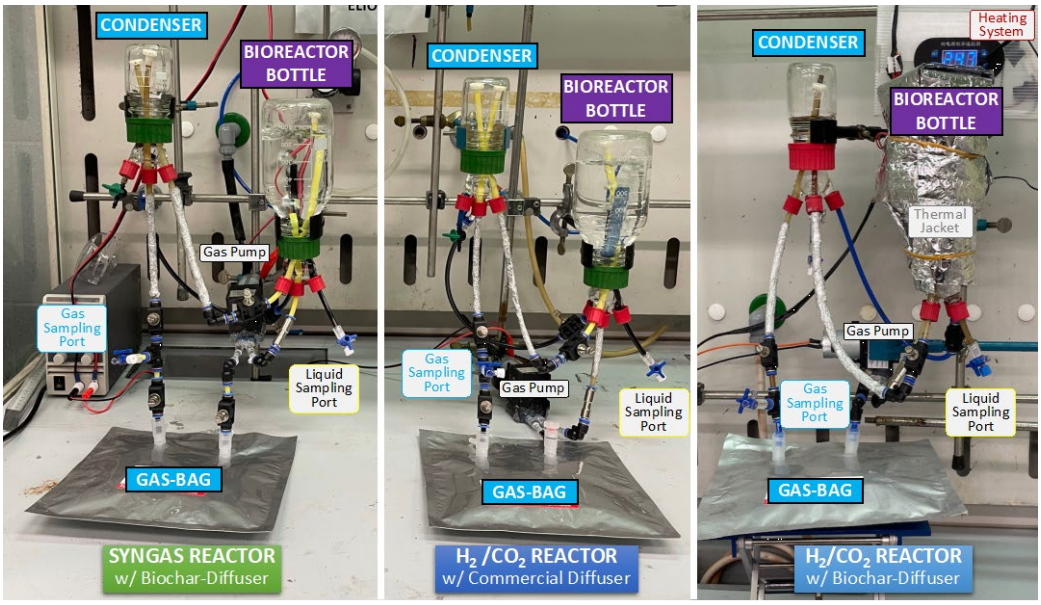

Figure D.2: Complete bioreactor set-up for the gas fermentation experiments.

Inoculum and medium

A digestate suspension previously obtained from an industrial anaerobic digester treating mainly grape pomace and wastewater treatment sludges (Caviro Extra S.p.A.) was used as the inoculum source. The refrigerated inoculum suspension had a characteristic as follow: pH 8.0, total COD 23.6 ± 0.0 g/L, and suspended COD 1.6 ± 0.1 g/L. Besides, a freeze-dried culture sample in milligrams levels was also available, which was originated from a previous syngas fermentation experiment conducted in Gebze Technical University laboratories during the previous research periods of the researcher's PhD study. This secondary MMC source was also used as an additional

source of already enriched gas-fermentative microbial source. The same modified anaerobic basal medium based was used as reported in previous sections (Table 3.3).

Microbial enrichment test of first CBSR

Prior to the real gas fermentation tests with a complete set-up, one of the reactors (R-3) were equipped with a biochar-diffuser. A preliminary anaerobic test was conducted to revive refrigerated inoculum and enrich the gas fermentative anaerobic bacteria with the presence of initial glucose and $CO_{2\,(aq)}$ existence and subsequent continuous H_2 feedings. At the same time, the new bioreactor set-up was tested, and the performance of biochar-diffuser was observed in a real anaerobic test first time. In this, 26-days long preliminary gas fermentation test, *power-to-material* approach was applied where hydrogen gas was used as the main energy source and carbon dioxide in a dissolved form (via bicarbonate salt additions) was the only carbon source in the continuous operational system.

A 500mL of start-up aqueous mixture was prepared to initiate the preliminary biological experiment which contains 5% of concentrated medium stock and 10% of digestate as inoculum source, by volume. Besides, 8.8 grams of Glucose as the initial energy source for the revival and enrichment of MMC, 50 grams of Sodium Bicarbonate ($NaHCO_3^-$) as the carbon dioxide representative inorganic carbon source, and 2.6 grams of BES as a chemical inhibitor for methanogenic cultures were included in the start-up solution of the preliminary test. In this way, the final concentrations were corresponding as; 20 g-COD/L of glucose, 25 mM of BES, 100 g/L of $NaHCO_3^-$. Start-up mixture's pH value was adjusted to 8.5, before and after the additions of bicarbonate salt to minimize the CO_2 dissolution.

Prior to the start-up of the preliminary MMC enrichment test, all the bioreactor system was continuously flushed with excess amount of Helium to scavenge all the atmospheric air. Then, the test was started by inoculation with the prepared start-up mixture liquid. Bioreactor was kept in alkaline environment throughout the operation to keep the CO_2 in a dissolved phase and overall average pH was corresponding as 8.8 (±0.25). During the first 13 days of operation bioreactor was operated in batch mode in terms of hydraulic feeding and was subjected to a semi-batch feeding of H_2 (Figure D.3). However, all the existing gas collected in the gasbag was continuously recirculated through the bioreactor system in a pulse feeding mode throughout the test (10sec bubbling in each minute). First VFA production were recorded in 5^{th} day, and

initially provided glucose content was completely consumed in day-9. Continued increase in total VFA concentrations, was verifying the bio-utilization of bubbled H_2 gas through the biochar-diffuser, since the first gas consumptions were observed 7th day and continued thereafter. Together with the change of operational mode from batch to continuous mode (at 13th day) with a 25 days of hydraulic retention time, H_2 gas feedings were standardized to 1.0 L per feeding day. VFA trend was showing a very compromising increasing trend and get stabilized during the continuous operational phase (Figure D.3). Consequently, VFA over COD ratio was showing an astronomical number, which was 100% (±3%) for the last 5 days of operation.

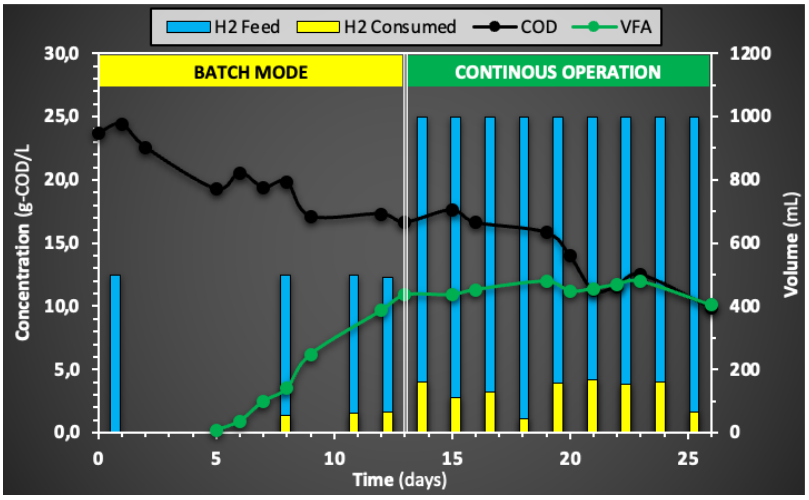

Figure D.3: An overall performance graph of the preliminary enrichment test

Operational details and start-up

The first reactor (R-1) was operated with Syngas feeding in the presence of biochar-diffuser, while R-2 with commercial diffuser was used for H_2/CO_2 fermentation, and lastly R-3 was also operated for H_2/CO_2 fermentation but equipped with a biochar-diffuser. All bioreactors were operated in daily-fed continuous way of operation where both liquid and gas materials were subjected to a continuous feeding/discharging cycles. The bioreactor bottles of all three reactors were heated and isolated to be kept under mesophilic temperature environment (36 °C). Total liquid volume was identical in all and corresponding a total half liter (500mL) of bioliquid. The daily liquid feeding and discharging volume was 20 mL/day and it corresponds 25 days of hydraulic retention time (HRT). Average gas COD loading rates were calculated as follows 0.53, 0.68, and 0.62 for R-1, R-2 and R-3 respectively. The

operational and set-up parameters of the gas fermentation bioreactor set-up was presented in Table D.2.

One of the particular methodologies applied in this study was recirculating the gaseous substrates throughout the integrated bioreactor system to increase the overall gas-utilization efficiency. In contrast, almost all the previous syngas fermentation studies available in literature, gas feedings were conducted by continuous sparging. Mini gas pump was operated in pulse mode by Arduino controlling system and was worked at 1.0 L/min flow rate. Gas flow calibration had been conducted by an external gas rotameter periodically before and during the continuous operation. Pulse working frequency of the pump was adjusted to work for 2.5 seconds in every 15 seconds of operation (≈ 10 sec/min).

Table D.2: Set-up and Operational Parameters of Gas Fermentation Experiments

Parameters		**R-1** Syngas Reactor	**R-2** H_2 Control Reactor	**R-3** H_2 Active Reactor
Substrate Material(s)	-	Syngas	$H_2 + CO_2$	$H_2 + CO_2$
Diffuser Type	-	Biochar	Commercial	Biochar
Operational Method	-	Daily Fed Continous	Daily Fed Continous	Daily Fed Continous
Temperature Set	*°C*	36.0	36.0	36.0
Total Wet Volume	*mL*	500.0	500.0	500.0
Hydraulic Retention Time	*days*	25	25	25
Avarage Gas Loading Rate	*g-COD/L-day*	0.53 ± 0.14	0.68 ± 0.26	0.62 ± 0.29
Gas Recirculation Flow Rate	*L/min*	1.0	1.0	1.0
Gas Feeding Regime	*sec*	2.5 ON / 12.5 OFF	2.5 ON / 12.5 OFF	2.5 ON / 12.5 OFF

First of all, 500 mL of start-up mixtures were prepared for each reactor (Table D.3). The first two start-up liquids were identical to be used in R-1 and R-2 which was going to be inoculated first time. For this reason, 200 mL of discharged bioliquids from the preliminary MMC enrichment test were included to the mixtures of the R-1 and R-2, to be used as the main microbial source for the aim of gas-fermentative biofilm growth on their clean diffusers. In addition, small amounts of freeze-dried syngas-fermentative culture source was dissolved in 3 mL of liquid and included to the start-up mixtures as an additional gas-fermentative culture source. A small amount of the anaerobic digestate which was used in the previous test {Microbial enrichment test of first CBSR}, was also added as a tertiary co-inoculant to all reactors. The reason

behind these supplemental co-inoculant additions was for enriching the initial biodiversity of anaerobic consortia, to increase the possibility of selecting a wide range of syngas fermentative microbial communities. The same concentrated medium stock was again included at small volumes (10 mL) to achieve the desired concentrations of nutrient. BES included again at a corresponding concentration level of 10.0 mM, which was previously used at 25.0 mM. Lastly, known amount of glucose feedstock were also added to ensure an overall 10.0 g-COD/L initial concentration in all reactors. One-time glucose amendment in the beginning was for providing initial energy source for the revival and enrichment of the MMC, which was found as an effective strategy in the previous experiments.

Table D.3: Set-up and Operational Parameters of Gas Fermentation Experiments

Compounds & Parameters	**R-1** (Syngas Reactor)		**R-2** (H_2 Control Reactor)		**R-3** (H_2 Active Reactor)	
	Added Amount	Corresponding Concentration	Added Amount	Corresponding Concentration	Added Amount	Corresponding Concentration
Distilled Water	277 mL	0,0 g-COD/L	277 mL	0,0 g-COD/L	477 mL	0,0 g-COD/L
Medium	10 mL	0,1 g-COD/L	10 mL	0,1 g-COD/L	10 mL	0,1 g-COD/L
Bioliquid of Preliminary Test	200 mL	4,0 g-COD/L	200 mL	4,0 g-COD/L	0 mL	0,0 g-COD/L
Lyophilized Syngas Culture	3 mL	0,0 g-COD/L	3 mL	0,0 g-COD/L	3 mL	0,0 g-COD/L
Digestate Inoculum	10 mL	0,0 g-COD/L	10 mL	0,0 g-COD/L	10 mL	0,0 g-COD/L
Glucose	2,35 g	5,0 g-COD/L	2,35 g	5,0 g-COD/L	4,45 g	9,5 g-COD/L
BES (at 10mM Level)	1,10 g	0,5 g-COD/L	1,10 g	0,5 g-COD/L	1,10 g	0,5 g-COD/L
Overall	500 mL	≈ 10 g-COD/L	500 mL	≈ 10 g-COD/L	500 mL	≈ 10 g-COD/L

Results and Discussion

All three reactors were started to work under continuous operation by inserting the start-up mixtures. Start-up mixtures had a similar composition and 10 g-COD/L concertation. As explained before, the initial start-up suspension was also included some amount of glucose to be used as an initial enrichment agent for the anerobic consortia. Available glucose content inside the bioreactor was monitored via GC-MS silylation analysis to confirm that it was completely consumed prior to the subsequent operational phases with only continuous gaseous substrates input. As expected, all the initial glucose content was rapidly consumed by the enriched anaerobic consortia at 3rd-day for R-1 and 2nd-day for R-2 and R-3. This initial few days with glucose-available environment were entitled as *enrichment phase*; which is referring that anaerobic MMC originated from three-different microbial source (Table D.3), were

expected to be enriched significantly in these initial ideal conditions. This initial phase was followed by a so-called ***selection phase*** for R-1 and R-2 when the already enriched anaerobic MMC did not have easy-to-degrade glucose substrate anymore. Since R-3 was already inoculated and successfully operated for 26 days-long preliminary H_2 fermentation test, it was assumed that its biochar-diffuser was already enriched and selected by the target gas fermentative cultures. In case of R-1 and R-2 reactors at this their first-time biological test, their enriched MMC were forced to grow only by gaseous substrates which were syngas and H_2 respectively. This secondary selection phase which continued until the 7^{th} days of operation was ended with the removal of suspended microbial cultures by externally centrifuging (for 15 minutes at 4000 RPM) all the available bioliquid inside the R-1 and R-2. In this way, most of the microbial communities rather than the attached-grown ones (i.e. biofilm onto the diffusers) were eliminated to investigate only the effect of using conductive carbonous diffuser as compared to a regular commercial diffuser (Figure D.1). As together with the removal of the suspended matters, biofilm onto the diffusers were expected to be become the only biological-active part of the system. Thereby, the biofilm onto the diffusers were exposed to the relatively same loading rate of challenging gaseous substrates, which previously should have been colonized by suspended MMC during the initial subsequent enrichment and selection phases. Thus, the four-days long tertiary transition phase was so-called as adaptation phase where unstable effluent concentrations with a negative trend was observed. Then a final longer phase with a regular continuous way of operation in terms of both gaseous and liquid feeding, was named as ***operational phase***, and considered to be in nearly stead-state conditions. In case of R-3 with an already bio-active carbonous-diffuser, was automatically be considered to work in operational phase with the consumption of initially provided glucose substrate (at 2^{nd} day). R-3 was operated under same continuous operational conditions until to the end, which corresponded a longer time period as compared to first two reactors. All these explained sub-operational phases were also indicated onto the profile graphs of the gas fermentation experiments (Figure D.4).

The total VFA content in terms of COD concentration in the R-1 reactor, where the acidogenic fermentation of syngas was targeted, started with a slightly upward trend during the initial enrichment phase with the presence of some glucose content. Shortly after, a sharp increasing trend was observed in total VFA concentration, and it reached around 9 g-COD/L levels which is corresponding that all COD content was

already made up mainly from organic acids. In the meantime, amount and the percentage of carbon monoxide fixation did also maximize during the selection phase when the total unit number of cultures were presumably at maximum level inside the bioreactor system (R-1). At the same time, both suspended microorganisms and biofilm attached to the biochar-diffuser of R-1, might have been still using the residual energy obtained from the utilization of initial glucose addition. Together with the microbial clarifying procedure (centrifuging) applied at the end of secondary sub-phase (selection phase), when the syngas-fermentable anaerobic acidogenic cultures were selected, an instant but reasonable decrease was observed for the VFA content and the CO-fixation of R-1. The reason behind this phenomenon can be <highly possibly> correlated to the fact that attached-grown microbes were exposed to much higher CO loading since previously similar amounts of syngas were co-utilized by a mixture of suspended and attached-grown cultures. However just in few days during this third operational period which was so-called as adaptation phase, the bioreactor was recovered itself and adapted to new harsh conditions, with a possible increase in the total unit number of syngas-fermentative attached grown microbes. Interestingly highest CO fixation was recorded in day-10 during this period, was corresponding more than 400 mL of CO from real syngas input, was removed just in one day. Later on, profile concentrations of effluent bioliquid were corresponding an almost complete stead-state conditions at the last period of the experiment. VFA composition was compromised dominantly from Acetic acid which corresponds the 90% and followed by 6% of Propionic acid and so on (i-Butyric, i-Valeric, and Butyric). During the last period of experiment; COD, VFA and pH profiles were stable around 7.0 g/L, 5.1 g/L, and 8.6 respectively. More importantly VFA-to-COD ratio was also steady around 75% which is found as very promising after 20-days long solo fermentation of untreated raw syngas. In contrast, unstable CO fixation amounts were recorded throughout experiment was correlated the fact of non-fixed CO feeding regime, that was related to stored syngas samples with varying gas compositions and varying amounts obtained from the previous pyrolysis experiments (Figure D.4-left).

A quite similar beginning was observed for COD and VFA profile of R-2, with an even sharper latter increasing trend, which was equipped with a commercial non-conductive diffuser and fed with H_2 gas in presence of solubilized CO_2 in the form of bicarbonate. On the other hand, the highest and equal concentrations of COD and VFA was recorded as 11.3 g-COD/L during the selection phase, when both suspended and

attached grown microorganisms were bio-available. Commercial diffuser of R-2 with a non-conductive but having possibly higher porosity, was providing finer and more homogenous bubbles, as compared to the biochar-based conductive and carbonous diffuser available in R-1. This differences in their characteristics, was expected to provide a more enriched attached-grown microbial community in biochar-diffuser, while commercial one could possibly ensure a slightly better bubbles may result better performance in case of bubbling-type of operation with suspended microbial cultures. Yet another different trend was observed for pH profile in R-2, since it was showing a slowly continuous increasing trend and ended up with a value of 9.4. In contrast, pH trend of R-1 was comprised of several ups and downs. This phenomenon can be correlated with a possible increase in consumption of bicarbonate content over time that ended up with a decreased concentration of available CO_2, which was the main source of acidity in the system. A similar decreasing trend was observed together with the passage to adaptation phase without suspended cultures, followed by a relatively stable conditions in terms of COD, VFA and pH profile during the operation phase. At the end, COD was around 6.5 g/L and VFA was over 5 g/L with an identical composition of organic acids in R-1.

Table D.4: Overall performance of the gas fermentation experiments

Parameters	**Unit**	**R-1** Syngas Reactor	**R-2** H_2 Control Reactor	**R-3** H_2 Active Reactor
Total Input	*g-COD*	10,57	12,26	12,51
Total Output	*g-COD*	9,98	10,40	10,35
COD Recovery	*%*	94%	85%	83%
Gaseous Input*	*g-COD*	2,77	7,50	7,50
Consumed Gas*	*g-COD*	1,40	3,13	4,29
Gas* Fixation Ratio	*%*	51%	42%	57%
Produced Total VFA	*g-COD*	3,15	3,19	7,02
Total VFA Yield (VFA_{TOT}/Gas_{FEED}*)	*%*	> 100%	42%	94%
$GLU_{extracted}$ VFA_{NET} Product	*g-COD*	0,70	0,73	2,37
NET VFA Yield (VFA_{NET} /Gas_{FIXED}*)	*%*	50%	23%	55%
$Diffuser_{BASED}$ VFA Productivity	*g-COD/L-day*	22,4	22,7	50,0
$Diffuser_{BASED}$ VFA_{NET} Productivity	*g-COD/L-day*	5,0	5,2	16,9
$Volumetric_{WET}$ VFA Productivity	*g-COD/L-day*	0,25	0,26	0,56
$Volumetric_{WET}$ VFA_{NET} Productivity	*g-COD/L-day*	0,06	0,06	0,19

** Only CO (for R-1) or H_2 (for R2 & R3) gases are taken into account in the estimations.*

In case of R-3 with an already bio-active biochar-diffuser was not contained selection and adaptation sub-phases. The feeding gas regime of the R-3 was identical to R-2 with a gradually increased amounts of H_2 inputs over time, which ended up with a gradually increasing trend of gas consumptions especially during the 3rd week of operation where the most promising results were also obtained. As can be tracked from the figures, R-3 was resulting with a better H_2 uptakes and higher COD and VFA concentrations as compared to the control reactor equipped with a commercial non-conductive filter (Figure D.4-right-up). While pH was showing a similar continuous increasing trend like in R-2, and it ended with a higher value over 9.5. That is indirectly referring an increased uptake of solubilized CO_2 which is required for the synthesis of organic acids from H_2 (Eq. 7.1). Besides, total VFA and COD concentrations were equal at the end of operation where nearly steady-state conditions already sustained. VFA and COD were corresponding over than 7.5 g-COD/L which is the highest end-concentration as compared to the other two reactors. Those differences in active reactor (R-3) as compared to control reactor (R-2) were implying of a gorgeous positive effect of conductive biochar-diffuser as a microbial-friendly biofilm-media, which possibly allowed a higher interaction between the gaseous substrates and the gas-fermentative attached-grown cultures.

$$4H_2 + 2CO_{2(aq)} \longrightarrow CH_3COO^- + H^+ + H_2O \qquad (7.1)$$

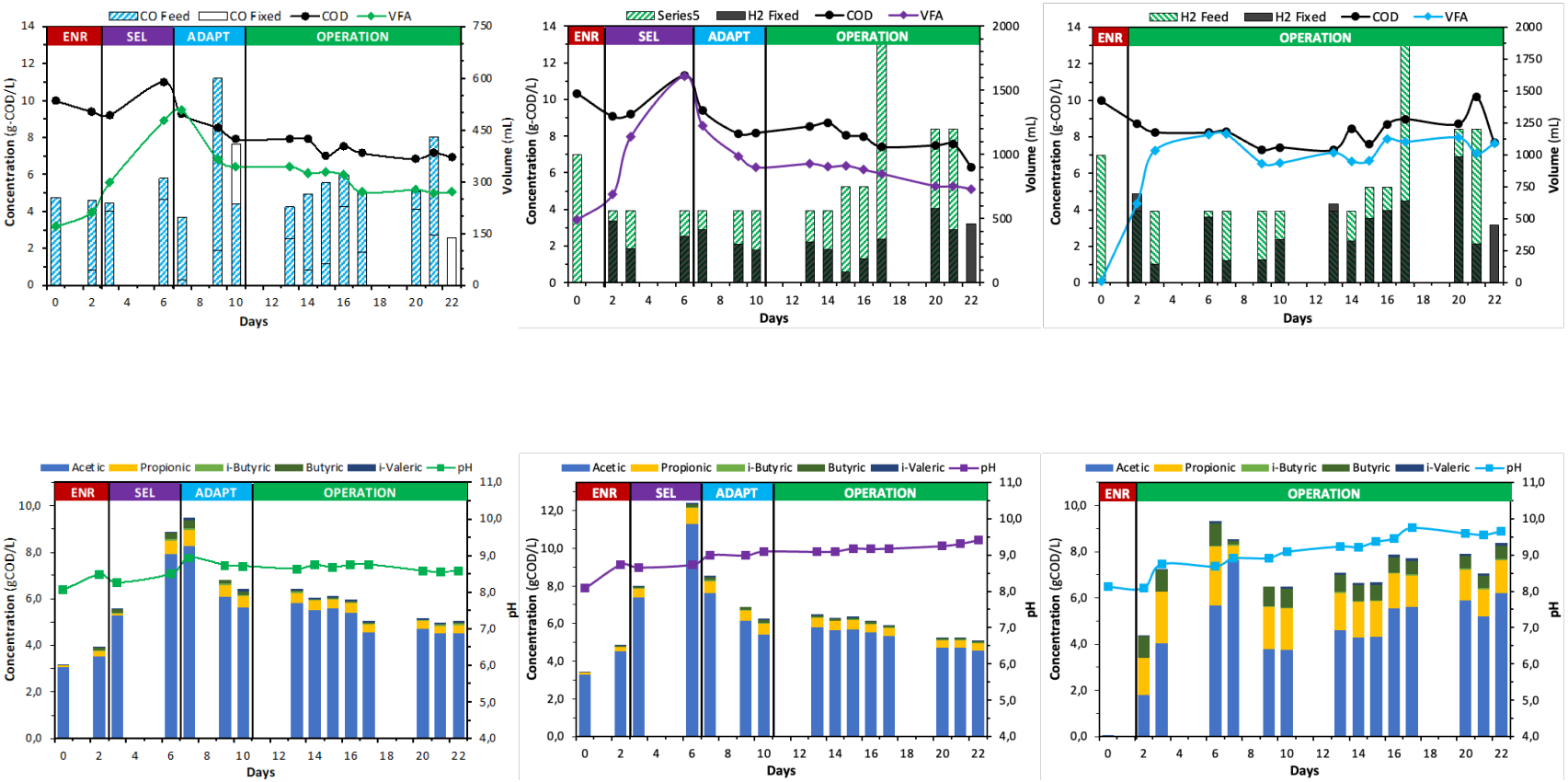

Figure D.4: Profile graphs of the gas fermentation tests conducted in R-1 (left), R-2 (middle) and R-3 (right).

Final Discussion

An overall performance summary of the conducted gas fermentation experiments is presented in Table D.4. All three gas fermentation tests conducted in the closed-loop bioreactor set-ups were ended up with a satisfactory mass balance with an average 86% ±6 of COD coverage. In the fact of raw syngas mixtures obtained from the intermediate pyrolysis of wooden biomass were corresponding a varying concentration in terms of COD, was ended up with a lower total COD and gas input in R-1, as compared to R-2 and R-3 with H_2 feeding. However, total VFA yield (VFA_{TOTAL}/Gas_{FEED}) and net VFA yield over consumed gas (VFA_{NET}/Gas_{FIXED}) was corresponding a very satisfactory results either better or very similar to the R-3 reactor which was fed with high-purity clean H_2 gas. In case of control reactor (R-2) with a non-conductive commercial diffuser was showing a considerably lower performance in terms of both total and net VFA yields together with a slightly lower gas fixation rate. In terms of VFA productivities, best performance was belong to the R-3 with a 50 g-COD/L-day which was calculated based on the diffuser's volume of the only bio-active part of the bioreactor system. Unlikely, the control reactor (R-2) was resulting more than halved performance (22.7 g-COD/L-day). On the other hand, R-1 with a syngas feeding regime was very similar to the R-2 which was fed with three times higher gas input in terms of COD. In case of, net VFA productivities based on the diffusers' volume, R-3 was corresponding an even better performance than the control reactor and again R-1 and R-2 was nearly identical. Furthermore, as correlated with the diffuser based volumetric productivity estimations, a clear resemblance was estimated also for the conventional total wet-volume based productivity parameter. An overall conclusion through the gas fermentation experiment would be the fact that the novel conductive biochar-diffuser developed by this work, was found as an effective way of stimulating the anaerobic microbial conversion of both syngas and H_2 into organic fatty acids as a green-way of production those building block value-added chemicals.